

Reducing production costs in offshore wind turbine tower design

O.B.A. Nekeman

Track: Aerodynamics & Wind Energy



Courtesy of Siemens Gamesa

Reducing production costs in offshore wind turbine tower design

by

O.B.A. Nekeman

to obtain the degree of Master of Science
at the Delft University of Technology,
to be defended publicly on September 30th, 2021 at 9:00 AM.

Student number: 4367642
Project duration: September 1, 2020 – September 30, 2021
Thesis committee: Prof. dr. ir. M.B. Zaayer, TU Delft, supervisor
Prof. dr. ir. D.A. von Terzi, TU Delft, Chair
Prof. dr. ir. J. Sinke, TU Delft, examiner
Ir. F. Wennekers, Siemens Gamesa Renewable Energy

This thesis is confidential and cannot be made public until September 30th, 2023.

An electronic version of this thesis is available at <http://repository.tudelft.nl/>.

Abstract

The objective of the thesis was to evaluate the cost reductions and tower design when production costs are included in the design process of an offshore wind turbine tower. First, a tower cost model had to be developed. Then, based on the findings, a cost optimization model was built with the tower design software from Siemens Gamesa Renewable Energy (SGRE). Three scenarios were developed to mimic different supply chains. The results show that the production costs can be reduced by [0.2, 2%]. Moreover, in each scenario, a different optimum tower design was found. Another study into the optimum number of shells per section showed wind turbine manufacturers could reduce production costs up to 20%.

Preface

This thesis studies the effect production costs have on tower design in the offshore tower design process. Wind turbine manufacturers are continuously searching for methods to reduce the cost of their turbines to reduce the cost of energy. This is important to speed up the transition from fossil fuels to renewable energy. Siemens Gamesa Renewable Energy initiated this study with the question: "how to optimize for costs in the tower design process?". The question was intriguing because I firmly believe that the transition speed from fossil to renewable energy depends mainly on the energy cost of both sources. Therefore, if wind energy becomes cheaper than burning fossil fuels, the industry will shift in a heartbeat. This thesis is basically my first concrete contribution to the energy transition and making the world a better place.

I have focused on various optimization methods in my studies, such as multi-disciplinary optimization and evolutionary algorithms. Besides my interest in engineering, I also have a keen interest in commercial projects. During my master wind energy and aerodynamics, I have learned about the technical influence on design. However, in reality, commercial aspects are a significant driver in decision-making. Once I noticed how little research was done on the commercial engineering of an offshore wind turbine tower, my interest increased. This thesis just might influence the way wind turbine manufacturers design their towers.

The thesis is meant for scientists, engineers, and managers in the wind industry. Scientists can use the cost model in structural optimization studies to finally optimize for costs instead of the mass objective. Engineers can use the findings to improve their tower designs. The conclusions provide valuable guidelines for tower design. Managers can decide whether it is worthwhile to change the manufacturing procurement from a bidding process to a framework agreement. A bidding process gives the procurer the lowest price. Still, it limits a tower engineer to design for a specific supply chain. This forces the engineer to create a generic design not optimized for any party. If framework agreements are made, the engineer knows upfront what the cost functions are and can design accordingly.

*O.B.A. Nekeman
Amsterdam, September 15, 2021*

Acknowledgements

A student in aerospace engineering can choose their own thesis topic and supervisor. When my time came, the first professor I went to was Michiel Zaayer for two reasons. First, because you had the most interesting research topics, and second, the way you help and engage with students is admirable. Every time I went to you for help, we first had a coffee break and discussed what was on our minds. During my thesis, I experienced how committed you are to your thesis students, and reading your feedback brings a smile to face. I am grateful for receiving your supervision and would recommend anyone to have your guidance in their thesis.

I wanted to do a commercial optimization of wind turbines, which can best be done at an industry partner. So when Sven Voormeeren of Siemens Gamesa proposed doing a cost optimization for off-shore towers, I did not doubt for a second. With Frits Wenekers and Joris Remijn, you supervised me, and I could not have wished for anyone better. Sven, your knowledge of tower engineering is admirable. I must say, the critical questions were intimidating, but they kept me sharp. Frits and Joris, your expertise in tower engineering were invaluable to this project. The industry perspective on this research was refreshing. I am glad to have experienced what life as an engineer entails. And thank you for taking me to the pancake shop on the Theresiastraat. The question "gehakt, spinazie, feta?" will always stick with me.

Besides the supervisors, I would like to thank everyone from SGRE. Showing what an engineer does was a valuable experience. Col, thank you for making all the students feel at home and Pim for organizing the student meetings. And finally, two fellow students, who started with me in the same cohort. Mees and Vincent, I enjoyed the beers when we were still allowed to. I wish you all the best in the future and hope we meet again.

To close off, I would like to thank my friends and family interested in my thesis. The thesis period is notorious for the roller coaster of emotions you go through. However, without you guys listening to me, I could not have succeeded. You kept me motivated throughout the process, and I am glad about the final result.

Contents

List of Figures	xi
List of Tables	xiii
Abbreviations	xv
1 Introduction	1
1.1 Background on offshore wind turbine tower design	1
1.2 Cost models for offshore towers	2
1.3 Challenges for cost-optimizing towers	3
1.4 Thesis objective and tasks	3
1.5 Thesis outline	4
2 Methodology	5
2.1 Developing the cost model	5
2.1.1 Industry interviews	5
2.1.2 Deriving cost functions	6
2.2 Building a cost optimization model	8
2.2.1 Tower design software	9
2.2.2 Conceptual cost optimization models	11
2.3 Case study explanation	12
3 A cost model for offshore wind turbine towers	15
3.1 Cost model structure	15
3.1.1 Cost model concept	15
3.1.2 CAPEX cost breakdown	16
3.2 Interview results	17
3.2.1 Interview results for the cost model	17
3.2.2 Acquired data sets	19
3.3 Material Procurement	20
3.3.1 Phase explanation	20
3.3.2 Material cost model	20
3.4 Material transport	24
3.4.1 Phase explanation	24
3.4.2 Transport cost model	24
3.5 Manufacturing	27
3.5.1 Phase explanation	27
3.5.2 Manufacturing cost model	27
3.6 Section transport	30
3.6.1 Phase explanation	30
3.6.2 Section transport cost model	30
3.7 Assembly	32
3.7.1 Phase explanation	32
3.7.2 Assembly cost model	32
3.8 Installation	33
3.8.1 Phase explanation	33
3.8.2 Installation cost model	33
4 Cost optimization model	35
4.1 Reasoning behind the optimization routine	35
4.1.1 Chosen optimization concept	35
4.1.2 Implementation of chosen concept	35

4.2	Tower parameterization	37
4.3	Optimization algorithm	38
4.3.1	Optimization model structure	38
4.3.2	Explanation of the Nelder-Mead algorithm	38
4.4	Optimization problem formulation	40
4.4.1	Objective	40
4.4.2	Design vectors	41
4.4.3	Rewriting constraints	41
4.5	Case study tower design	43
4.5.1	Outer geometry	44
4.5.2	Baseline tower design	44
4.6	Optimization model vulnerabilities	46
4.6.1	The local minima study	46
4.6.2	Structural integrity in the cost optimization	54
4.6.3	Convergence in tower design loop	56
4.6.4	Mitigation of the vulnerabilities	57
5	Case studies	59
5.1	High manufacturing cost scenario	59
5.1.1	Scenario parameters	59
5.1.2	Cost analysis	60
5.1.3	Tower design analyses	62
5.2	Low manufacturing cost scenario	64
5.2.1	Scenario parameters	64
5.2.2	Cost analysis	64
5.2.3	Tower design comparison	66
5.3	Sensitivity study into number of shells	68
5.3.1	Scenario parameters	68
5.3.2	Cost analysis	68
6	Conclusions and recommendations	73
6.1	Conclusions	73
6.2	Recommendations for future research	74
A	Qualitative interview data	77
B	Derivation of plate dimensions	81
B.1	Cylindrical shell - plate mass	81
B.2	Conical shell - plate mass	81
	References	85

List of Figures

1.1	Phases over the lifetime of a wind turbine tower. The red-outlined phases are the Capital Expenditure (CAPEX) phases.	2
2.1	Example of polynomial functions up to order 3.	8
2.2	Effect of tuning parameters on a sigmoid function.	8
2.3	Effect of tuning parameters on stacked sigmoid function.	9
2.4	Flow diagram of tower design software.	11
2.5	Changing objective from mass to cost	12
2.6	Optimization process for a separate tower design and cost optimization algorithm.	13
3.1	Schematic representation of the cost model.	16
3.2	Indicative CAPEX cost breakdown.	16
3.3	Tower cost breakdowns for the same tower design with two different supply chains.	17
3.4	Indicative material cost breakdown.	20
3.5	Indicative plate cost breakdown.	21
3.6	Price of hot rolled steel plates over time per continent.	21
3.7	Cost data and functions with respects to plate height, length and thickness.	22
3.8	CO ₂ prices over time for Europe, British Columbia (CA), and China.	23
3.9	Cost data for steel grade qualities.	23
3.10	Supplier-Manufacturer network.	24
3.11	Material transport cost data and functions with respect to plate length.	26
3.12	The five main actions in the manufacturing phase.	27
3.13	Indicative manufacturing cost breakdown.	27
3.14	Cutting & beveling cost curve fits.	28
3.15	Rolling & welding cost curve fits.	29
3.16	Painting cost curve fits.	29
3.17	Section transportation process from manufacturer to landing site.	30
3.18	Example overview of landing site layout.	32
3.19	Schematic representation of the installation process.	33
3.20	Indicative installation cost breakdown.	33
4.1	Tower parameters in the optimization problem.	37
4.2	Cost optimization flowchart	38
4.3	Example of a Nelder-Mead optimization.	40
4.4	Value of constraint violation.	42
4.5	Structural integrity assumption.	43
4.6	Initial tower geometry.	44
4.7	baseline tower geometry.	45
4.8	Example of a local and global minimum.	46
4.9	All minima found by the optimization model.	47
4.10	Thickness distributions of the global minimum and Baseline Tower Design (BTD) minimum for section 1.	48
4.11	Shell heights of the global minimum and BTD minimum plotted on the plate height cost function.	49
4.12	Shell heights of all minima with $\Delta C > 0$ plotted on the plate height cost function.	49
4.13	Optimized design vector of section 2 for the global optimum and result of case study 2.	50
4.14	Difference between a conical shell mass and the rectangular plate mass with respect to shell height (h) and bottom diameter (d_2) with a fixed cone angle β	51

4.15 Shell heights of the global minimum, BTD minimum, and third dominating minimum M3 plotted on the plate height cost function.	52
4.16 Distribution of the initial value of the h_{38} variable for the global minimum, local minimum - CS1, and third minimum - M3.	53
4.17 Cost optimized designs for the global minimum, BTD minimum, and third dominating minimum M3.	53
4.18 Thickness deviation between Cost-Optimized Design (COD) and Cost-Optimized Design - Structural Integrity Design (COD-SID).	54
4.19 Thickness distributions for the COD and COD-SID.	55
4.20 Cost results per section for the tower design loop.	56
4.21 Steps in the cost optimization model.	57
5.1 Section cost breakdowns of the baseline tower design for supplier 1 and manufacturer 4.	60
5.2 Optimization cost deviations per section.	61
5.3 Thickness distributions for the BTD and COD.	62
5.4 COD cost breakdown of section 2.	63
5.5 Scaled manufacturing cost functions used in case study 2.	64
5.6 Section cost breakdowns of baseline design for supplier 1 and the scaled manufacturing cost functions.	64
5.7 Phase costs and section mass results for the COD-SID-CS1 and COD-SID-CS2.	65
5.8 Thickness distributions for the BTD and COD.	67
5.9 Results for varying number of shells in section 1 for several case studies.	69
5.10 Results for varying number of shells in section 2 for several case studies.	70
5.11 Results for varying number of shells in section 3 for several case studies.	71
B.1 Necessary plate shape for cylindrical and conical shells.	81
B.2 Plate geometry of a conical shell.	83
B.3 Plate and shell mass difference w.r.t to shell height and bottom diameter.	83

List of Tables

2.1	Overview of conducted interviews.	7
2.2	Overview of tower design methods for wind turbine towers	10
3.1	Summary of interview results	18
3.2	Cost data summary.	19
3.3	Parameters for the calculation of the transport costs from manufacturer to landing site.	31
3.4	Vessel parameters for the calculation of the total installation time.	34
4.1	Overview of parameters affected by the tower design software and cost optimization model.	36
4.2	Section diameters and height, fixating the tower outer geometry.	44
4.3	Final design vectors for the global minimum and BTD optimization results.	48
4.4	Final design vectors for the global minimum and BTD and M3 result for section 3. Values represent the percentage of the original shell heights.	52
4.5	Relative thickness deviation between the COD and COD-SID per section.	54
4.6	Bandwidths of the tower design loop	57
4.7	Tower design loop performance.	57
5.1	Results for the COD and COD-SID. Comparison against the baseline tower design.	61
5.2	Results for the COD-SID-CS1 and COD-SID-CS2. Comparisons made against the baseline tower design of each case.	65
5.3	Parameters for the sensitivity study into the number of shells per section.	68
A.1	Answers to interview questions.	77

Abbreviations

- ANMS** Adaptive Nelder-Mead Simplex algorithm. 40
- BTD** Baseline Tower Design. xi, xii, 46–50, 52–55, 57, 59, 62–64, 66, 67
- CAPEX** Capital Expenditure. xi, 1–3, 5, 16, 36, 40
- COD** Cost-Optimized Design. xii, 12, 46, 54–56, 60, 62, 63, 67, 73, 74
- COD-SID** Cost-Optimized Design - Structural Integrity Design. xii, 54–56, 60, 62, 64–66, 68
- COM** Cost Optimization Model. 73, 74
- IEC** International Electrotechnical Commission. 1, 10, 44
- LCoE** Levelized Cost of Energy. 2
- LMA** Levenberg-Marguardt Algorithm. 6, 7
- OPEX** Operation Expenditure. 15
- RNA** Rotor-Nacelle Assembly. 1, 32, 34, 37
- SGRE** Siemens Gamesa Renewable Energy. iii, 9, 10, 35, 43, 73
- SID** Structural Integrity Design. 12, 46, 56, 60, 73, 74
- TDS** Tower Design Software. 60, 73, 74

Introduction

The world will likely warm up beyond 1.5°C if we do not take immediate action to reduce greenhouse gas emissions [1]. One of those actions to shift from fossil fuels to renewable energy, with offshore wind energy playing a major role in that new energy system. The best way to accelerate the shift is by making renewable energy economically more attractive than its fossil counterpart. Decreasing the cost of turbine components, among which the tower, contributes towards that goal. Much effort is put into towers' technical design, while historically, little attention is given to cost optimization. The best practice in the industry is to minimize tower mass, which reduces material costs. This is done under the assumption that tower mass is the main cost driver in CAPEX. However, this assumption has not been validated and leaves room for improvement in the tower design process. That is why in this study, the effect of including CAPEX in the design process is studied. To reach that goal, first a background on tower design and cost modeling is given in sections 1.1 and 1.2. When the state-of-art is known, the current challenges in tower cost optimization are explained in section 1.3, from which naturally follow the research objectives in section 1.4. The outline of the report is given in section 1.5.

1.1. Background on offshore wind turbine tower design

The design of an offshore wind turbine tower is an iterative process between the Rotor-Nacelle Assembly (RNA) and the support structure design [2]. In that process, engineers focus on six primary design drivers fatigue, minimizing resonance, preventing buckling, withstanding ultimate material stress, tower clearance, and cost-efficiency [3]. The goal is to develop a tower that meets all certification criteria against the lowest cost.

Finding the best tower design can be done with structural optimization models. The purpose of these structural optimization methods is to aid engineers in developing site-specific towers. Every wind farm has a unique tower because of the different environmental conditions at that location. Wind turbine manufacturers have found it to be worthwhile to develop a tower for each wind farm [4]. Moreover, the International Electrotechnical Commission (IEC) demands a certification process for each wind farm [5].

An optimization problem consists of the objective, the value to be minimized, and the constraints, relations that cannot be violated. The technical design drivers are the constraints to the tower optimization problem and the industry objective is cost-efficiency. Over the course of 30 years, several researchers studied the best objective, optimization method, and which constraints are most important.

Many researchers used tower mass as the objective [6], . Minimizing the mass reduces material costs, which is an important cost driver for CAPEX. Some researchers tried other objectives. In 2000, Negm and Maalawi [7] established that the weighted sum of natural frequencies resulted in the best tower design. It was one of the first studies in structural optimization of steel towers and the objective has not been used in later studies. Seven years later, a study of Uys, Farkas, Jármai, *et al.* [8] used the material and manufacturing cost to find the optimum tower design. The idea was to evaluate the effect of including more cost functions than just mass. However, a more recent study questions "to what degree the Farkas and Jármai cost model can be used for wind turbine design" [10]. With all this research, the industry best practice is to use tower mass as the design objective [4].

Also, several optimization methods have been proposed. Gradient-based [11], [8], evolutionary algorithms [12], [13], or a combination of both [6] were used and showed promising results. Unfortunately, there is not a consensus on the best approach. It is known that the design space has many local minima and most variables are continuous. Evolutionary algorithms perform better in finding a global optimum but are very time consuming in establishing continuous variables. Gradient-based algorithm have the exact opposite properties. Finding the right balance is still an undergoing topic.

Finally the constraints. The technical design drivers set the design space in which the optimizer can find the best solution. In most studies, ultimate stress (ULS) is chosen [8], [7]. However, the study of Maljaars considered all design drivers and showed that the governing constraint can be also fatigue, depending on the environmental conditions and tower design. The goal of that study was to optimize CAPEX but due to the lack of available cost models, the objective was switched to tower mass.

1.2. Cost models for offshore towers

Several researchers developed cost models for wind turbine towers. Before discussing the models, the overview of CAPEX phases in figure 1.1 must be discussed. The tower costs are split into eight phases, material, material transport, manufacturing, section transport, tower assembly, installation, operation & maintenance, and decommissioning, shown in figure 1.1. The first six phases together make up the CAPEX of a wind farm project.

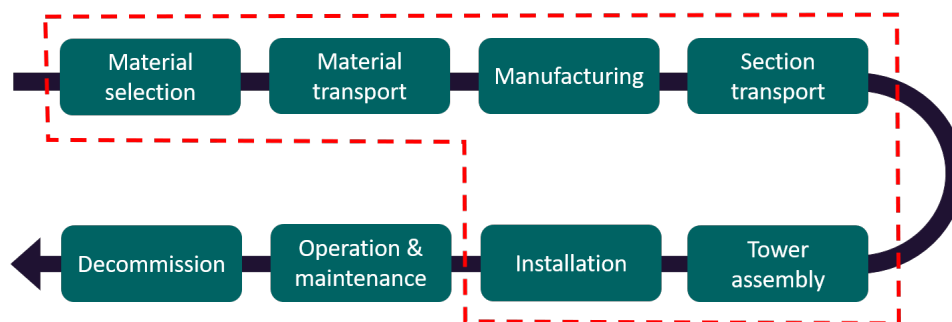


Figure 1.1: Phases over the lifetime of a wind turbine tower. The red-outlined phases are the CAPEX phases.

The topic of cost modelling for offshore towers started in 1993 with a study of Harrison and Jenkins [14]. He was the first to develop a routine for building the lowest-cost turbine. In that study, a cost factor per unit weight of the tower was used to determine the optimum height of the tower with respect to the cost of energy. The researchers already recognized that *"due to the simple nature of the costing multipliers that have been used, no reliance should be placed on the actual level of the costs"* [14]. Nevertheless, the industry practice of mass minimization of the tower has the underlying assumption that the cost of the tower can be estimated by a cost factor multiplied with its mass.

The pitfall of Harrison and Jenkins's study was recognized by Fingersh, Hand, and Laxson [15]. In an extensive study of wind farm components, production, installation, and operation costs, the researchers established cost relationships based on top-level turbine parameters rated power, swept area, and hub height. These relationships enabled studies into Levelized Cost of Energy (LCoE) optimization studies [16]. Although it allows conceptual studies, in reality, these relationships are too coarse to use in actual tower design [10]. The top-level parameters used for the cost relations do not account for the different wind, sea, and soil conditions. According to the model of Fingersh, Hand, and Laxson, a tower built in a high-speed wind environment should bear the same cost as one built in a low wind speed location. In reality, this is not true.

A study into the cost of production of wind turbine towers by Farkas and Jármai established relationships on a process level for ring-stiffened wind turbine towers. It is a grouping of several earlier studies of the researcher into production costs. It covered the cost of material, plate bending, welding and painting. This model was used in the least-cost tower optimization study of Uys, Farkas, Jármai, *et al.* [8]. It only considered buckling and bending stress as design drivers. Thus it is unsure whether the final result would meet the fatigue requirements. Researchers argued that this cost model has the potential to be used in industrial tower design [10].

Shafiee, Brennan, and Espinosa [17], studied the whole-life cost of a wind farm, similar to Fingersh,

Hand, and Laxson [15]. The cost relationships combine regression analysis of previous wind turbine projects and a cost factor approach for phase costs, such as transport and installation. The coverage of all phases is a major step forward in cost modeling, but it does not cover tower costs in specific. The cost functions are too coarse to be used in the tower design phase.

The cost of transportation can be a large share of the wind farm CAPEX. Irawan, Akbari, Jones, *et al.* [18] studied a supply chain optimization that focused on transport costs, the capacity of factories, and storage costs. The case study in that article showed that transportation could be up to 10% of the CAPEX cost of a tower.

A cost model for installation of a wind farm was covered by Sarker and Faiz [19]. The cost was found by multiplying the vessel day rate and the total installation time. The latter was found by decomposing each step of the process and estimating the time per step.

More recently, a study into multi-objective optimization of steel towers was done by Cicconi, Castorani, Germani, *et al.* [20]. One of the objectives was the cost, which was calculated by a material, transport, and manufacturing cost with cost factor over the tower mass and length. Unfortunately, the exact cost factors are not publicly available.

1.3. Challenges for cost-optimizing towers

The biggest problem in tower cost modeling is that no integral cost model links specific tower parameters to the costs in all phases of production. It prevents engineers from designing the lowest-cost tower. Instead, engineers rely on mass minimization that was already criticized by the researcher that invented it in 1993 [14].

The challenge of developing such a model is finding the appropriate relationships between tower parameters and costs in each production phase. It requires input from industry and is often confidential information, which wind turbine companies, steel suppliers, and tower manufacturers are reluctant to share.

Another difficulty in cost modeling is the fluctuation of prices, especially for the cost of the material. Steel, coal and electricity prices change over time. Therefore, at the time of design, the material cost can be different than at the time of actual procurement. Also, material, manufacturing, transport, and installation procurement is an open market, meaning supply and demand set the price. The market conditions influence the markup in each phase depending on their capacity.

Fourthly, in every step of production, each company has its cost structure and limitations. Local labor rates, equipment costs, overhead, and markup determine the price per action in each phase. The equipment also has its limits regarding the material it can handle. For large-sized towers, there are a limited number of manufacturers around the world to produce them.

1.4. Thesis objective and tasks

The objective of this thesis is:

”Evaluate the difference in the production costs and tower design between a cost-optimized tower against a reference tower.”

Two main components are essential to reach the objective. First, a cost model covering all CAPEX phases and a cost optimization method. An earlier study into cost models and tower design methods by Nekeman and Zaayer [3] has shown that there is not a good cost model for detailed tower design. Since such a cost model is unavailable, a cost optimization routine for towers must also be investigated. Therefore, the objective can be split into three tasks:

- develop a cost model for offshore wind turbine towers covering all phases that contribute to the tower CAPEX;
- propose a cost-optimization method for the primary structure of an offshore wind turbine tower;
- compare the cost-optimized tower with a reference tower on production costs and tower design.

1.5. Thesis outline

This chapter introduced the process and research on offshore wind turbine tower design, cost modeling for offshore towers, and the challenges for optimizing towers for cost. Based on these findings, the research goals were formulated. To achieve these goals a firm methodology is established, explained in chapter 2. Chapter 3 introduces the cost model, which was developed based on cost models from literature, help of industry experts, and cost data. It covers all phases of production, from material procurement to installation of the tower. With the cost model, the tower cost optimization model was developed in chapter 4 and tested in several case studies in chapter 5. The conclusions that can be drawn from this report are given in chapter 6.

2

Methodology

Answering the research objective requires a firm methodology. Section 1.2 established that there is no accurate cost model available for offshore wind turbine towers. The new cost model was developed through a mix of industry interviews and, if available, cost data, further explained in section 2.1. Once the model has been established, the gap between optimizing for costs and mass can be studied. The cost optimization methods that fill specific gaps of the cost functions are explained in section 2.2. The best optimization method is chosen based on the cost relations found in the cost model. In section 2.3, several case studies were developed through which the effect of including CAPEX cost in the tower design process can be analyzed.

2.1. Developing the cost model

A new cost model suited for tower design optimization has to be developed because it is not present in literature [3]. Building a new model categorizes this study as exploratory research [21]. *"Exploratory designs begin with a primary qualitative phase, then the findings are validated or otherwise informed by quantitative results. This approach is usually employed to develop a standardized (quantitative) instrument in a relatively unstudied area"* [21]. Paragraph 2.1.1 explains the qualitative industry interviews, which were structured to find the most relevant parameters for modeling costs in each production phase. Following is the methodology for deriving quantitative cost functions in paragraph 2.1.2.

2.1.1. Industry interviews

The methodology for the industry interviews was developed according to a qualitative research framework [22]. A qualitative study is a different approach from regular engineering research. Therefore, a comparison between the two is given first. Then the qualitative research method is explained, with the interview perspective, data collection method, interviewee list, and the qualitative data analysis method.

Differences between qualitative and engineering research

There are three major differences between qualitative and quantitative (engineering) research. The first difference is the moment when theory is developed. In the former, a framework for interviews is made, and a theory is developed based on the interview results. Thus the theory is part of the results. For the latter, the theory is developed upfront in the methodology, and the tests are the results. The theory is part of the methodology. Thus, in this study, the cost model is developed after the interviews were conducted.

The second difference is the generalizability of the results. In quantitative engineering research, the focus is on generalizability, meaning that the results can be generalized to other situations. In qualitative studies, the focus is on transferability, meaning that the reader of the study has to judge whether the results apply to their situation [21]. For this reason, the context of the interview and interviewee must be provided. This was done by providing the structure and topic of each interview and the job description of the interviewee.

A final difference between standard qualitative research and this study is that the former studies the interaction between people, while in this study, the focus is on the costs of a tower. Since there is no human interaction in the phenomenon, the need for a different perspective and the extent of the interview analysis is reduced.

Interview perspective

The epistemological perspective is the lens through which the interviews are conducted. In this part of the study, the post-positivist perspective is used because the industry experts and cost data are provided by one industry partner. This means the results (truths) found in this study are based on the acquired data and might not apply to other tower manufacturers. Also, the cost dynamics can change over time, as well as the knowledge of the industry experts. Therefore, the results are specific to the context of the study.

This also aligns best with the perspective of a regular quantitative engineering study which is either positivist or post-positivist. This means the researchers assume there is an absolute truth to be found. In positivist research, this phenomenon occurs independently of the context. In post-positivist studies, the results or phenomenon depend on the context of the study, and if the study is redone in a different context, the results may vary [22].

Data collection method

Interview questions

The interviews with industry experts were semi-structured. Semi-structured interviews have predetermined questions but allow the interviews to deviate if relevant information was presented [22]. The interview questions were designed to find the current truth of tower cost modeling in industry, complying with the post-positivist perspective.

The predetermined questions used in all interviews were:

1. What are the most important tower parameters that contribute to costs in the production phase?
2. What are the current cost estimation methods for the production phase used in industry?
3. What is your opinion on the presented cost model from literature?
4. Do you know more tower cost experts on a phase in the tower production process?

Sampling

Most participants in this study were found using snowball sampling. Snowball sampling means *"seeking the assistance of initial study participants to generate contacts ... that are potentially highly informative for the topic"* [22]. The interview overview in table 2.1 shows that the study started with an expert on overall tower costs. Due to confidentiality reasons, only the topic of the interview and the job title of the expert can be given. As the interviews progressed, the interview topic and expert knowledge became more specific to a production phase.

Qualitative data analysis method

The answers to the interview questions were sorted and categorized. Because of the semi-structured interviews, sorting can be done in order of the interview questions [22]. Categorizing the answers is the process of extracting relevant passages and summarizing those into small phrases called 'codes'. The codes in this study relate to relevant parameters for cost modeling. The results of the categorization process of the interviews are given in appendix A and the summary is given in paragraph 3.2.

2.1.2. Deriving cost functions

Cost functions were derived via curve fitting if there is was data available for a production phase. The Levenberg-Marquardt Algorithm (LMA) curve fitting method from the Python package Scipy [23] was used. The quality of a curve fit depends on the input function and the scattering of the data. The input functions are discussed in this section. The acquired data sets are discussed in chapter 3.

Table 2.1: Overview of conducted interviews.

Date	Topic	Phase	Job title
12-10-2020	General cost modelling.	All	Quotation engineer
26-10-2020	Follow up on cost modelling.		Quotation engineer
10-11-2020	Optimizing for cost in the offshore tower design process.	-	Tower engineer
15-12-2020	Cost engineering for offshore towers	All	Cost engineer
05-01-2021	Cost engineering for offshore towers	All	Cost engineer
05-02-2021	Procurement of materials	Material	Plate procurer
09-02-2021	Pre-assembly costs	Assembly	Project manager
11-02-2021	Pre-assembly strategies and costs	Assembly	Commercial site manager
12-02-2021	Procurement of flanges	Material	Flange procurer
19-02-2021	Cost of welding	Manufacturing	Production procurer
23-02-2021	Follow-up on pre-assembly costs	Assembly	Commercial site manager
24-02-2021	Case study project costs	All	Project manager
26-02-2021	Transport of sections	Transport	Transport procurer
03-08-2021	Cost in the installation phase	Installation	Installation procurer

LMA curve fitting algorithm

The Levenbach-Marquardt algorithm was used to estimate the parameters of the input function [24], [25]. It minimizes the sum of squared errors through a combination of gradient descent and the Gauss-Newton method. In short, the gradient-based step update h_{gd} is found by a linearization of the gradient at p , shown in equation 2.1. The Gauss-Newton method converges faster for parameters near the optimal solution. The step update h_{gn} is found by a first-order Taylor series expansion, shown in equation 2.2. The LMA adapts the method of the step update through the damping parameter λ , as is shown in equation 2.3. A large damping parameter increases the effect of the gradient descent method, and for small values, the weight is shifted to the Gauss-Newton method. The damping parameter is chosen based on the change in the objective function. An improvement in the objective function means the algorithm is getting closer to the optimum. Thus the Gauss-Newton method becomes more effective. However, when the objective function decreases, λ is increased to emphasize the gradient descent method, which works better if the algorithm is far from the objective.

$$h_{gd} = \alpha J^T W (y - \hat{y}) \quad (2.1)$$

$$[J^T W J] h_{gn} = J^T W (y - \hat{y}) \quad (2.2)$$

$$[J^T W J + \lambda I] h_{lm} = J^T W (y - \hat{y}) \quad (2.3)$$

Input functions

The suit of input functions was developed for two scenarios. The first is for cost data which displays a step function; the second is for scattered data. The best curve fit was selected based on the R^2 score and a visual inspection of the researcher.

Polynomial functions

Polynomial functions of various degrees, described in equation 2.4 and shown in figure 2.1. With the parameters a_i , the polynomial can be fitted to data.

$$f(x) = \sum_{i=0}^{n=3} a_i x^i \quad (2.4)$$

Sigmoid activation function

The sigmoid activation function, shown in equation 2.5, can be used to model discrete steps. The shape parameters a is the start value, b is the step size in the y -direction, c is the steepness factor, and

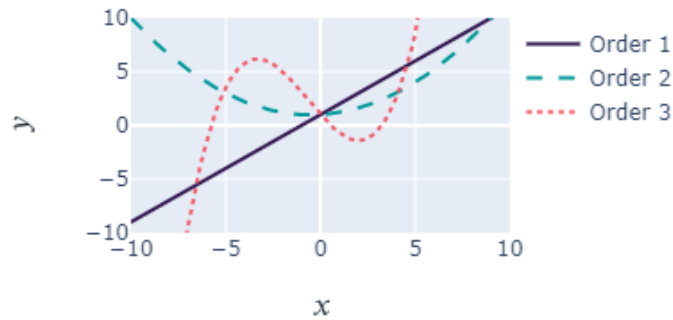


Figure 2.1: Example of polynomial functions up to order 3.

d is the shift in the x -direction. From figure 2.2 shows that with these four parameters, any single step function can be fitted.

$$f(x) = a + b * \frac{1}{1 + e^{-c(x-d)}} \quad (2.5)$$

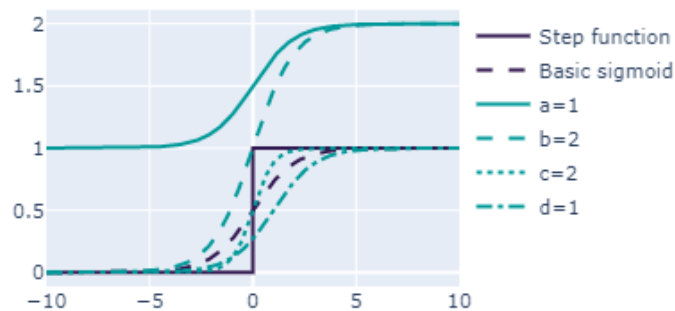


Figure 2.2: Effect of tuning parameters on a sigmoid function. Basic sigmoid base parameters are $a = 0$, $b = 1$, $c = 1$, $d = 0$.

Stacked sigmoid activation function

The curve fit can be done with a stacked sigmoid function for cost functions with several discrete steps. For a discrete cost function with n steps, n sigmoid functions can be summed up to reproduce the discrete function, as is shown in equation 2.6. Similar to the sigmoid function 2.5, the parameter a is the start value, b_i the step size in the y -direction, c_i the steepness factor, and d_i the x -value of the step. The steepness factor can be tuned for each step. A simplification is to take the same steepness factor in each step, of which the effect is shown in figure 2.3.

$$f(x) = a + \sum_{i=1}^n b_i * \frac{1}{1 + e^{-c_i(x-d_i)}} \quad (2.6)$$

2.2. Building a cost optimization model

The cost optimization model will be implemented in a tower design model. Most tower design models apply for one or several design drivers and have the objective to minimize mass Nekeman and Zaayer.

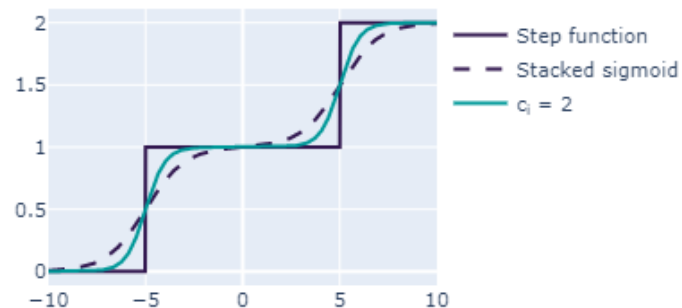


Figure 2.3: Effect of tuning parameters on stacked sigmoid function. Stacked sigmoid base parameters are $a=0$, $b_i=1$, $c_i = 1$, $d_1=-5$, $d_2=5$.

In this study, the focus is to research the effect of including production costs, thus developing a tower design model is not the main focus. Moreover, extending a proven model will add to the applicability of such a model in the industry tower design processes. First, a tower design method has to be selected. The choice was made to use the SGRE tower design software. Paragraph 2.2.1 explains the rationale behind the choice and software in detail. In an earlier literature study, it was found that tower design models optimize mass instead of costs [3]. Although little is known on the exact cost functions and relevant tower parameters, several cost optimization strategies were developed based on the tower design software, explained in paragraph 2.2.2. The best strategy is chosen in chapter 4 after the cost functions are known. Then, through a series of case studies, the effect of the cost optimization can be analyzed, which is explained in the final paragraph.

2.2.1. Tower design software

The choice was made to use the SGRE tower design software in the cost optimization model, based on the comparison of methods developed by academics and companies. The criteria and literature models found in an earlier literature study have been extended with models from industry [3], explained in the first paragraph. The second paragraph explains the SGRE tower design software.

Tower design models

The literature models were analyzed in an earlier study by Nekeman and Zaayer [3] and extended with an analysis of tower design tools from industry. In literature, costs are often estimated based on a curve fit on top-level tower parameters. In industry, it was found that actual production costs act on the component that is procured. The cost optimization model must estimate costs on a detailed level; thus, the tower design model must do so as well. The component design level of the model is the first comparison criterium. The second criterium is the optimization method. Gradient-descent methods cannot handle discrete cost functions, while genetic algorithms can. Thus, the optimization method determines if discrete step cost functions must be approximated with the approach described in section 2.1.2. Finally, the goal is to develop a cost optimization model that can directly be applied in industry. The tower design model must account for all design drivers or limit states, of which the most important are fatigue, natural frequency, and buckling, which is the final criterium. All criteria are summarized below, and the overview is given in table 2.2.

1. Design level of the software; which component is being optimized.
2. Applied optimization method.
3. Coverage of design drivers; most important are the limit states fatigue [1], natural frequency [2], and buckling [3].

The comparison in table 2.2 show the Yoshida [12] and SGRE [4] models cover all limit states and design the tower on a shell level. All other models are either too coarse to be used in practical tower design or do not account for all limit states.

Table 2.2: Overview of tower design methods for wind turbine towers

Author	Year	Research criteria		Limit states		
		Design level	Opt. method	1	2	3
Negm [7]	2000	Tower	Several	✓	✓	✓
Yoshida [12]	2000	Shells	GA	✓	✓	✓
Uys [8]	2007	Shells	Gradient-descent			✓
Karpat [13]	2015	Shells	PSO			✓
Lagaros [26]	2015	Shells	GA			✓
Maljaars [6]	2017	Sections	Gradient-descent	✓	✓	✓
O'leary [11]	2019	Sections	Gradient-descent		✓	✓
Ciccioni [20]	2020	Shells	Gradient-descent			✓
SGRE [4]	2021	Shells & flanges	Gradient-descent	✓	✓	✓
DNV-GL [27]	2021	?	?	✓	✓	✓
Bentley [28]	2021	?	?	✓	✓	✓

The choice was made to use SGRE tower design software because it also accounts for practical industry limitations, such as shell ovalization and maximum thickness transition. In fact, it is industry-grade tower design software, meaning the resulting tower design is close to IEC certification level. Another benefit of this software package usage is that it is used in industry, meaning a cost optimization model build has a larger chance to be implemented in the industry and lower the cost of wind energy. Finally, SGRE is the industry partner in this research and can provide the necessary support for software issues.

A drawback is that the SGRE software is a proprietary technology which may limit the applicability of the cost optimization model in other industry tower design routines.

Selected tower design model

The SGRE tower design software uses a fixed tower outer geometry and calculates the minimum shell thicknesses to satisfy the limit states. The process is shown in figure 2.4. The fixed outer geometry and initial thickness distribution are given to the optimization loop. First, the tower mass m_i is calculated which is followed with the structural integrity checks, covering the most important load cases and limit states in [5] and [2]. If a limit state is exceeded, the shell thicknesses are adjusted, and the loop starts over. If none of the limit states are exceeded, the new tower mass m_i is compared against the former mass m_{i-1} and if it has converged within the tolerance ϵ , the loop is finished. If the tower mass has not converged, the loop starts over.

The software employs a gradient-descent algorithm to find the minimum tower mass. Several strategies can be developed to minimize the tower cost with cost functions found in the cost model research. The best method depends on the found cost relations and their relevant tower parameters.

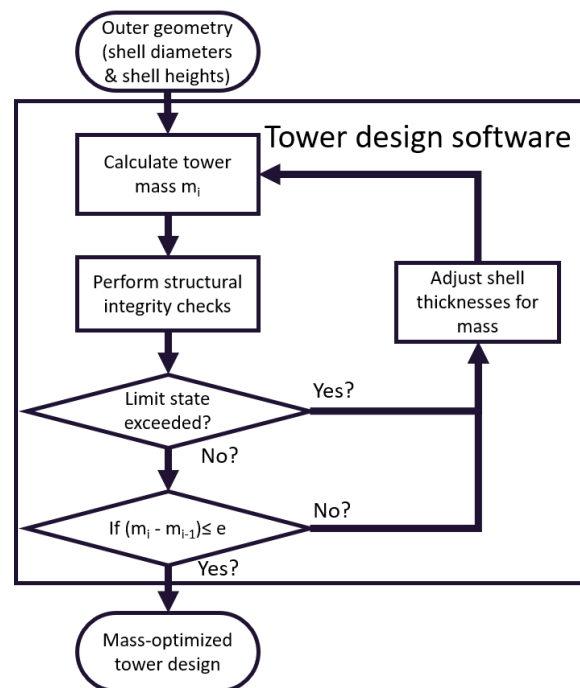


Figure 2.4: Flow diagram of tower design software.

2.2.2. Conceptual cost optimization models

Two conceptual cost optimization models are explored in this section. The first option is a change in the selected tower design software where the objective is switched from minimum mass to minimum cost. The second option is to develop a separate cost optimization model and use the tower design software as a black box. In each model, the steps where changes are applied are shown in green blocks. Purple blocks are part of the current tower design process. The best optimization model is chosen in section 4.1 based on the cost functions found in the cost model in chapter 3.

Implement in tower design software

The first option is to change the objective in the tower design software from mass to cost, shown in figure 2.5. This requires changes in three steps, shown in the green blocks, and the changes are made bold. First, the tower cost must be calculated instead of tower mass. The second change is in the convergence criteria, and finally, the shell thickness must be adjusted for costs. The result is a cost-optimized design. This approach has the following benefits:

- If implemented successfully, it will directly decrease the cost of towers build in industry.
- Optimization algorithm is already built and validated. No need to develop and test a new algorithm.

However, this approach also has the following disadvantages:

- Optimization is limited to use the shell thickness as design variables.
- No freedom to choose optimization algorithm. If the cost functions have many local minima, the current algorithm will not be able to find the global optimum at all times.
- Implementation is specific to this software architecture. Therefore, applicability to other research and companies may be limited.

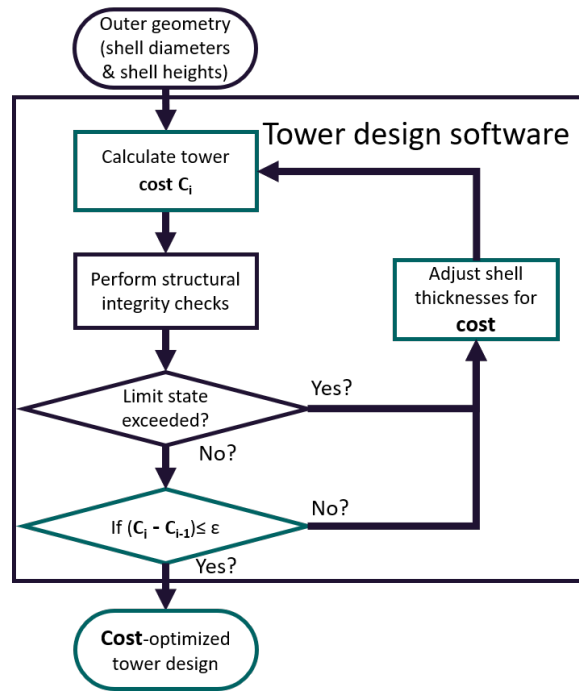


Figure 2.5: Changing objective from mass to cost

Separate cost optimization model

The second option is to develop a cost optimization separately from the tower design software. The result is the tower design loop, shown in figure 2.6. The tower design software is used a black-box and a cost calculation step and cost optimization model are added. The loop is converged if the difference in tower cost between two subsequent loops, $C_i - C_{i-1}$, is within the tolerance ϵ , and the COD is similar to the Structural Integrity Design (SID). This approach has several advantages:

- Freedom to choose cost estimation and optimization methodology. Several techniques can be applied.
- Can choose design variables such that all cost functions are included.
- Universal methodology; can be applied to any tower design software.

However, the approach can also cause the following problems:

- No convergence between tower design software and cost optimization routine because of the black-box approach.
- Many local minima because of additional cost functions.
- Cost optimization model results may be unreliable because the structural integrity is not maintained that model.

2.3. Case study explanation

The case studies help to study the cost optimization model and answer research objective 4. In these studies, a tower from a currently developed wind farm project of the industry partner is used for this purpose. The effect production costs have on tower design is studied by running the cost optimization model in three scenarios, a high manufacturing cost, a low manufacturing cost, and a high material cost scenario. The first three case studies evaluate one scenario each. In a fourth case study, the optimum number of shells per section is studied for each scenario. The summary of case studies is given below.

1. High manufacturing cost scenario, regular material costs.

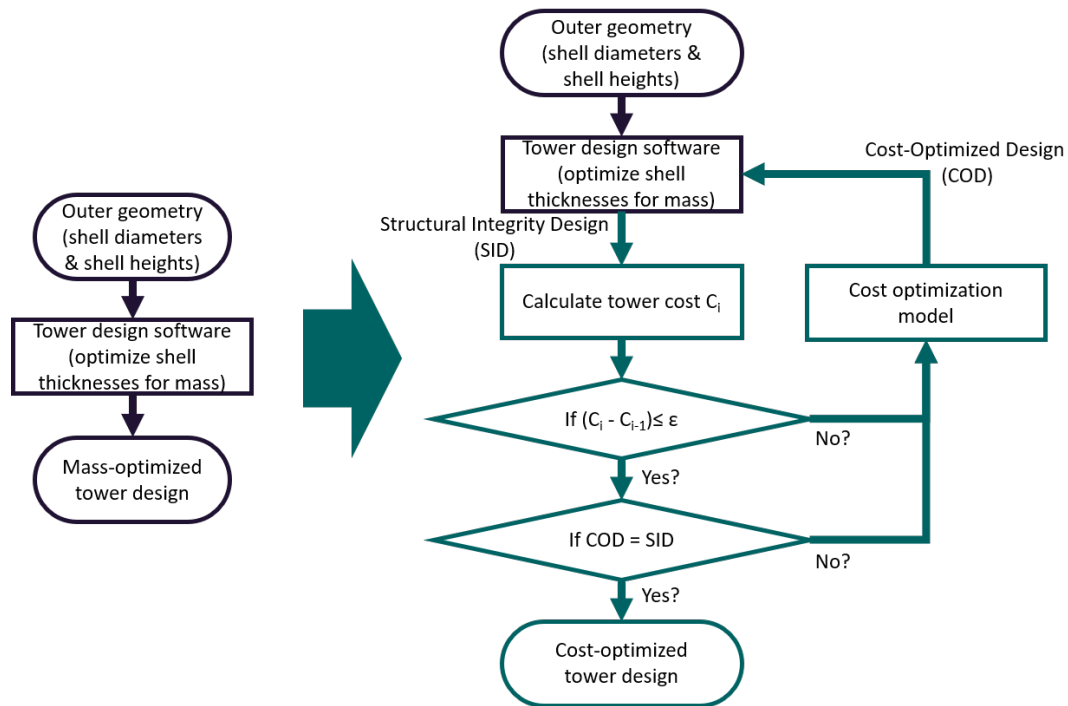


Figure 2.6: Optimization process for a separate tower design and cost optimization algorithm.

2. Low manufacturing cost scenario, regular material costs.
3. High material cost scenario, low manufacturing costs.
4. Optimum number of shells for scenarios 1, 2, and 3.

3

A cost model for offshore wind turbine towers

The cost model was build based on the knowledge from industry experts and curve fitting. The general concept is to follow the flow of material over the course of the tower production, further explained in section 3.1. The results from the industry interviews, summarized in section 3.2, show which parameters contribute most to the phase costs. Moreover, whether it is feasible to build a quantitative cost function based on tower parameters. This is important because non-tower parameters are difficult to include in an optimization routine. This is followed by an explanation of each phase of production, from material cost to the offshore tower installation, in sections 3.3 to 3.8. Every section starts with an explanation of the phase, followed by the phase cost model and if applicable the quantitative cost functions.

3.1. Cost model structure

The cost model follows the materials and parts over its entire production process. It starts at the raw material procurement and ends at the installation of the wind farm. The focus is on cost drivers that are affected by tower parameters. First, the concept is further explained in section 3.1.1. This is followed by a cost breakdown of the entire production process.

3.1.1. Cost model concept

The concept behind this cost model is to estimate costs in each production phase on the relevant component level, as is shown in figure 3.1. This means that the actual procurement materials, material transport, manufacturing, assembly, and installation are modeled process-wise. It covers all phases from material selection up to installation, after which the wind farm is commissioned. The operation & maintenance and decommissioning phase are not covered in this model, because these phases are covered by Operation Expenditure (OPEX), which is a different field of research.

What can be derived from figure 3.1, is that the material, material transport and manufacturing can be modeled on a shell level. The section transport and assembly deal with tower sections and thus require a cost model on that level. Finally, in the installation phase fully or partly assembled towers are installed at sea. This means cost should be modelled on that level.

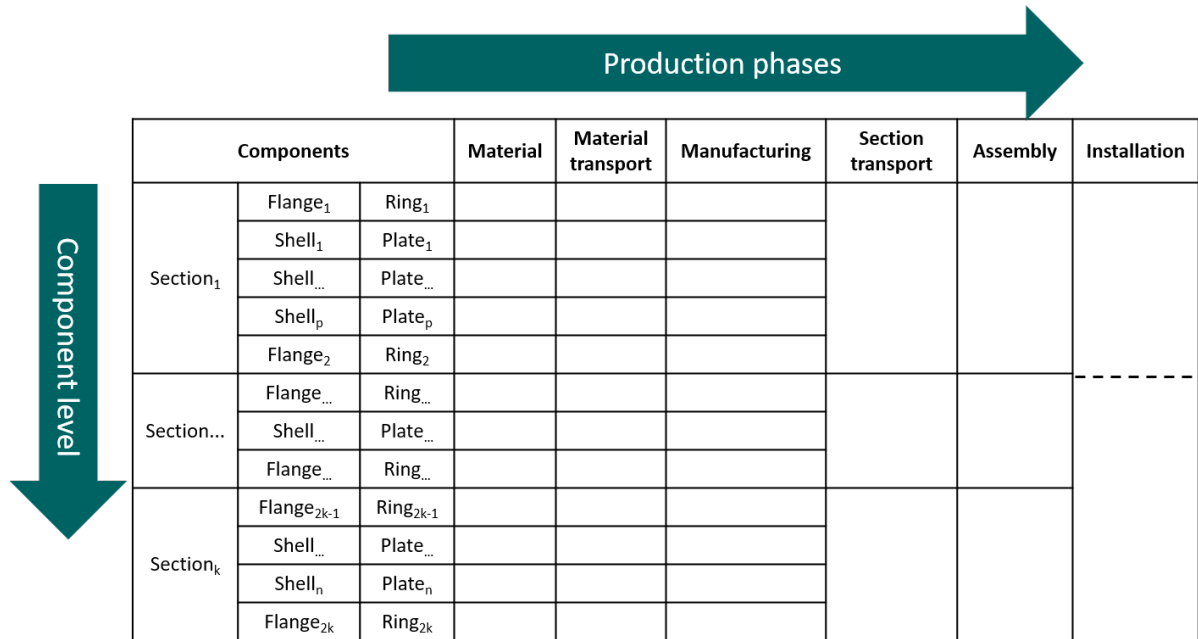


Figure 3.1: Schematic representation of the cost model.

3.1.2. CAPEX cost breakdown

The cost of all CAPEX phases is not distributed evenly, as can be seen in the indicative cost breakdown in figure 3.2. Material cost has the largest share of CAPEX. Manufacturing, section transport, and installation each have a one-sixths share. The smallest cost contributors are the material transport and assembly phase.

The most important cost driver for material costs is tower mass, which explains the industry’s focus to minimize mass. Unfortunately, it only covers 45% of CAPEX, which means the other 55% is not accounted for in the tower design process. Including all phases in a cost optimization routine may result in new tower designs.

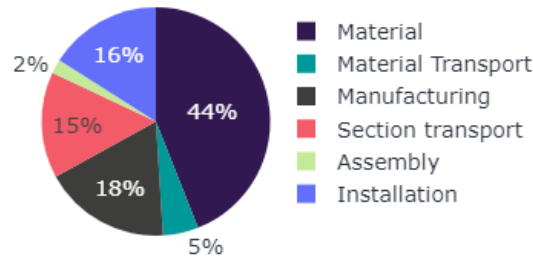


Figure 3.2: Indicative CAPEX cost breakdown [3].

A problem is that in reality, the relative shares of each phase vary per supply chain used. Figures 3.3a and 3.3b show the cost breakdown of two supply chains, from material to section transport phase, for the same tower. CAPEX was roughly the same for both. The section transport costs more than tripled in supply chain 2, while the material, material transport, and manufacturing cost declined. The implication of these figures is that in supply chain 1, the minimizing of steel mass has a larger effect on CAPEX than in supply chain 2. In supply chain 2, it is more beneficial to minimize costs in the section transport phase.

The main reason for the different cost breakdowns is the global locations of suppliers and manufacturers. Material and manufacturing costs in Asia-Pacific region are lower than in Europe. However if the project is in New York, the transport the manufactured sections becomes a costly exercise, as is shown in figure 3.3b. Because the relative cost shares vary, tower manufacturers may need to design the tower for a specific supply chain.

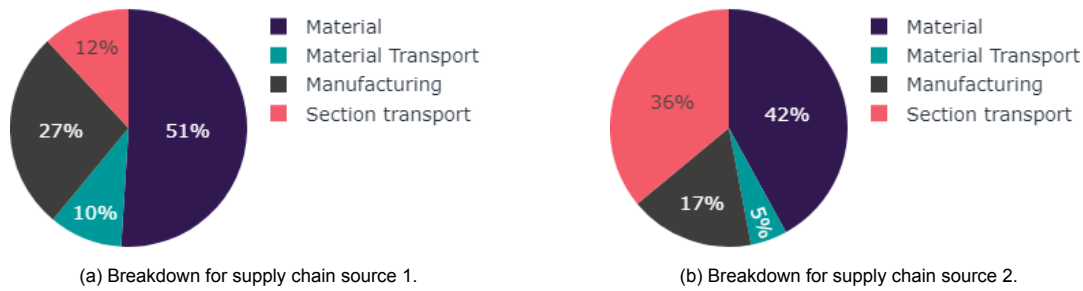


Figure 3.3: Tower cost breakdowns for the same tower design with two different supply chains.

3.2. Interview results

The main results of the industry interviews are summarized in table 3.1. The results are categorized per phase, and the main cost components are shown. The relevant parameters for costs in each phase are categorized as a tower design parameter if the parameter can be influenced in the tower design phase or a non-tower design parameter if external factors predominantly influence the parameter. The industry experts also commented on the feasibility of building a quantitative cost model for tower design.

3.2.1. Interview results for the cost model

Reasons for quantitative modeling of the material procurement, material transport, and manufacturing phase

What can be derived is that a quantitative cost model for the design of offshore wind turbine towers is only feasible for the material, material transport, and manufacturing phase. The reason is that the most important relevant tower design parameters are known at the time of design in these phases. At the same time, from the section transport onwards, costs depend mainly on external parameters or decisions taken at a later stage of wind farm development. In the material phase, the two non-tower design parameters are non-destructive testing and commodity material price, which are both quantifiable.

Reasons for excluding the section transport, assembly, and installation phase

The two main factors why the section transport, assembly, installation phase are too difficult to model quantitatively are the complexity of estimating vessel stow and determining the installation strategy.

The first is the complexity of estimating the vessel stow. Vessel stow is the number of sections that fit in one transport ship. Determining this parameter is a manual process done for each transport ship. Which transport ships are used depends mainly on the availability at the time of installation and is often not known at the time of tower design. Moreover, a small section length or diameter deviation can affect the number of sections that fit in the cargo hold. Finally, market conditions on the transport vessel have a large influence on the costs in this phase. Given these three influences, it was concluded that a reliable quantitative cost model is extremely complicated to build.

The other significant influence is the installation strategy. In most wind farm projects, the strategy is to build the wind farm in the shortest time frame possible. The cost in this phase largely depends on the installation vessel rent. An important factor in the choice of vessels is the maximum lifting capacity and lifting height of a vessel. The tower is the heaviest component of the turbine; thus, the tower mass and tower height are important decision parameters. The complicating parameters are the availability of vessels, round-trip time of a vessel, weather conditions, turbines storage capacity, and the number of installation vessels to be used. Moreover, the tower mass and height do not have to limit the vessel choice because the lifting crane can be adjusted to the tower specifications. However, the adjustments incur additional costs, which are unknown at the time of tower design.

The final complicating factor is the interdependent influence of the parameters. The installation strategy determines the required inflow of turbine components. The inflow of components influences the number of transport vessels to be used. Also, the uncertainty in weather conditions influences the buffer for the tower. This is a risk decision an installation procurer has to make. Given these interdependent phase effects, it is hard to build a quantitative model for the last three phases.

Table 3.1: Summary of interview results.
* Only applies to conical shells.

Phase	Feasible	Main cost components	Tower parameters	Non-tower parameters
Material	✓	Plates	Shell diameters, height, thickness, steel grade	Testing, commodity prices, supplier
		Flanges	Shell diameters, steel grade	Testing, commodity prices, supplier
		Internal structure	-	commodity prices, supplier
Material transport	✓	Plate transport	Shell diameters, mass	supplier-manufacturer combination
		Flange transport	Shell diameters, mass	supplier-manufacturer combination
Manufacturing	✓	Cutting*	Shell diameters, height, thickness	Manufacturer
		Beveling	Shell diameters, height, thickness, bevel-shape	Manufacturer
		Rolling	Shell diameters, thickness	Manufacturer
		Welding	Shell diameters, height, thickness, weld-type	Manufacturer
		Painting	Tower area	Manufacturer
Section transport	✗	Vessel	Section diameters, height, mass, number of sections	Vessel stow, manufacturer location, assembly port, installation / assembly strategy
Assembly	✗	Crane	Tower mass, height, number of sections	Installation / assembly strategy
		Land-lease	Buffer zone size	Installation strategy
Installation	✗	Installation vessel	Tower mass, height	Installation / assembly strategy, weather conditions, turbine storage capacity, number of vessels, crane adjustments

3.2.2. Acquired data sets

The quantitative cost functions in this cost model are build with the acquired cost data through the industry interviews. The data consisted of a 6 cost functions for the material procurement phase, 8 cost functions for the material transport phase, and 133 data points for the manufacturing phase. The data was filtered to make a reliable fit. The criteria was a minimum of 15 data points for one manufacturer with an even spread.

Table 3.2: Cost data summary.

	Number of data points
Total data set	133
Material phase	
Plates	6 (cost functions)
Flanges	-
Transport phase	
Plate transport	8 (cost functions)
Manufacturing phase	
Cutting - Weveling	100
Bending - Welding	105
Surface treatment	102
Paint	79

3.3. Material Procurement

3.3.1. Phase explanation

In this phase, the raw plates, flanges, and material for the internal structure are procured. The plates and flanges alone can account for 70% of the material cost. The internal structure, consisting of ladders, platforms, electrical systems, and attachments, accounts for 30% of phase costs. The biggest cost component is the steel plates, although industry sources say that as the tower increases in bottom diameter, the share of the flanges can increase up to 30% of the material costs [29].

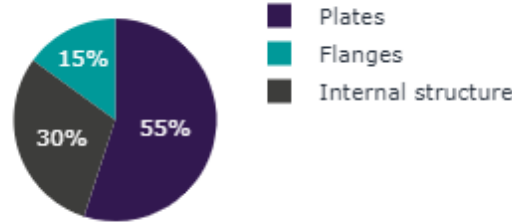


Figure 3.4: Indicative material cost breakdown.

3.3.2. Material cost model

The material cost model aims to improve the current best practice in material cost estimation by calculating the cost on component level. The best practice in industry [4] and literature [15], [9], [17] uses a mass cost factor c_m (\$/kg) multiplied with the tower shell mass m_{tower} , shown in equation 3.1. In the proposed material cost formula, shown in equation 3.2, the distinction is made between the cost factor of a steel plate $c_{m,plate_i}$ and flanges $c_{m,flange_i}$. Moreover, the cost factors are not assumed to be constant. Another difference is that the mass of the plates is used instead of the shell. More explanation is the paragraph on plate costs. The cost of the internal structure $C_{internal}$ is calculated as the cost of all internal components. Although covering 30% of material costs, no in-depth analysis was done because the internals is not part of the primary structure.

$$\text{Best practice: } C_{mat} = c_m m_{tower} \quad (3.1)$$

$$\text{Proposed: } C_{mat} = \sum_{i=1}^n c_{m,plate_i} m_{plate_i} + \sum_{i=1}^{2k} c_{m,flange_i} m_{flange_i} + C_{internal} \quad (3.2)$$

The difference between the shell mass and plate mass for conical sections in the baseline design in paragraph 4.5.2 is 4.7%. A conical shell is made from a semiring cut out of a rectangular plate in the manufacturing phase. Calculating the height h_{plate} and length l_{plate} of the rectangle which fits around the semiring is given in equation 3.3 and 3.4 respectively. In this equation, θ is the angle of the semiring, l the outer radius, and h' the hypotenuse of the shell. The full trigonometric derivation of these formulas is given in appendix B. It shows that the plate mass can be up to 90% higher for shells with a steep cone and small height.

$$h_{plate} = l(1 - \cos \theta) + h' \cos \theta \quad (3.3)$$

$$l_{plate} = 2l \sin \theta \quad (3.4)$$

The supplier's location is an influential factor in the material cost because of local labor rates, steel prices, and regulations. Thus in all following paragraphs, the effect of supplier location is studied.

Plate costs

Figure 3.5 shows all factors that influence the plate costs. All elements are cost factors, meaning that they are calculated as a price per unit mass (\$/kg). Thus, the plate costs are split into plate mass and the cost factor. Equation 3.5 shows the plate cost factor function, which consists of commodity materials (iron ore, scrap metal, energy) c_{base} , manufacturing cost c_{man_i} , CO2 emissions tax c_{CO_2} and

price increases for higher quality steel grades c_{grade} . Each element has explained in its own dedicated paragraph.

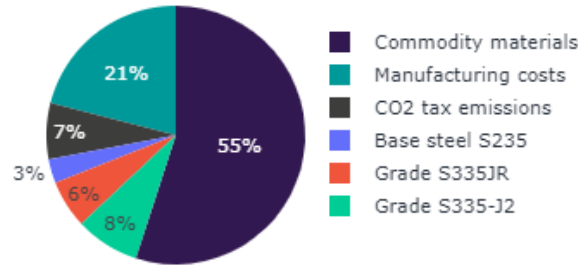


Figure 3.5: Indicative plate cost breakdown.

$$c_{m,plate_i} = c_{base}(t) + c_{man_i}(l_i, w_i, t_i) + c_{CO2}(t) + c_{grade}(grade_i) \quad (3.5)$$

Commodity Materials

The price of commodity materials consists of iron ore, scrap metal, energy use, heat, and several other factors. These factors fluctuate over time t and per continent, according to the material procurer [29]. The steel price fluctuations shown in figure 3.6, confirm these statements. For the past five years, steel prices have fluctuated between [600-1000]USD. However, in July 2021, the steel price increased to 1825USD/tonne [30], which is a 300% increase from July 2020. These fluctuations can affect the tower cost tremendously, and it is useful to design for such a scenario. The prices also depend on the continent, but the deviations are a magnitude smaller (20-30%) than the time dependency.



Figure 3.6: Price of hot rolled steel plates over time per continent. [31], [32], [33].

Manufacturing costs

Through the interview with the material procurer, it was found that suppliers' manufacturing cost of a plate depends on the plate height h_{plate} , length l_{plate} , and thickness t_{plate} , shown in equation 3.6. Reasons for this dependency are that the supplier's equipment limitations or it affects the production speed of the machinery [29]. Cost data shown in figure 3.7 was acquired from the procurer. It can be derived that each supplier has its own set of step cost functions with respect to plate height, length, and thickness. These prices are fixed, but for confidentiality reasons, they are normalized with the supplier's base price at that time. In extreme cases, the manufacturing cost can amount to $0.22 \cdot c_{base}$, which is a large amount that is ignored in the current best practice.

$$c_{man_i} = c_h(h_{plate_i}) + c_l(l_{plate_i}) + c_t(t_{plate_i}) \quad (3.6)$$

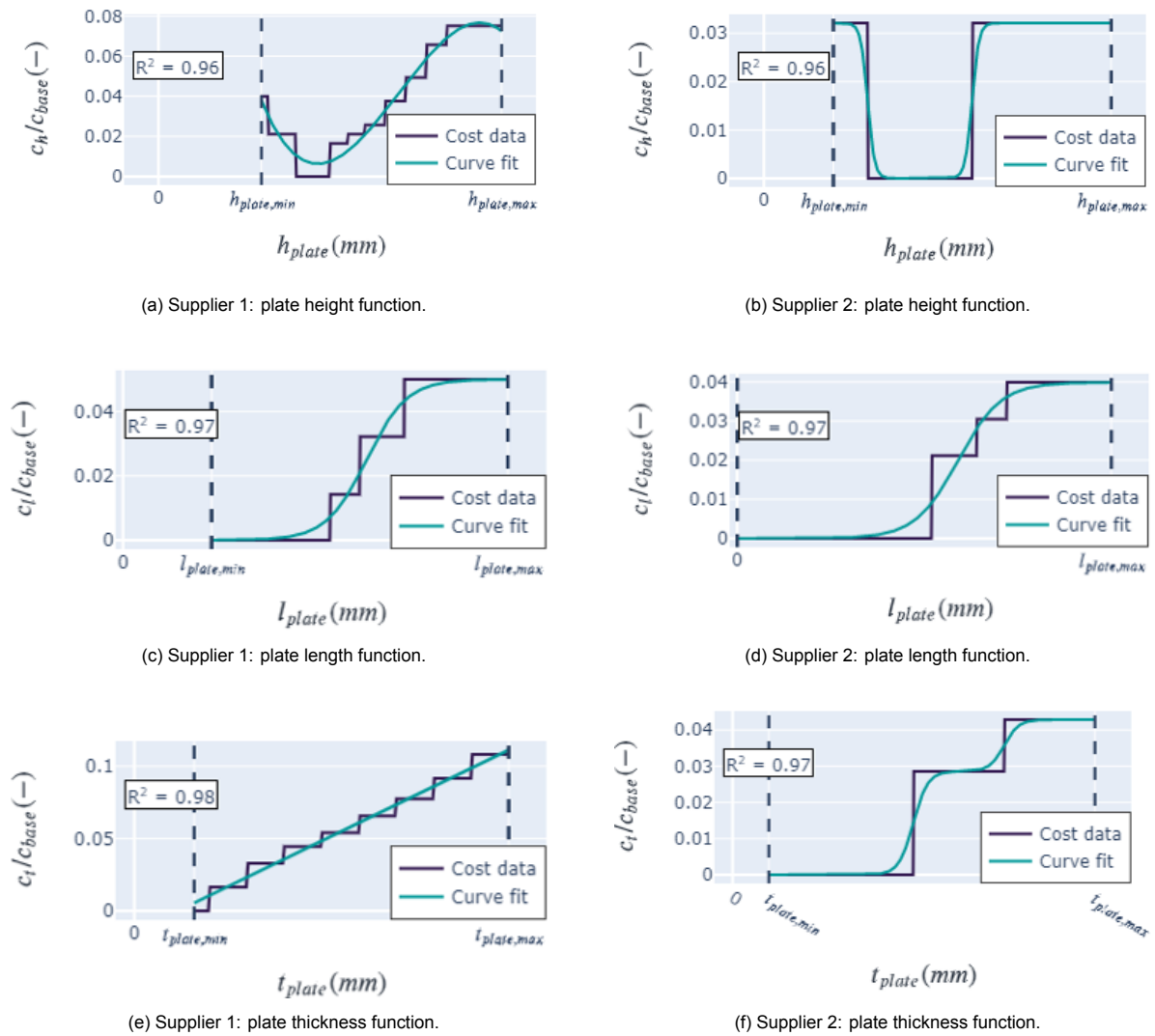


Figure 3.7: Cost data and functions with respects to plate height, length and thickness. All data is normalized with the respective suppliers' base price c_{base} .

CO₂ emissions tax

CO₂ tax emissions are charged as a price per tonne CO₂. The price fluctuates over time and is only applied in Europe according to the material procurer [29]. The carbon price data in figure 3.8 shows the fluctuation over time. Moreover, it is increasing rapidly in Europe due to the yearly reduction of carbon emissions rights in the European Trading System [30], so further increases can be expected. The CO₂ price must be converted to a price per tonnage of steel, taking into account that the carbon intensity of production also varies per country, ranging from 1086 kg CO₂/tonne in Europe to 2148 kg CO₂/tonne in China [34]. Moreover, the carbon emissions tax is not limited to Europe. There are 63 emission tax systems in effect, spread across all continents as of August 2021 [35]. Moreover, 22 are currently under development. It is likely that some form of emissions tax will be applied in each country, making it an increasingly important factor in the material cost.

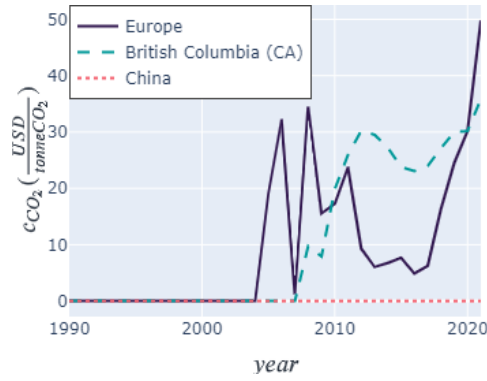


Figure 3.8: CO₂ prices over time for Europe, British Columbia (CA), and China.

Steel grade costs

Finally, the steel grade can increase the price of steel. Higher quality steel requires a more intensive production process, which inflicts higher costs [29]. The cost data in figure 3.9a and 3.9b confirms the steel price increase for higher qualities. Higher material strength requires less material mass to be used. However, in the offshore tower industry, S355J2 is the most common steel grade [4].

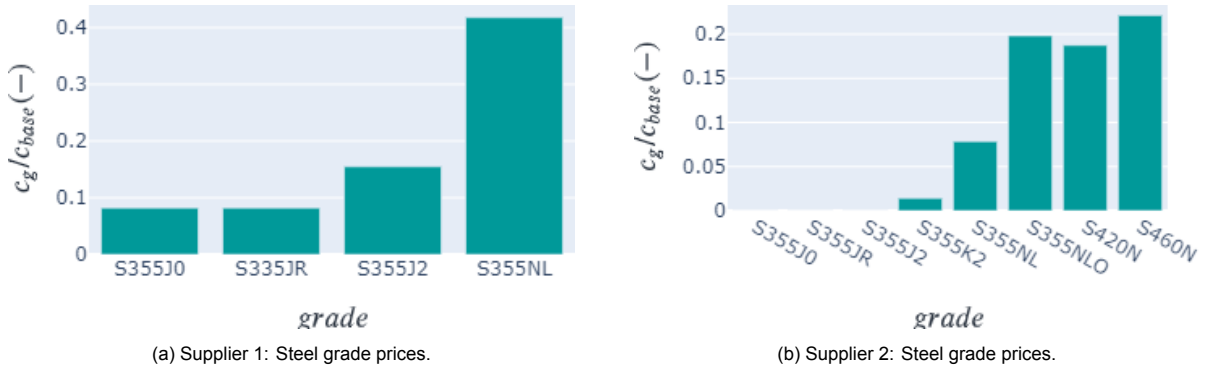


Figure 3.9: Cost data for steel grade qualities. All data is normalized with the respective suppliers' base price c_{base} .

Flanges

Flanges are made from steel rings that are forged and machined to their final shape. Because flanges are forged instead of hot-rolled, they bear a higher cost per unit mass. From the interviews, the main cost driver for the flange cost factor is the diameter which results in the following function

$$c_{m,flange_i} = c_{flange}(d_i)m_{flange_i}$$

where c_{flange} is the flange cost factor and d_i the flange diameter. Unfortunately, this could not be confirmed by cost data.

Internal structure

The internal structure of a tower consists of several components. The cost is dependent on the tower height, diameters, and the configuration determined by engineers. The internal structure provides a complete overview of the cost model components. However, it is not elaborated on because it is not part of the primary structure.

3.4. Material transport

3.4.1. Phase explanation

In this phase, the plates and flanges are transported from the supplier to the manufacturer over sea. The process starts at the supplier, where the raw material is loaded onto the transport vessel. This requires the appropriate loading equipment. In sea transport, there are no limitations regarding the size of the cargo. On arrival at the manufacturer, the material is unloaded and stored for further processing. Here, the manufacturer must again have the appropriate equipment to handle the components [36].

3.4.2. Transport cost model

The best practice in literature is the material transport cost model from Irawan, Akbari, Jones, *et al.* [18]. It applies a fixed cost for the plates and flanges between supplier i and manufacturing j , shown in equation 3.7 and graphically in figure 3.10. The interview with the transport procurer has shown that this model is too simplified to represent reality [36]. The first modification is to split the cost factor in a price for plate transport and a price for flange transport. The second modification is to replace the fixed transport price with a cost function depends on the component parameters. The final modification is to change the unit N_{ij} for the mass of the component. The result is shown in equation 3.8

$$\text{Irawan: } C_{trans} = w_{ij}N_{ij} \quad (3.7)$$

$$\text{Proposed: } C_{trans} = \sum_{i=1}^n c_{transplate,i} m_{plate,i} + \sum_{i=1}^{2k} c_{transflange,i} m_{flange,i} \quad (3.8)$$

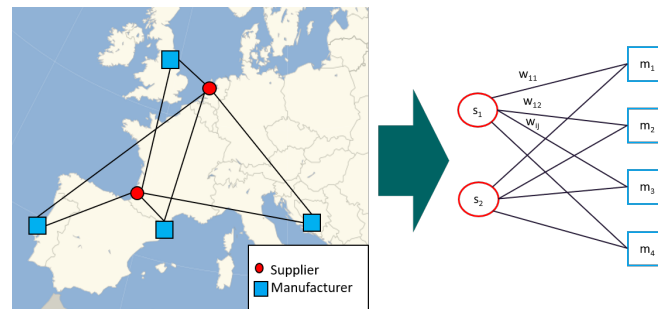


Figure 3.10: Supplier-Manufacturer network.

Plate transport

The transport cost factor $c_{transplate,i}$ depends on the plate length. The reason is that plates of a certain length do not fit in the cargo hold of the low-cost transport ships, and a larger vessel has to be rented, which inflicts an additional cost. The transport cost factor data of supplier 1 to any manufacturers show the stepwise increase at a certain plate length. However, the cost data from supplier 2 does show a constant cost factor. Another observation is that the transport cost from supplier 1 is three to four times higher than supplier 2. In case the tradeoff is between decreasing mass or decreasing manufacturing costs, it would be more beneficial to decrease mass in supplier 1.

$$c_{transplate,i} = c_{transplate}(l_i) \quad (3.9)$$

Flange transport

The flange cost factor $c_{transflange,i}$ can be modelled with the flange diameter $d_{flange,i}$, shown in equation 3.10. It is assumed that the cost functions vary for each supplier - manufacturer combination. Unfortunately, no data was acquired on the flange transport cost. Therefore, the validation could not be done.

$$c_{transflange,i} = c_{transflange,i}(d_{flange}) \quad (3.10)$$

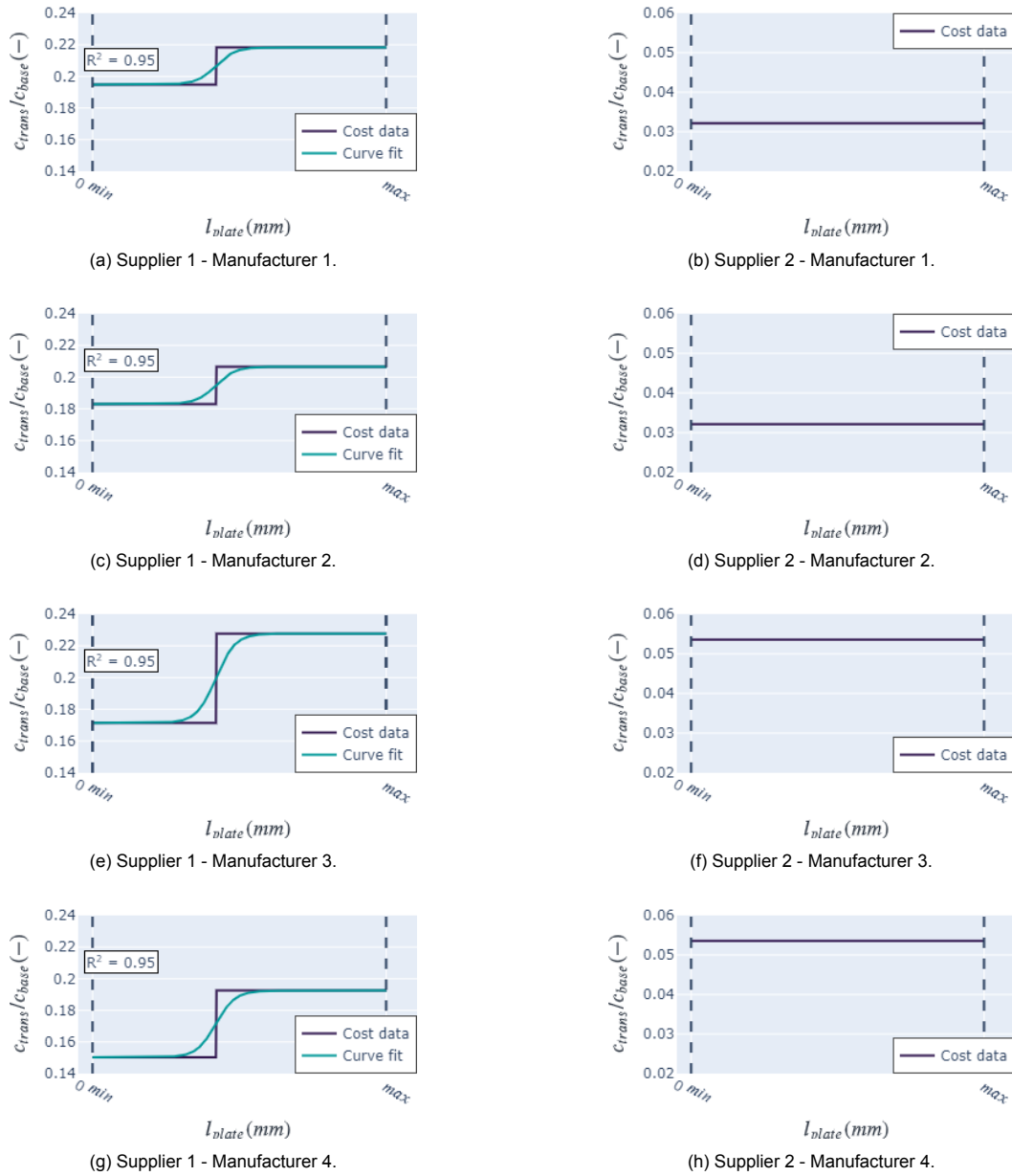


Figure 3.11: Material transport cost data and functions with respect to plate length. All data is normalized with the respective suppliers' base price c_{base} .

3.5. Manufacturing

3.5.1. Phase explanation

The plates and flanges are converted into sections in the manufacturing phase. The manufacturing process, shown in figure 3.12, consists of five main steps cutting, beveling, rolling, welding, and painting. The rectangular steel plates and forged flanges arrive at a manufacturer. If the plates are for a conical shell, a banana-shaped cut-out is made. For a cylindrical shell, this step is not necessary. The next step is preparing the edges of the plate for the welding step, called beveling. The flat plates are then bent to a cylinder or semi-cone with heavy-duty bending equipment. A longitudinal weld binds the bent plate into a shell. Next, the shells are hoisted onto a holding beam, where circumferential welds join the shells to create a section. At the two ends of the section, flanges are welded, and the primary structure of the section is finished. The final step is to paint the section on the inside and outside to prevent corrosion and make it blend in more with its environment. The internal structure (power cables, platforms, ladders, etc.) is built in the section after the painting process.



Figure 3.12: The five main actions in the manufacturing phase.
*Only applies to conical shells.

Figure 3.13 shows the cost breakdown manufacturing process. The data for the cutting and beveling phase and bending and welding phase thus, only statements about the groups can be made. Nevertheless, the figure shows that the Bending & welding costs dominate the manufacturing process. The manufacturing materials are used in all steps of the process, thus can be spread evenly. The construction of the primary structure, all steps of figure 3.12 together, contribute to roughly 75% of manufacturing cost.

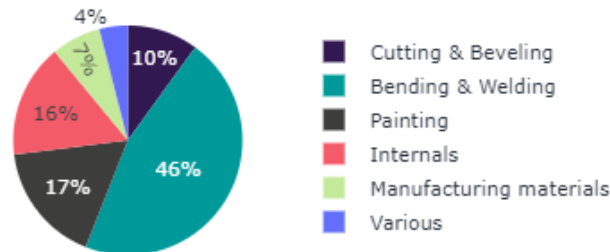


Figure 3.13: Indicative manufacturing cost breakdown.

Similar to the material procurement phase, the cost structure is different for each manufacturer due to local labor rates, cost of equipment, or manufacturer markup. In addition to different cost structures, there are also market conditions that affect the price. For example, when there is little production capacity in the market, the manufacturer markup will increase [37]. Moreover, each manufacturer has its limitations due to its equipment. The result is a manufacturer can have a monopoly on the production of towers of certain dimensions. This influences the price quoted to wind turbine companies.

3.5.2. Manufacturing cost model

The Farkas and Jármai manufacturing cost model [9], shown in equation 3.11, is the best practice in literature. It considers the bending cost $C_{bend,i}$, longitudinal welding cost $C_{weld-long,i}$, circumferential welding cost $C_{weld-circ,i}$ as a function of shell parameters, and painting cost as a function of tower area inside and outside. Muskulus and Schafhirt has questioned whether this cost model applies to industrial tower design. This model was analyzed through industry interviews and the acquired data and assessed whether it applies to industrial tower design.

The improved model includes functions for all steps from figure 3.12. The acquired data had grouped the cutting and beveling step and the bending and welding step, which results in three cost functions. Each cost function is explained separately.

$$\text{Farkas: } C_{man} = \sum_{i=1}^n (C_{bend_i} + C_{weld-long_i} + C_{weld-circ_i}) + C_{paint} \quad (3.11)$$

$$\text{Proposed: } C_{man} = \sum_{i=1}^n (C_{bevel_i} + C_{weld_i} + C_{paint}) \quad (3.12)$$

Cutting & Beveling

The cost for cutting and beveling is not considered in literature [3]. The dominant cost element in this step is the beveling cost C_{bevel} [37]. For every weld, the edge has to be beveled. Thus the logical cost driver would be weld volume V_{weld} . Figure 3.14, shows the cutting and beveling costs plotted against the weld volume. The linear curve fits explain close to all variance in the data because $R^2 > 0.95$, implying that the weld volume is a reliable estimator for beveling cost.

Another observation is that the curve fits both nearly cross the origin (0, 0). This implies that manufacturers do not charge startup costs for manufacturing a tower.

Finally, figure 3.14 shows that the manufacturers use a different beveling cost factor c_{bevel} . This shows that the choice of manufacturer influences the beveling cost and should be taken into account in the tower design phase.

$$C_{bevel_i} = c_{bevel} \cdot V_{weld_i} \quad (3.13)$$

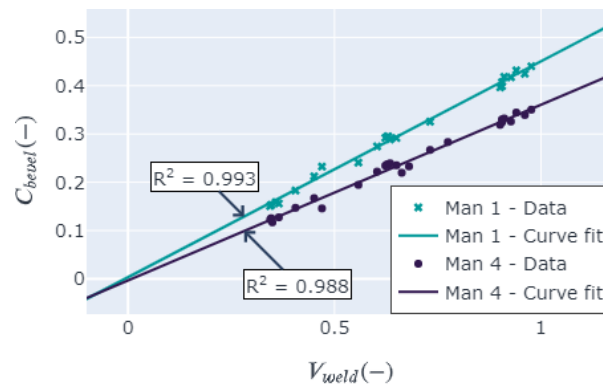


Figure 3.14: Cutting & beveling cost curve fits.

Rolling & welding

The industry interviews have shown that the main cost driver in the welding cost is the weld volume [37]. The curve fits from figure 3.15 show that most of the variance can be captured by fitting a linear function $R > 0.9$. This means that weld volume can also be used as an estimator for weld cost.

Another observation is the welding cost factor c_{weld} for manufacturing 1 is 50% higher than manufacturer 4 uses. Designing a tower for manufacturer 1 may involve fewer welds and fewer plates per section, than when designing a tower for manufacturer 4. It shows that a tower design can depend on the manufacturer that is being used.

$$C_{weld_i} = c_{weld} \cdot V_{weld} + \text{constant} \quad (3.14)$$

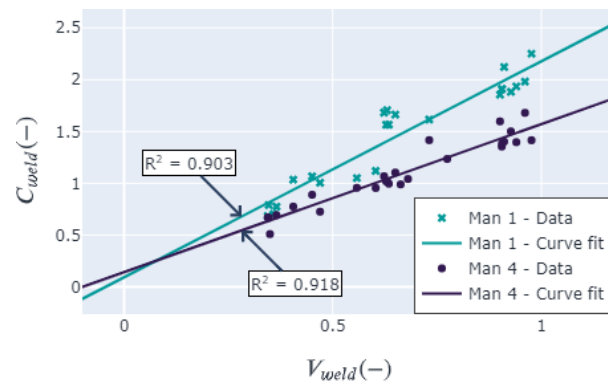


Figure 3.15: Rolling & welding cost curve fits.

Painting

The cost of the painting was modeled in literature with a cost factor c_{paint} and the area A , as is shown in equation 3.15. This was also confirmed in the interviews [37]. From the curve fit in figure 3.16, it can be seen that a linear function provides a good fit $R^2 > 0.8$. This confirms the painting cost function.

Another observation is the different rates the manufacturer applies. Manufacturer 4 charges a higher price than manufacturer 1. This proves again that the supply chain can influence the tower design.

$$C_{paint} = c_{paint}A \quad (3.15)$$

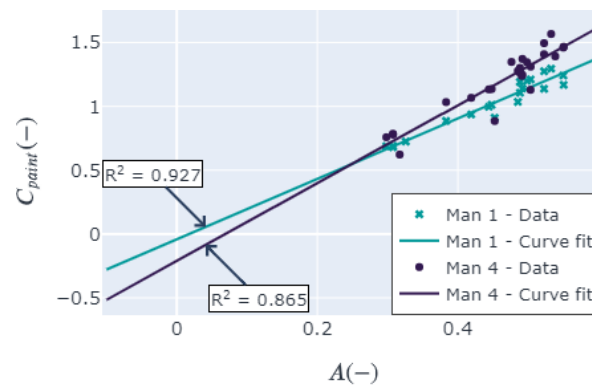


Figure 3.16: Painting cost curve fits.

3.6. Section transport

3.6.1. Phase explanation

The section transport of offshore towers is done via ships. The process is as follows. First, at the manufacturing site, the sections are lifted onto the brackets in the ship. Often, these brackets are custom-made for a tower. The lifting can be done with the crane on the vessel or a rented crane on land. The chosen method depends on the lifting capacity and maximum lifting height of the onboard crane. If the section supersedes these constraints, a separate crane has to be rented, which incurs an additional cost. When the sections are loaded, the ship sails to the landing site. At the landing site, the sections are offloaded with either the onboard crane or a rented crane because for the same reasons as with the on loading. The sections are transported to a storage area, where they are waiting to be assembled for installation. An overview of the transport process is given in figure 3.17.



Figure 3.17: Section transportation process from manufacturer to landing site.

The vessel rental is the largest share in the transport costs [36]. This is due to the high vessel day rate and the number of vessels that are necessary for transport to meet the turbine installation speed. In an offshore wind farm project, the installation is most expensive. Therefore, the installation speed dictates the flow of incoming towers to the landing site. Thus, multiple transport vessels may be necessary to match the rate of turbine installation.

3.6.2. Section transport cost model

The cost for the transport of the sections is the summation of the crane rental, vessel rental, and port fees, as shown in equation 3.16. The parameters for each equation are explained in table 3.3. The formulas are the mathematical formulation of the transport process, explained in paragraph 3.6.1 and schematically shown in figure 3.17.

$$C_{sec-trans} = C_{crane} + C_{vessels} + C_{port} \quad (3.16)$$

Cranes

The optional crane cost is dependent on the crane day rent price c_{rent} , the maximum section mass $m_{sec,max}$, and the total installation time. The crane day rate is a discrete cost function [38].

$$C_{crane} = c_{rent}(m_{sec,max})T_{inst} \quad (3.17)$$

Vessels

The vessel cost is calculated according to equation 3.18.

$$\begin{aligned} C_{vessels} &= N_{vessel} \cdot c_{vessel-day} \cdot t_{inst} \\ t_{round} &= t_{loading} + 2 \cdot t_{trans} + t_{offloading} \\ t_{trans} &= \frac{d_{landing-site}}{v_{vessel}} \end{aligned} \quad (3.18)$$

The inflow of towers at the landing site must meet the outflow of turbines by the jack-up vessels because of the limited storage capacity at the landing site. The outflow of towers is determined by the installation schedule. With that information, the number of required vessels can be calculated with the derivation in 3.19.

$$Q_{in} = Q_{out} \quad (3.19)$$

$$N_{vessel} \cdot \frac{N_{stow}(l, d_{top}, d_{bottom})}{t_{round}} = \frac{N_{turbines}}{T_{inst}}$$

$$N_{vessel} = \frac{t_{round}}{T_{inst}} \cdot \frac{N_{turbines}}{N_{stow}(l, d_{top}, d_{bottom})}$$

Determining the vessel stow

The stow of the vessel is determined manually. This is where cost engineers analyze the cargo hold of each vessel and determine the number of sections that fit. The fit is determined by the tower section dimensions. It is a manual process, which is highly dependent on the tower parameters. A slight change in the diameter or length of the section influences the number of sections that fit, and in turn, affects the number of vessels that are needed in the process.

Port fees

The port fees are a price per tonnage of on- or offloading cargo, shown in equation 3.21 [36]. The only model that covers the port fees is the life-cycle cost model of [17], where the port fees are taken as a fixed cost [17], shown in equation 3.20. The mass of the tower determines in large part the port fees and thus, should be accounted for.

$$\text{Literature: } C_{port} = C \quad (3.20)$$

$$\text{Improved: } C_{port} = c_{port} \cdot m_{tower} \quad (3.21)$$

Table 3.3: Parameters for the calculation of the transport costs from manufacturer to landing site.

Symbol	Parameter
$C_{sec-trans}$	Total section transport costs
C_{crane}	Total crane rental costs
$C_{vessels}$	Total vessel rental costs
C_{port}	Total port fees
N_{vessel}	Number of vessels necessary for transport
$c_{vessel-day}$	Vessel day rate
t_{round}	Transport round trip time per vessel
$t_{loading}$	Loading time of the towers
t_{trans}	Transport time
$t_{offloading}$	Offloading time per vessel
$d_{landing-site}$	Distance from manufacturer to landing site
v_{vessel}	Vessel speed
Q_{in}	Inflow of towers for pre-assembly
Q_{out}	Outflow of towers for installation
N_{stow}	Tower stow per vessel
$N_{turbines}$	Total number of turbines in the wind farm
T_{inst}	Total installation time

3.7. Assembly

3.7.1. Phase explanation

In the assembly phase, the stored sections are assembled into a complete tower, ready to be loaded onto the installation vessel. The process starts with a crane lifting one section on top of another. The sections are bolted together by assembly workers. This process is repeated until a full tower is complete. The number of assembled towers is determined by the loading capacity of the installation vessel. When the vessel returns from one installation round, the assembled towers are loaded. It can happen that this process requires two separate cranes because of the maximum lifting weight and height [38].

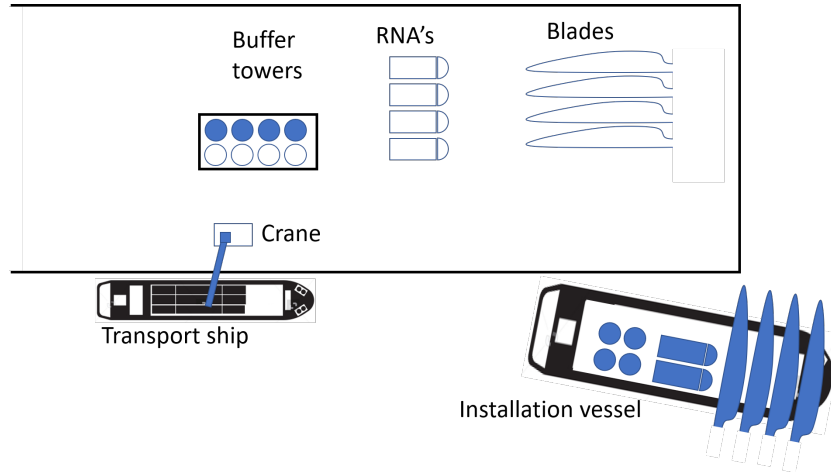


Figure 3.18: Example overview of landing site layout.

The assembly requires a storage area for the sections, nacelles and blades in the port, as can be seen in figure 3.18. This area is rented from the port and can take up a large share of the assembly phase costs, called land lease costs. The larger the area, the more space there is for buffer components. This is necessary because there is a flow of incoming and outgoing goods. One disturbance in either flow increases the cost of the wind farm. Determining the buffer level is a complex problem, which involves a lot of human judgement. One can model the uncertainty in installation, but problems in manufacturing or transport of sections can also affect the buffer. Also, the layout of the buffer area is made manually. It is very complex to capture this cost element with a model, given the amount of manual work and human judgement [38]. Therefore, it was chosen not to model the land lease costs.

3.7.2. Assembly cost model

The major components in the assembly costs are the crane rental and land lease, given in equation 3.22.

$$C_{ass} = C_{crane} + C_{land-lease} \quad (3.22)$$

Crane

The crane costs can be calculated with the crane day rate, $c_{crane,i}$, and the total installation time T_{inst} . There are k number of crane needed for the process, depending on the installation strategy.

$$C_{crane} = \sum_{i=1}^k c_{crane,i}(m_{tower}) \cdot T_{inst} \quad (3.23)$$

Land lease

The land lease costs are not modeled based on tower parameters because of the complexity. The required area is determined based on the RNA assembly and the size of the blades, and is done manually. Moreover, the port and layout is not a design choice for tower designers.

3.8. Installation

3.8.1. Phase explanation

According to Sarker and Faiz [19], there are six steps to be undertaken in this phase, schematically shown in figure 3.19. First, the tower sections are pre-assembled in the port. From there the sections are loaded onto a jack-up vessel and transported to the wind farm site. At the turbine location, the vessel needs to be jacked-up and the tower is installed along with the rotor-nacelle assembly and the blades. Then the vessel has to jack down and move to the next turbine location in the wind farm. When all turbines on deck have been installed, the vessel returns to the port to load the next set of turbines until the wind farm is finished [39].

The largest cost component in the installation phase is the vessel rent, as can be seen in figure 3.20.

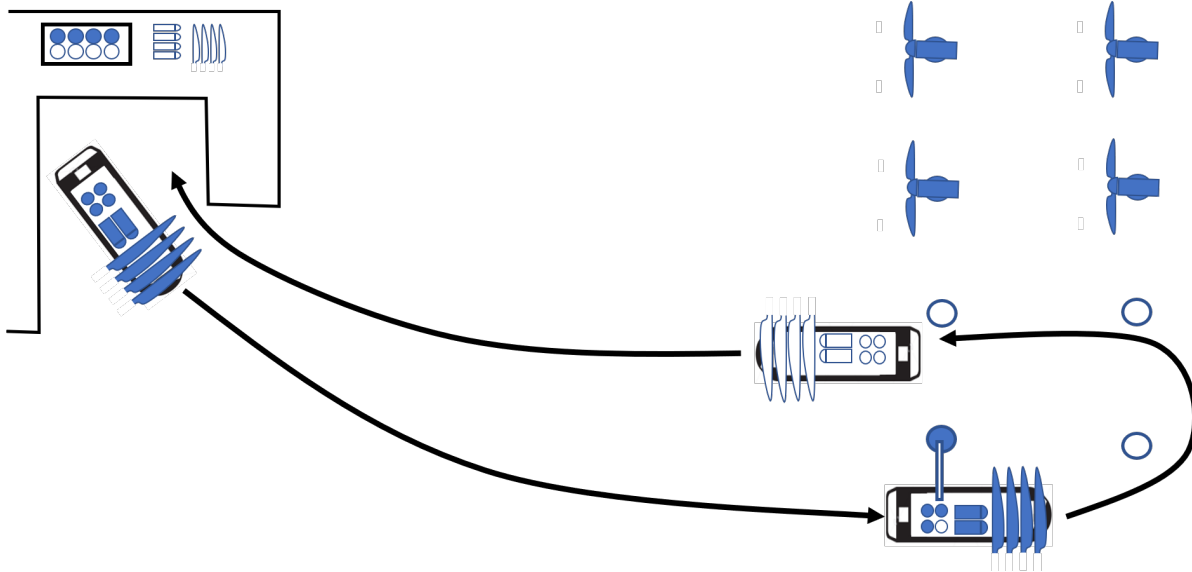


Figure 3.19: Schematic representation of the installation process.

What can be derived from figure 3.20, is that roughly 80% of the total costs is vessel rent. Thus the focus of the cost model is on the vessel rent.

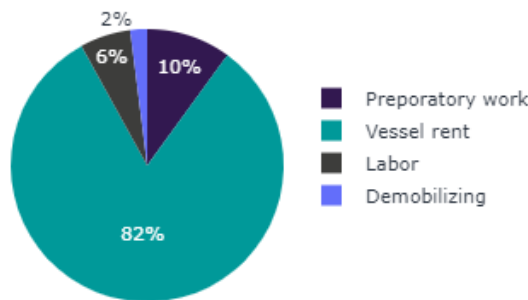


Figure 3.20: Indicative installation cost breakdown.

3.8.2. Installation cost model

The installation cost model is based on the study of Sarker and Faiz [19], because the methodology is the same as the current methods. In that model, the installation cost per vessel is calculated based on the total operating time and the vessel day rate, shown in equation 3.24. Based on the steps in figure 3.19, one can calculate the time spend per step with the wind farm and vessel parameters, shown in table 3.4. In this part of the cost model, only publicly available information was used. The effect

was that some parameters were not available and engineering estimates had to be used. It is noted whenever this applies.

The formula for the total installation time per vessel is given in equation 3.25. The round trip time, t_{round} , is the sum of the time for each installation step in figure 3.19. This can be seen in equation 3.26. Equations 3.27 to 3.31 show the formulas for calculating the time, where the subscript represents the step in process. In the equations, the jack-up speed is the same as the jack-down speed.

$$C_{inst} = c_t(m_{tower}, l_{tower}) \cdot t \quad (3.24)$$

$$t = \text{ceil}\left(\frac{N_{WF}}{N_{vessel}}\right) \cdot t_{round} \quad (3.25)$$

$$t_{round} = t_2 + t_3 + t_4 + t_5 + t_6 \quad (3.26)$$

$$t_2 = t_{jack-up} + t_{loading} = \frac{d_{port}}{v_{jack-up}} + t_{loading} \quad (3.27)$$

$$t_3 = t_{jack-down} + t_{transport} = \frac{d_{port}}{v_{jack-up}} + \frac{D}{V_{cruise}} \quad (3.28)$$

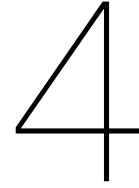
$$t_4 = t_{jack-up} + t_{installation} = \frac{d_{WF}}{v_{jack-up}} + t_{tower} + t_{RNA} + t_{blades} \quad (3.29)$$

$$t_5 = t_{jack-down} + t_{travel} = \frac{d_{WF}}{v_{jack-up}} + \frac{d_{turbine}}{v_{vessel}} \quad (3.30)$$

$$t_6 = t_{transport} = \frac{D}{V_{cruise}} \quad (3.31)$$

Table 3.4: Vessel parameters for the calculation of the total installation time.

Symbol	Parameter
D	Distance from shore
d_{port}	Water depth in the port
d_{WF}	Water depth at the wind farm
v_{cruise}	Vessel cruise speed
$v_{jack-up}$	Vessel jack-up speed
t_{tower}	Tower installation time
t_{RNA}	RNA installation time
t_{blades}	Blade installation time
$t_{loading}$	Loading time at the port
N_{vessel}	Number of towers on the vessel
N_{WF}	Number of towers in the wind farm



Cost optimization model

To evaluate the effect of optimization of a wind turbine tower for costs, the developed cost model must be integrated in a tower design routine. The cost optimization routine is developed independently from the SGRE tower design software. First, the tower parameterization and initial design are discussed in section 4.2. With these parameters, the cost model can be developed reasoning behind the cost optimization method is based on the results from the cost model research. This is followed by an explanation of the optimization algorithm and the problem formulation, all discussed in section 2.2, which is developed based on the cost model.

4.1. Reasoning behind the optimization routine

From the cost model found in chapter 3, ten cost functions have been found for the material procurement, material transport, and manufacturing phase. Table 4.1, shows an overview of cost functions, cost drivers and which parameters are included in the tower design software and cost optimization model. The tower design software from SGRE calculates the minimum required shell thickness for structural integrity. The thickness cost factor, cutting & beveling, and rolling & welding cost are fully or partially dependent on shell thickness.

4.1.1. Chosen optimization concept

In paragraph 2.2.2, two conceptual cost optimization models were developed:

1. implementation cost optimization in tower design software or;
2. a separate cost optimization model from tower design software.

The second option was chosen because the tower design software is limited to changing the shell thicknesses and thus only affects one cost function fully and two partially. To see the effect of production cost in tower design, as many cost functions as possible have to be included in the process and a separate cost optimization model provides the freedom to do so. Also, it may provide a model that can be applied in the wind industry and research.

4.1.2. Implementation of chosen concept

In the separate cost optimization, one has the freedom to choose which tower parameters to optimize, but the downside is that the structural integrity of the tower is not maintained. The output from the tower design software has to be used to ensure the structural integrity. Three possible optimization parameters are identified:

- Section diameters
- Section heights
- Shell heights

The choice was made to optimize the shell heights and keep the outer geometry intact for three reasons. First of all, the shell heights affect six out of seven cost functions with cost drivers. Together, these cost functions cover an additional 25% of CAPEX. Unfortunately, the fixed outer geometry does not affect the total painting cost of the tower, which accounts for 17% of manufacturing cost according to figure 3.13. This can be studied in a future into the optimum section diameters and heights. Secondly, because the optimum shell height distribution is not known and can be important knowledge for optimizing section heights and diameters. Changing a section height directly affects the shell heights, thus knowledge on the best distribution is critical. The second reason concerns the modeling complexity in the cost optimization model. The software deals with numerous inputs, ranging from door frames, all sorts of attachments, flange connections, dampers, fatigue curves, and more. These are defined by tower engineers based on the outer geometry. By keeping the section geometry constant, information on the shell thickness distribution might be enough for maintaining the structural integrity. The thickness assumption eliminates any additional load modeling in the cost optimization. This adds to the universality of the optimization.

Table 4.1: Overview of cost functions affected by the tower design software and cost optimization model. Only applies to conical shells.

Phase	Cost function	Cost driver	Relevant shell parameters	TDS	COM
Material	Base price	-	-	-	-
	Height cost factor increase	Plate height	Diameters*, Height	- -	✓ ✓
	Length cost factor increase	Plate length	Diameters, Height*	- -	✓ ✓
	Thickness cost factor increase	Plate thickness	Thickness	✓	✓
	CO2 emission tax	-	-	-	-
	Steel grade	-	-	-	-
Material transport	Length cost factor	Plate length	Diameters Height*	- -	✓ ✓
	Manufacturing	Cutting & beveling cost	Weld volume	Diameters Height	- -
Weld volume			Thickness	✓	✓
Rolling & welding cost		Weld volume	Diameters Height	- -	✓ ✓
		Weld volume	Thickness	✓	✓
Surface treatment & painting cost	Area	Diameters, Height	- -	- -	

4.2. Tower parameterization

The relevant tower parameters are the shell heights, diameters and thicknesses. A tower has n number of shells, each with a height h_i , top diameter d_i , and thickness t_i . The number of sections k is 3. Each section can have a different number of shells, denoted by the letters p , q , and r for the top, middle and bottom section respectively.

The parameters of shells 1, 2, 3, and 4 are kept constant in the optimization routine because they are provided by the RNA engineers. These shells only account for 4% of tower mass and 4.3% of tower costs. Thus the influence on the result of the optimization is minor. Moreover, such design decisions are common in the industry, and testing the cost optimization routine with these constraints adds to the applicability of the methodology in industry-grade tower design.

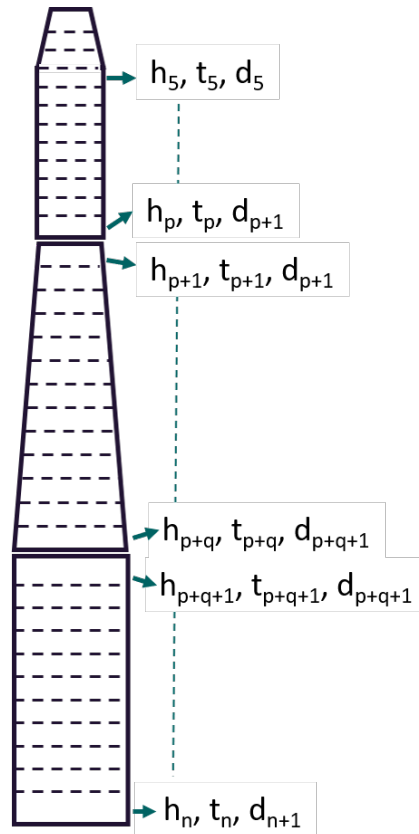


Figure 4.1: Tower parameters in the optimization problem. Parameters of shells 1-4 are fixed.

4.3. Optimization algorithm

The cost optimization routine optimizes the shell heights in a tower section, given a fixed diameter and thickness distribution. The cost functions cover the material, material transport, and manufacturing cost.

4.3.1. Optimization model structure

A direct search method is chosen for the cost optimization with the steps shown in figure 4.2. The first step is to input a tower design consisting of k sections. The sections are fed into the tower cost optimizer and optimized individually by the section cost optimizer. In this routine, the shell heights are varied, and the new section cost c_i is calculated and compared against the value of the previous iteration c_{i-1} . If the solution has converged within the error ϵ , the section design is finished and combined to define the new tower. If the cost deviation is larger than ϵ , another iteration is done.

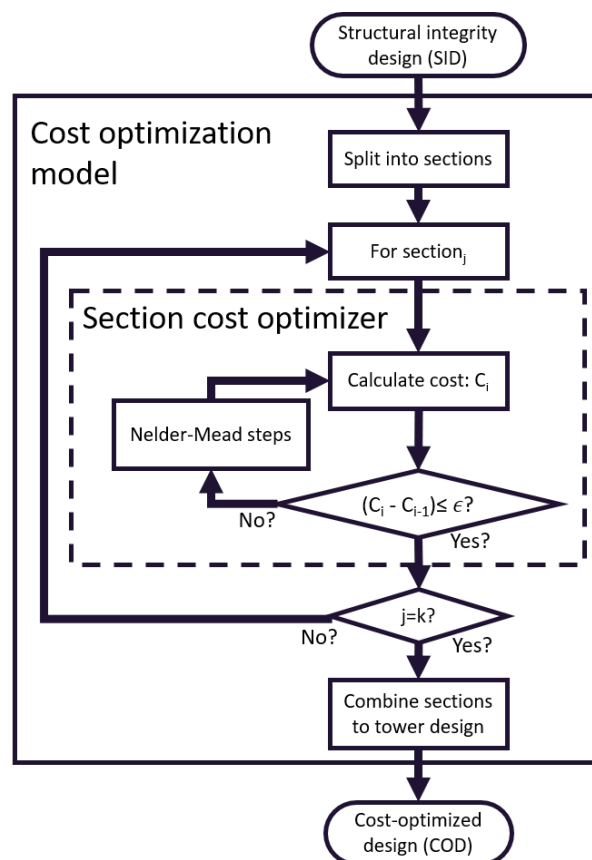


Figure 4.2: Cost optimization flowchart

4.3.2. Explanation of the Nelder-Mead algorithm

The Nelder-Mead algorithm [40], [41], [42] from the Python package Scipy [23] is chosen to work within this study. It was chosen because it yielded the most stable results after a minor study into the minimization methods provided in the Scipy package. The gradient-based methods could not resolve the constraint violations. It is recognized that the best optimization method can be studied but is left for the future, given the purpose of comparing mass optimized versus cost-optimized designs. It is an unconstrained bounded optimization algorithm, which means that any constraints must be resolved by a smart design of the optimization problem.

The algorithm steps are as follows. First, the initialization of the problem. The problem is defined by equation 4.1 with vectors \mathbf{x} and the initial simplex.

$$\min(f(\mathbf{x})) \quad , \text{ where: } \mathbf{x} \in \mathbb{R}^n \quad (4.1)$$

with vectors: $\Delta = \mathbf{x}_1, \dots, \mathbf{x}_{n+1}$

From here on, the iterative process starts.

1. Sort the vectors according to their function value in ascending order.

$$f(\mathbf{x}_1) \leq f(\mathbf{x}_2) \leq \dots \leq f(\mathbf{x}_{n+1}) \quad (4.2)$$

2. Calculate centroid of points 1, ..., n.

$$\bar{\mathbf{x}} = \frac{\sum_i^n \mathbf{x}_i}{n} \quad (4.3)$$

3. Reflection: mirror the vector with the highest function value \mathbf{x} over the centroid $\bar{\mathbf{x}}$ with a factor α . The result is the mirrored vector \mathbf{x}_r .

$$\mathbf{x}_r = \bar{\mathbf{x}} - \alpha (\bar{\mathbf{x}} - \mathbf{x}_{n+1}) \quad (4.4)$$

$$(4.5)$$

Evaluate its function value $f_r = f(\mathbf{x}_r)$. If $f_1 < f_r < f_n$, replace the vector \mathbf{x}_{n+1} with \mathbf{x}_r .

4. Expansion: if $f_r < f_1$, expand the vector \mathbf{x}_r away from the centroid with a factor γ to find \mathbf{x}_e

$$\mathbf{x}_e = \bar{\mathbf{x}} + \gamma (\mathbf{x}_r - \bar{\mathbf{x}}) \quad (4.6)$$

and calculate $f_e = f(\mathbf{x}_e)$. If $f_e < f_r$, substitute \mathbf{x}_{n+1} with \mathbf{x}_e , else substitute with \mathbf{x}_r .

5. Outside contraction: if $f_n \leq f_r < f_{n+1}$, pull the reflected vector \mathbf{x}_r towards the centroid with a factor ρ to find \mathbf{x}_{oc}

$$\mathbf{x}_{oc} = \bar{\mathbf{x}} + \rho (\mathbf{x}_r - \bar{\mathbf{x}}) \quad (4.7)$$

and calculate $f_{oc} = f(\mathbf{x}_{oc})$. If $f_{oc} < f_{n+1}$, substitute \mathbf{x}_{oc} for \mathbf{x}_{n+1} . Otherwise, go to step 7.

6. Inside contraction: if $f_r \geq f_{n+1}$, pull the original vector \mathbf{x}_{n+1} towards the centroid with a factor σ to find \mathbf{x}_{ic}

$$\mathbf{x}_{ic} = \bar{\mathbf{x}} + \rho (\mathbf{x}_{n+1} - \bar{\mathbf{x}}) \quad (4.8)$$

Calculate $f_{ic} = f(\mathbf{x}_{ic})$. If $f_{ic} < f_{n+1}$, substitute \mathbf{x}_{ic} for \mathbf{x}_{n+1} . Otherwise, go to step 7.

7. In the rare case that $f_{ic} > f_{n+1}$ and $f_{oc} > f_{n+1}$, so none of steps 3, 4, 5, and 6 improve the worst result, shrink the simplex towards the best vector \mathbf{x}_1 by a factor σ to find new vectors for $\mathbf{x}_2, \dots, \mathbf{x}_{n+1}$.

$$\mathbf{x}_{s_i} = \mathbf{x}_1 - \sigma (\mathbf{x}_i - \mathbf{x}_1) \quad (4.9)$$

Substitute \mathbf{x}_{s_i} with \mathbf{x}_i for $i \in \{2, \dots, n+1\}$.

In the original Nelder-Mead algorithm [40], the values for parameters α , ρ , γ and σ were set to 1, 0.5, 2 and 1 respectively. For larger dimensional problems where $n > 10$, the algorithm performance reduces sharply. Therefore, Gao and Han [42] implemented adaptive parameters to create the Adaptive Nelder-Mead Simplex algorithm (ANMS), making the algorithm more efficient for higher dimensional problems.

The steps in algorithm are graphically shown in figure 4.3, which shows a contour plot for the function 4.10 with $n = 2$ variables, x_1 and x_2 , and arbitrary coefficients a and b . In this example, points 1, 2, and 3 are the initial simplex. Point four was found through expansion. Points 5, 6, and 7 were only reflections, and point 8 was found by outside contraction. For points 9 and 10, inside contraction was used.

$$f(x, y) = ax_1^2 + bx_2^2 \quad (4.10)$$

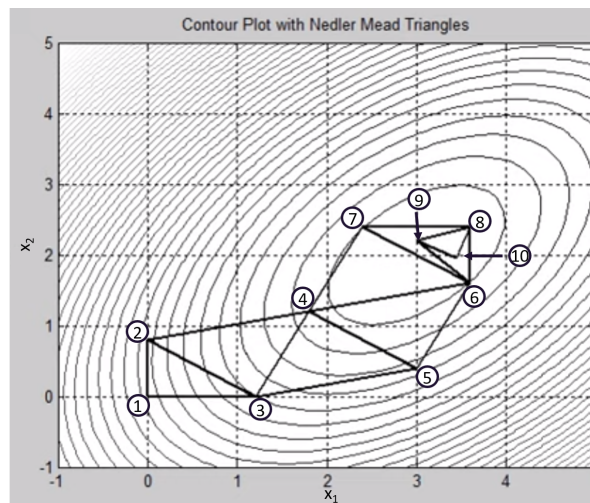


Figure 4.3: Example of a Nelder-Mead optimization.

4.4. Optimization problem formulation

Any optimization problem is composed of the objective function, design vector, and constraints. In this study, an unconstrained optimization method was used, which means the constraint violation value has to be used as a penalty term in the objective function. For clarity purposes, the constraint is discussed in a separate paragraph.

4.4.1. Objective

The objective of the optimization corresponds to research objective 4:

”Optimize the primary structure of an offshore wind turbine for CAPEX.”

In section 3.2, it was found that only the material, material transport, and manufacturing phase are feasible for cost optimization because the costs are driven by tower parameters. In the section transport, assembly, and installation phase, too many non-tower parameters influence the phase costs. Therefore, only the cost of the first three phases of the production process is included in the cost function C_i . The cost is calculated by the summation of the material cost C_{m_i} , material transport cost C_{t_i} and manufacturing cost function for beveling C_{bevel_i} , welding C_{weld_i} and painting C_{weld_i} . The algorithm is an unconstrained method. Thus any constraint violations CV are added to the objective value as a penalty function, shown in equation 4.11.

$$\min (C_i + CV^2) = \min \sum_{i=4}^n (C_{m_i} + C_{t_i} + C_{bevel_i} + C_{weld_i} + C_{paint_i} + CV^2) \quad (4.11)$$

$$(4.12)$$

4.4.2. Design vectors

The design variables in the cost optimization are the shell heights in each section, excluding the last plate in the section. If sections 1, 2, and 3 have p , q , and r number of shells, this results in three separate design vectors 4.13, 4.14, and 4.15.

$$\text{Design vector - Section 1: } [h_4, h_5, \dots, h_{p-1}] \quad (4.13)$$

$$\text{Design vector - Section 2: } [h_{p+1}, h_{p+1}, \dots, h_{p+q-1}] \quad (4.14)$$

$$\text{Design vector - Section 3: } [h_{p+q+1}, h_{p+q+2}, \dots, h_{p+q+r-1}] \quad (4.15)$$

4.4.3. Rewriting constraints

The cost optimization has two constraints, which have to be rewritten to a form that suits the unconstrained Nelder-Mead algorithm. The inequality constraint on the plate height is added as a penalty term to the objective value. The equality constraint on the fixed section length is resolved by eliminating the bottom shell height from the design vector and making it a function of the other shell heights in the design vector.

Plate height constraint

The first constraint is set on the plate height, shown in 4.16. The plate height must stay above a minimum and below a maximum value. This minimum and maximum value can be provided by any party in the supply chain because of manufacturing machines that cannot handle such plate sizes.

$$h_{plate_{min}} < h_{plate_i} < h_{plate_{max}} \quad (4.16)$$

The Nelder-Mead algorithm is an unconstrained optimization method, thus cannot handle constraints. Therefore, the value of the constraint violation is converted to a linear formula given in equation 4.17 and graphically shown in figure 4.4.

$$\begin{aligned} h_{plate_{min}} > h_{plate_i} &: CV = h_{plate_{min}} - h_{plate_i}; \\ h_{plate_i} > h_{plate_{max}} &: CV = h_{plate_i} - h_{plate_{max}}; \\ \text{else: } & CV = 0 \end{aligned} \quad (4.17)$$

Section height constraint

The second constraint is an equality constraint derived from the fixed section height. It was chosen to fix the section height to ease the transition from the cost optimization to the tower design software. The tower design software is of industrial grade and considers attachments, doorframes, slosher, and other practical components necessary for creating a real-world tower. Varying the shell heights can result in errors in the software and does not contribute to the objective of comparing a mass optimized design with a cost-optimized design. Therefore, the choice was made to keep each section's height constant. However, this does add a constraint to the optimization, which has to be dealt with. This was done by eliminating the bottom plate height in each section.

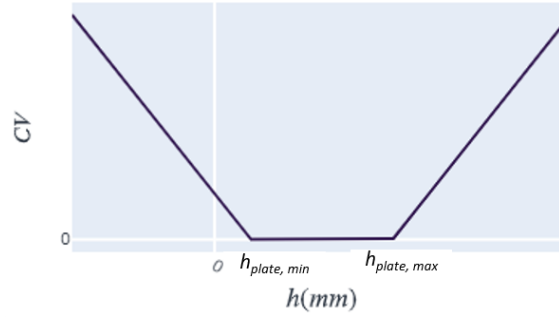


Figure 4.4: Value of constraint violation.

$$\text{Section 1: } h_{section_1} = \sum_{i=4}^p h_i \quad (4.18)$$

$$\text{Section 2: } h_{section_2} = \sum_{i=p+1}^{p+q} h_i \quad (4.19)$$

$$\text{Section 3: } h_{section_3} = \sum_{i=p+q+1}^{p+q+r} h_i \quad (4.20)$$

This shell height equality constraint would be a major problem in the optimization if all shell heights would also be in the design vector. Any change the algorithm does to the design vector would immediately result in a constraint violation. Therefore, the algorithm would be stuck in the initial values. This problem is resolved by eliminating the bottom shell (h_p , h_{p+q} , and h_{p+q+r}), from each design vector and calculating the height of that shell as the difference between the section height $h_{section}$ and the summation of the shell heights, shown in equations 4.22, 4.23, 4.21.

$$\text{Section 1: } h_p = h_{section_1} - \sum_{i=4}^{p-1} h_i \quad (4.21)$$

$$\text{Section 2: } h_{p+q} = h_{section_2} - \sum_{i=p+1}^{p+q-1} h_i \quad (4.22)$$

$$\text{Section 3: } h_{p+q+r} = h_{section_3} - \sum_{i=p+q+1}^{p+q+r-1} h_i \quad (4.23)$$

Shell thickness constraint

The shell thickness in the cost optimization model is constrained to the interpolated line of bottom shell thickness. The assumption is that with this constraint, the structural integrity of the tower is maintained. The reasoning is as follows.

The tower design software calculates the minimum thickness for each shell to handle the critical fatigue and ultimate loads over its lifetime. The assumption is that the critical loads occur at the bottom of each shell. The interpolation of the bottom shell thickness is shown in figure 4.5. Left of the interpolation line is the green area. This part of the tower is bearing the load. The area on the right is excess steel, which has no function. Therefore, it is only the green area that has to be maintained.

The change in shell height from one shell affects the elevation of other shells. In every step, the shell thicknesses are assigned by its new bottom elevation.

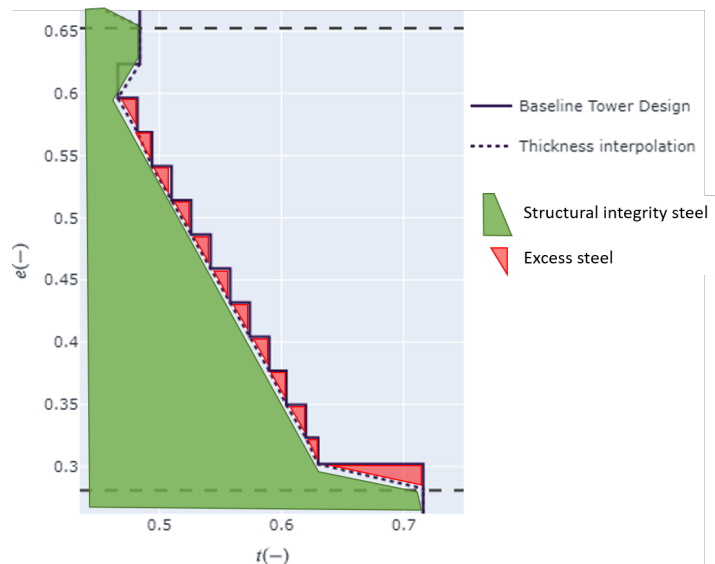


Figure 4.5: Structural integrity assumption.

Fixed outer geometry constraint

The optimization has the constraint that the outer geometry is fixed. In cylindrical sections, the diameter is constant over the section; thus, changing the shell heights does not cause any problems in the optimization.

$$d(e) = \text{constant} \quad (4.24)$$

$$d_{top_i} = d_{top_i} \quad (4.25)$$

$$d_{bottom_i} = d_{bottom_i} \quad (4.26)$$

However, for conical sections, the diameter has a linear relation to the shell elevation. To maintain the outer geometry when changing the height of shell i , new top and bottom diameters are assigned by the linear diameter distribution function

$$d(e) = a \cdot e + b \quad (4.27)$$

$$(4.28)$$

with the coefficient of the formula a , the elevation of the shell e , and the start value b . With this formula, the top and bottom diameters can be found through the calculation of the shell's position in the section.

$$d_{top_i} = d(e_{i-1}) \quad (4.29)$$

$$d_{bottom_i} = d(e_i) \quad (4.30)$$

Other constraints

In reality, there are more constraints to a tower design. Limitations in the material phase on plate length and thickness, transport limitations on material weight, or manufacturers having limits on the section weight, section length, for example. All these constraints can be dealt with by a smart design of the optimization problem.

4.5. Case study tower design

The tower used in the case studies is from a project of SGRE.

4.5.1. Outer geometry

The top section consists of $p = 14$ shells. As can be seen in figure 4.6a, the first three plates in the top section are conical, which are followed by cylindrical shells 4-14. The parameters of these conical shells are prescribed by the RNA design and are kept constant throughout the optimization. The middle section is conical, consisting of $q = 14$ shells. The diameter distribution is linear, from $d_{top}=0.927$ to $d_{bottom}=1.000$. The bottom section consists of $r = 13$ shells and has the maximum diameter of the tower. The section diameters and heights are summarized in table 4.2.

The diameters are non-dimensionalized with the bottom diameter d_n of the tower and the shell thicknesses with the top shell thickness t_1 , which are fixed. The same values are used for all subsequent figures showing non-dimensional diameter and thickness distributions.

Table 4.2: Section diameters and height, fixating the tower outer geometry.

Section (index)	N_{shells}	d_{top}	d_{bottom}	h_{top}	h_{bottom}
Top (1)	11	0.708	0.927	1.000	0.654
Middle (2)	14	0.927	1.000	0.654	0.281
Bottom (3)	13	1.000	1.000	0.281	0.000

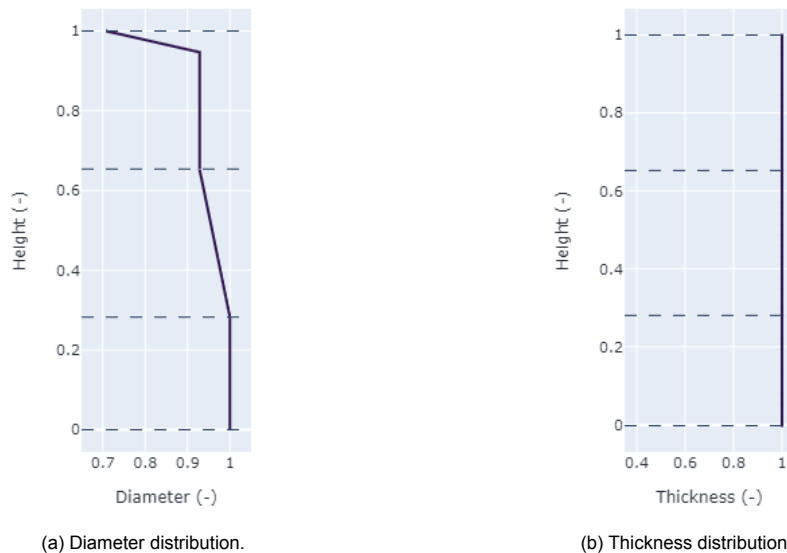


Figure 4.6: Initial tower geometry.

4.5.2. Baseline tower design

The tower design software takes the initial design as input and optimizes the shell thicknesses for minimum mass while complying with the IEC structural integrity requirements. The design variables are the shell thicknesses; the shell heights and diameters are kept constant. The result is the baseline tower design shown in figures 4.7a and 4.7b. The thickness distribution at the tower top three shells are fixed and then quickly minimizes to a value of $t_4=0.4$. From there on, the thickness is gradually increased. This follows from the increasing lever arm of the rotor thrust at lower heights.

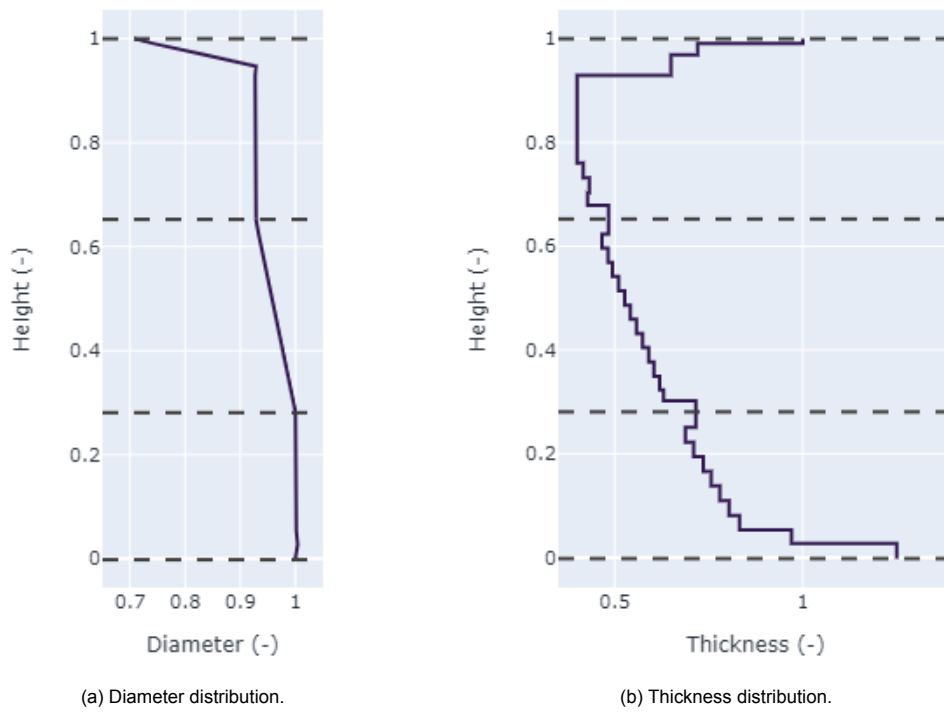


Figure 4.7: baseline tower geometry.

4.6. Optimization model vulnerabilities

The three vulnerabilities were identified in paragraph 2.2.2. In the first paragraph, the local minima problem is discussed, which is a common pitfall in optimization studies. This is followed by the problem of structural integrity in the cost optimization model. If large changes are required by the tower design software to maintain the structural integrity, the cost estimation is not very reliable. This problem is further elaborated on in paragraph 4.6.2. The final vulnerability can be the convergence between the COD and the SID and is explained in paragraph 4.6.3. The analysis of the possible pitfalls is done based on the results from case study 1. The cost and tower design analysis is given in section 5.1.

4.6.1. The local minima study

Any optimization algorithm can get stuck in a local minimum. However, the goal is to find the lowest value of the objective function, called the global minimum. Figure 4.8 illustrates a function with local minima. An optimizer searches for the lowest point of a function based on the information it has on its current point. With the Nelder-Mead algorithm, the only information is the current function value. It is like standing on a mountain blindfolded and having to find the valley. The only information at hand is the current altitude. The best way to find the valley is to move in the direction where the altitude declines. This is how an optimizer works. Now, if the optimizer starts close to $x = -0.5$, it will likely find the local minimum. However, if the optimizer starts at $x > 0.5$ it is likely to find the global minimum. Therefore, the starting point decides what path will be traveled to a minimum. The methodology for finding the minima is explained first, after which the results are analyzed.

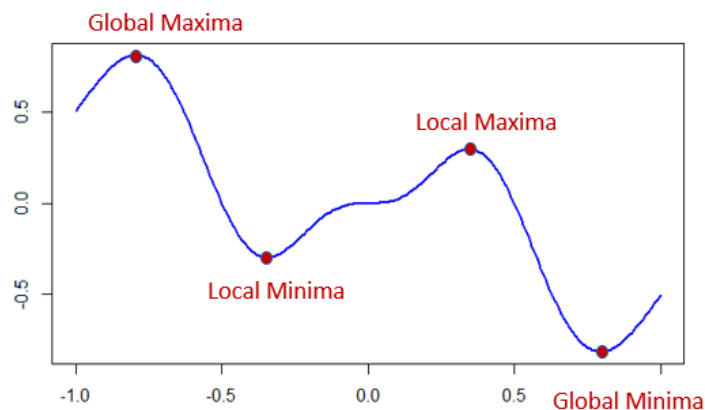


Figure 4.8: Example of a local and global minimum.

Methodology

The methodology for finding the local minima is to explore the design space from several starting points. Another name for the starting points is the initial design vector. Currently, the initial design vector consists of the shell heights from the BTD. In the cost optimization model, the shell heights in the initial design vector are normalized to create a vector of ones. The normalization of the design vector eliminates the dominance of large variables over smaller ones. Although the values of the variables in this study do not differ in order, it does come in handy for this study.

Instead of a vector of ones, the design vector is filled with randomly assigned values between $[0.5, 1.5]$, and the cost optimization is run. The initial and final design vectors are stored for analysis. This process was repeated 300 times over to search the design space from many different starting points. One might call this a brute force approach. The cost reductions per starting point are plotted.

Two results are given special attention. Firstly, the results are obtained by starting with the design vector from the BTD. Secondly, the design vector that results in the largest cost reduction, which is suspected to be the global minimum.

Local minima results

The main results of the local minima study are shown in figures 4.9a, 4.9b, and 4.9c. The result

from the BTD design vector is highlighted in red, and the assumed global minimum (GM) is highlighted in blue. For sections 1 and 3, the cylindrical top and bottom sections, there appear to be dominant local minima. In section 2, the conical middle section, the local minima are spread over the range of $[-1.5, -0.5]\%$. Another observation is that there are optimization results that increase the tower costs ($\Delta C > 0$). In the tower design loop, these results have to be disregarded. The final observation is that the BTD design vector does not find the assumed global minimum. In sections 1 and 3, it got stuck in the most dominant local minima. A positive note is that for all sections, the BTD design vector did reduce costs.

From these results, it appears that the shape of the section influences whether the optimizer has dominant local minima or is spread over a range. To analyze this further, the design vectors are analyzed per section.

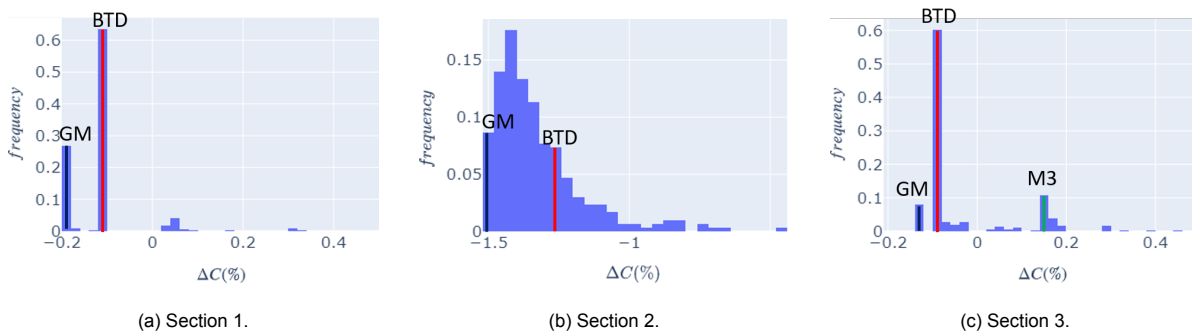


Figure 4.9: All minima found by the optimization model.

Local minima in section 1

Figure 4.9a shows that in section 1, there are two dominant local minima on $\Delta C = -0.19$ and $\Delta C = -0.11$. The former is suspected to be the global minimum, and the latter is the result of the BTD shell height distribution. The difference in results can be explained by a closer evaluation of the final design vectors, shown in table 4.3. The associated section designs are shown in figure 4.10.

Table 4.3: Final design vectors for the global minimum and BTD result. Values represent are relative change with the original shell heights.

	Design variable									
	h5	h6	h7	h8	h9	h10	h11	h12	h13	h14
GM	0.89	0.92	0.88	0.88	0.88	0.88	0.86	0.96	1.99	1.0
BTD	0.96	0.99	0.95	0.95	0.95	0.95	0.89	0.98	1.46	1.0

The largest difference can be observed at shell 13, where the global minimum vector has a value of $h_{13} = 1.99$ and the BTD vector a value of $h_{13} = 1.46$. It is difficult to give a definite reason for the two distinct local minima. The most logical reason is the local minima in the plate height cost function. The initial, global minimum, and BTD minimum design vectors are plotted on the plate height cost function, shown in figure 4.11. Due to the plate height limitation and the curve fit, two minima are created in the function, one at $h_{plate} = 0.6$ and one at $h_{plate} = h_{plate,max}$. Just before $h_{plate,max}$ there is a hump. The GM vector is on the right side of the hump, while the BTD minimum is on the left side. In the BTD scenario, the gradient in h_{13} is larger than the gradients of the other variables. Therefore, increasing h_{13} has no benefit. In the global minimum scenario, the gradient of h_{13} is opposite to the other variables, thus decreasing its shell height has a doubled negative effect on costs. This is the most compelling argument why the cost optimization model can get stuck in the two dominant local minima.

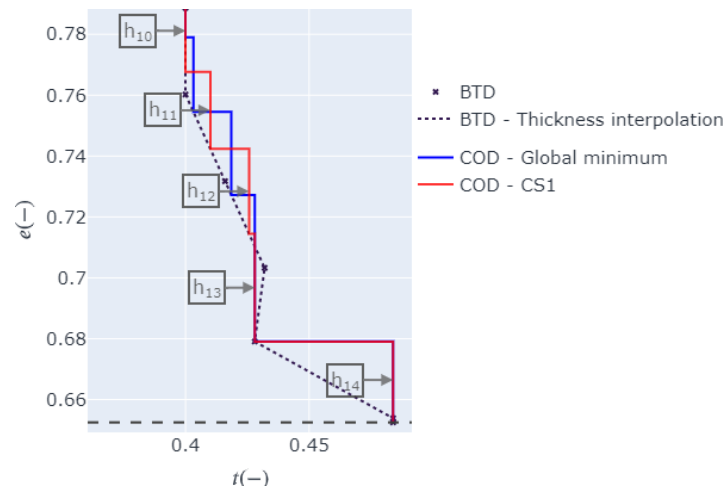


Figure 4.10: Thickness distributions of the global minimum and BTD minimum for section 1.

There are also minima in section 1 that increase the cost ($\Delta C > 0$). The corresponding design vectors are plotted on the plate height cost function in figure 4.12. What all these vectors have in common is that shell height 13 is in the local minimum A and one of h_5, \dots, h_{12} is in B at $h = h_{plate,max}$. Two variables in the local minimum result in a cost increase. If this occurs, the optimizer tower design loop continues with the initial design vector.

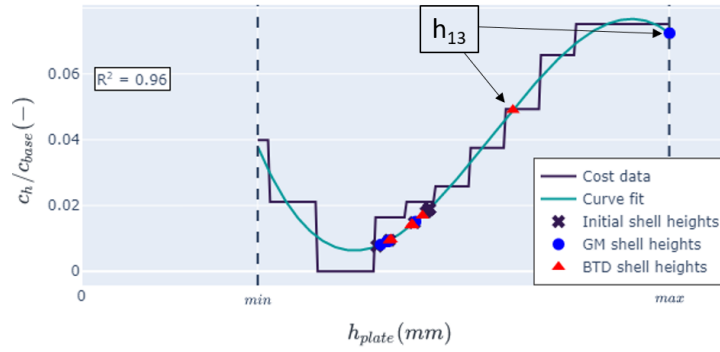


Figure 4.11: Shell heights of the global minimum and BTD minimum plotted on the plate height cost function.

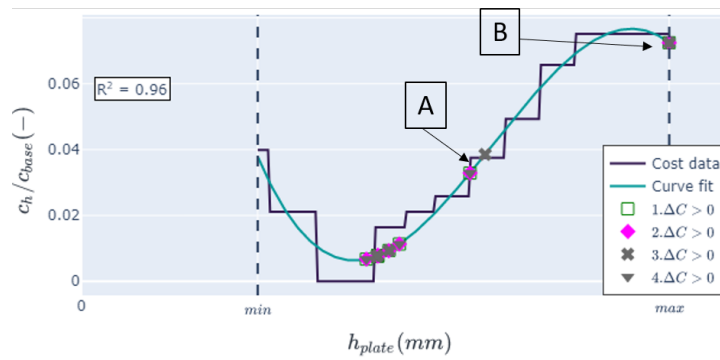


Figure 4.12: Shell heights of all minima with $\Delta C > 0$ plotted on the plate height cost function.

Local minima in section 2

Different from section 1, shows section 2 a spread of local minima over the range of $\Delta C = [-1.5, -1]$. Fortunately, all minima show a cost reduction, and 95% are smaller than $\Delta C < -1\%$. Again, the BTD result is not the global minimum. The best way to explain the dynamics of the optimizer is through the probability density function of each variable, shown in figure 4.13.

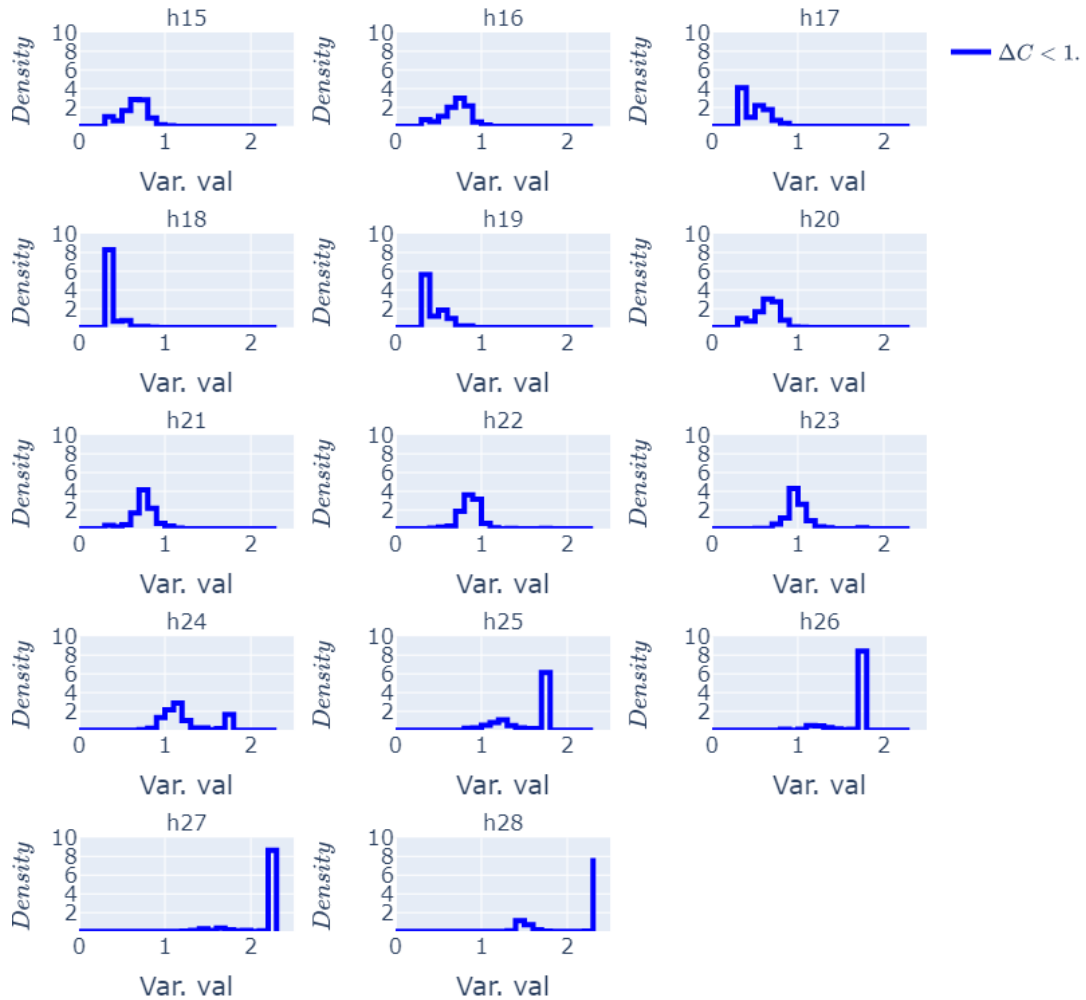


Figure 4.13: Optimized design vector of section 2 for the global optimum and result of case study 2.

First of all, the guideline that can be deduced from the figure is to increase the bottom shell heights and decrease the top shell heights. Although some shell heights show a distribution of minima, a general trend can be observed.

Secondly, shells 15-17 and 20-24 show almost a normal distribution of variables values, while shells 18, 19, and 25-28 have a more distinct value. The reason for the range of local minima found in figure 4.9b lies in the variables with a distribution of minimum values. The reason for the distribution of variables may be that in this conical, the transition function from conical shells to rectangular plates is added. A conical shell is created from a banana shape which is cut from a rectangular plate. These cutting losses have to be accounted for. The formula for the required plate size is derived in appendix B. The difference between the mass of a conical shell increases with height h and cone angle β . In the conical section, θ is fixed, and the bottom diameter d_2 and shell height h vary. The mass difference between the shell and plate in figure 4.14 shows a complex surface that creates the range of local

minima.

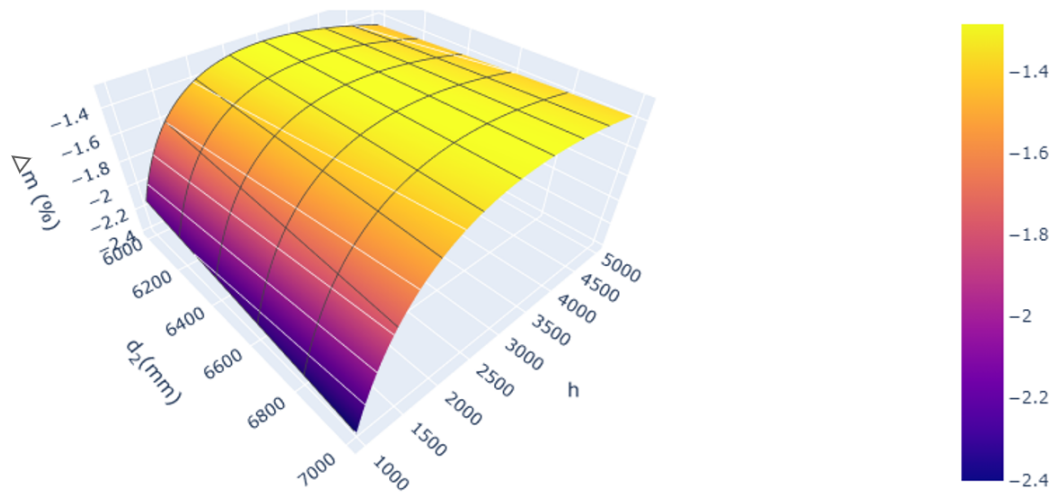


Figure 4.14: Difference between a conical shell mass and the rectangular plate mass with respect to shell height (h) and bottom diameter (d_2) with a fixed cone angle β .

Local minima in section 3

Figure 4.9c that in section 3, there are three dominant local minima on $\Delta C = -0.14\%$, $\Delta C = -0.11\%$, $\Delta C = 0.12\%$. The results are coined the assumed global minimum, BTD minimum, and a third dominant minimum M3. The design vectors for each local minima are given in table 4.4 and shown in figures 4.17a and 4.17b.

Table 4.4: Final design vectors for the global minimum and BTD and M3 result for section 3. Values represent the percentage of the original shell heights.

	Design variable									
	h29	h30	h31	h32	h33	h34	h35	h36	h37	h38
GM	0.88	0.97	0.73	0.81	0.90	0.96	1.04	1.73	0.99	1.01
BTD	0.94	1.06	0.80	0.87	0.97	1.03	1.11	1.22	0.99	1.01
M3	0.83	0.90	0.68	0.78	0.87	0.94	1.00	1.10	1.16	1.78

The first observation is the trend of increasing the bottom shell heights and decreasing the top shell heights, similar to sections 1 and 2.

The minor difference between the global minimum and BTD minimum can be explained by plotting the shell heights on the plate height cost function, shown in figure 4.15. The same happens as in section 1, where the hump closer to $h_{plate,max}$ creates a local minimum on the right. In the global minimum, shell 36 reaches over the hump, while in the BTD minimum, this does not happen. This benefit explains the minor difference in cost reduction.

The same figure can be used to explain the minimum M3. Instead of shell 36 having the maximum height, in this case, shell 38 finds that minimum. This happens because in most cases the h_{38} start value is close to $h_{plate,max}$, shown in figure 4.16. The outcome is very dependent on the starting point. This is unwanted behavior in an optimization model. It is clear that the valley at $h = h_{plate,min}$ is difficult to escape from. A solution would be to change the input function of the curve fit to a double sigmoid function, which has the ability to create plateaus. This can eliminate that local minimum near $h_{plate,max}$.

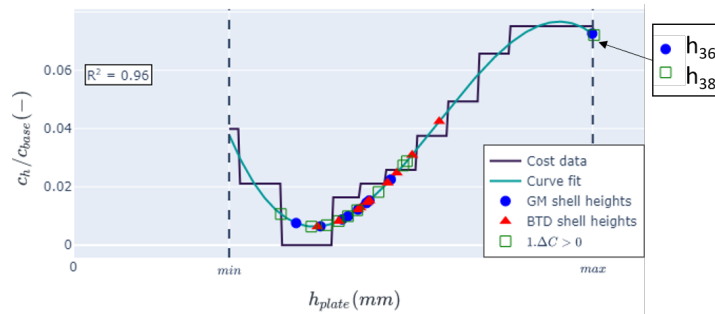


Figure 4.15: Shell heights of the global minimum, BTD minimum, and third dominating minimum M3 plotted on the plate height cost function.

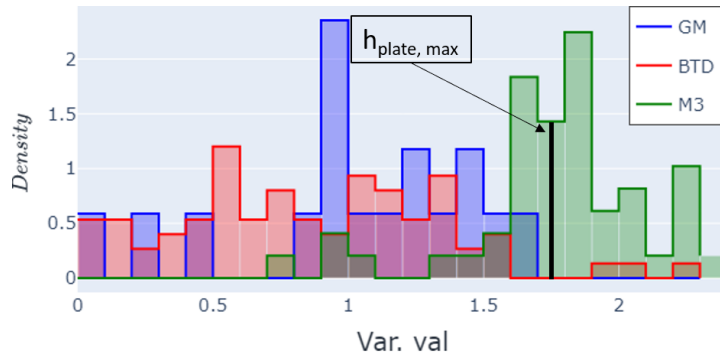
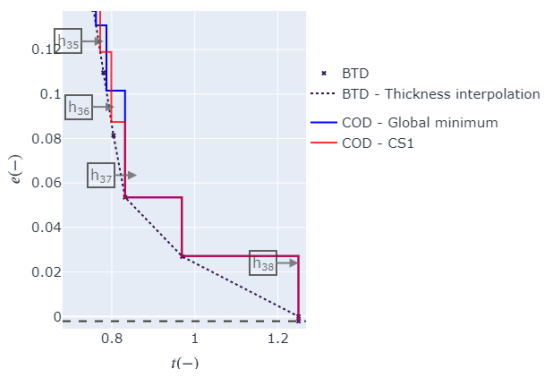
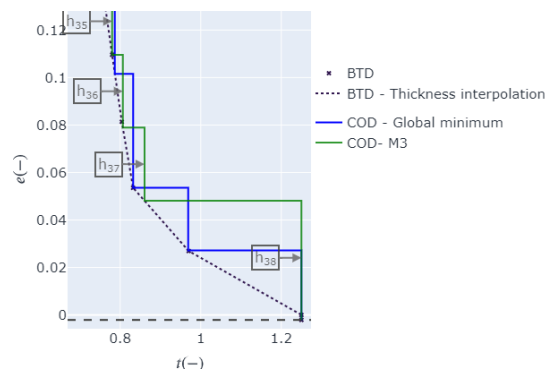


Figure 4.16: Distribution of the initial value of the h_{38} variable for the global minimum, local minimum - CS1, and third minimum - M3.



(a) Global minimum vs. CS1.



(b) Global minimum vs. M3.

Figure 4.17: Cost optimized designs for the global minimum, BTD minimum, and third dominating minimum M3.

4.6.2. Structural integrity in the cost optimization

In the cost optimization, the structural integrity of the tower is maintained by assigning the new shell thicknesses to the interpolated thickness interpolation of the structural integrity design. The concept is explained in paragraph 4.4.3 and visualized in figure 4.5. For the cost optimization, it is important to provide reliable cost estimates. The better the structural integrity is maintained in the cost optimization, the more reliable the cost estimates are. This is studied by a comparison of the COD and COD-SID and resulted in two findings. The first is that the thickness deviations are small in away from stress concentration factors and large close to stress concentration factors.

Reasonable approximation of structural integrity

The thickness deviations are summarized in table 4.5. What can be derived is that the mean thickness deviation σ and standard deviation μ in each section is tiny. This is important for the cost optimization model to give reliable cost estimates on the optimized design. The assumption performs well on the parts with minor changes in thickness gradient. In parts where the thickness gradient suddenly increases, the deviations between the COD and COD-SID increase but remain acceptable for parts where the sign of the gradient changes, the thickness interpolation assumption does not perform well.

The standard deviation in section 2 is the highest, which is the result of the transition in thickness gradient in shells 15-16 and 16-17 of the BTD. This change in gradient sign is caused by the stress concentration factor applied on all shells that connect to a flange. This is illustrated in figure 4.19c. In the bottom sections, the stress concentration factor introduces an increase in this thickness gradient, which is the optimizer can handle reasonably well. In top flanges, it causes a negative thickness gradient, which causes problems in the optimization.

The transition of gradient sign can also be seen in shells 12 and 13 of section 1 in figure 4.19b. This is the effect of an attachment that introduces a stress concentration factor.

Table 4.5: Relative thickness deviation between the COD and COD-SID per section.

	μ	σ
Section 1	0.03%	0.08%
Section 2	0.17%	0.80%
Section 3	0.1%	0.35%

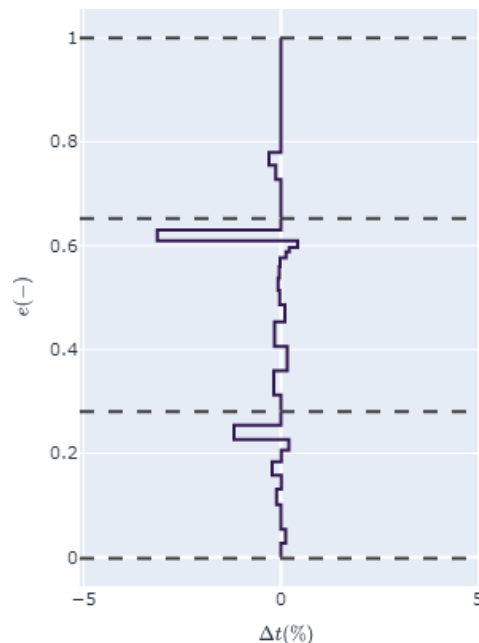


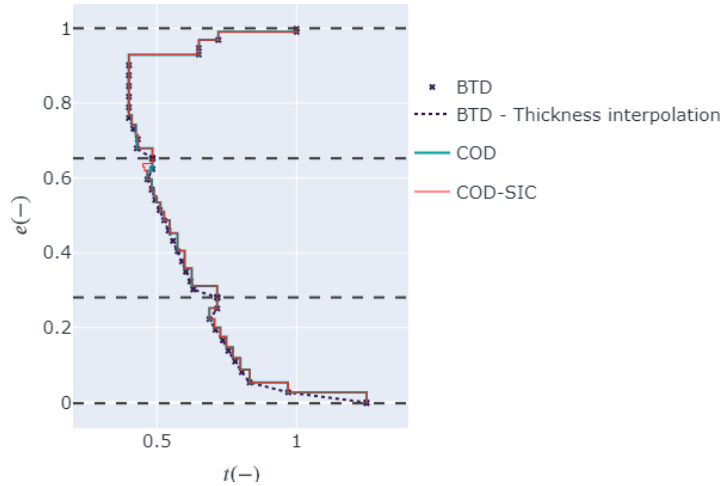
Figure 4.18: Thickness deviation between COD and COD-SID.

Thickness deviations away stress concentration factors

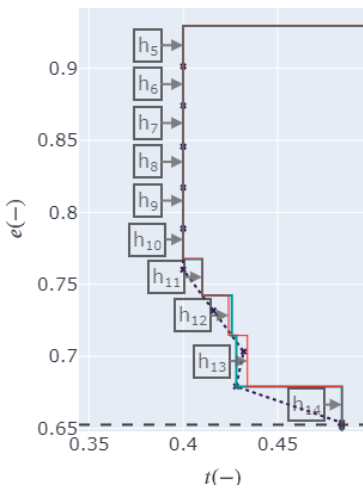
In the middle part of sections 2 and 3, the relative difference between the COD and COD-SID are small $\Delta t < 0.3\%$. This means the cost estimates in this part of the section will be very accurate.

Thickness deviations at stress concentration factors

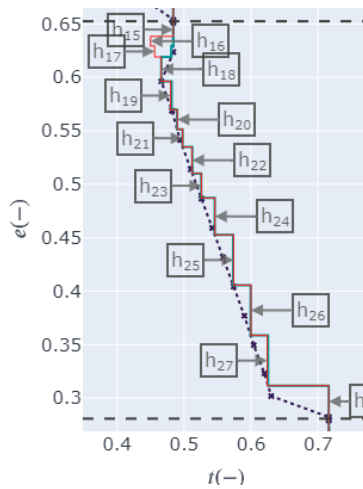
The differences in cost and mass of section 1 and 2 can be explained by figures 4.19b and 4.19c. They are caused by attachments and shells modeled with a local stress concentration factor, which increases the shell thickness. This effect can be seen in shells 13, 15, and 29. The shell thickness constraint is implemented by the linear interpolation of the BTD, which is very coarse due to the limited amount of points that are available. Because the optimizer is forced to follow this coarse thickness distribution, the thickness of the COD is off near the stress concentration factor.



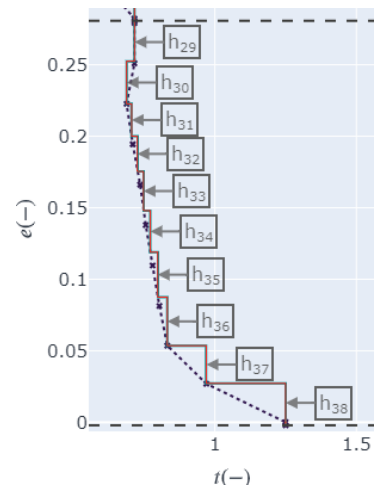
(a) Full tower.



(b) Section 1.



(c) Section 2.



(d) Section 3.

Figure 4.19: Thickness distributions for the COD and COD-SID.

4.6.3. Convergence in tower design loop

The convergence between the SID and COD was tested by running the tower design loop 12 times. The time per loop is roughly 15 minutes which resulted in total in a run time of 3 hours. In a regular engineering setting, this is a reasonable time for cost optimization. In each loop, the cost optimization model was run 100 times with a randomized start vector to increase the probability of finding the global optimum in each loop. The cost reductions per loop for section 1, 2, and 3 are given in figures 4.20a, 4.20b, and 4.20c respectively.

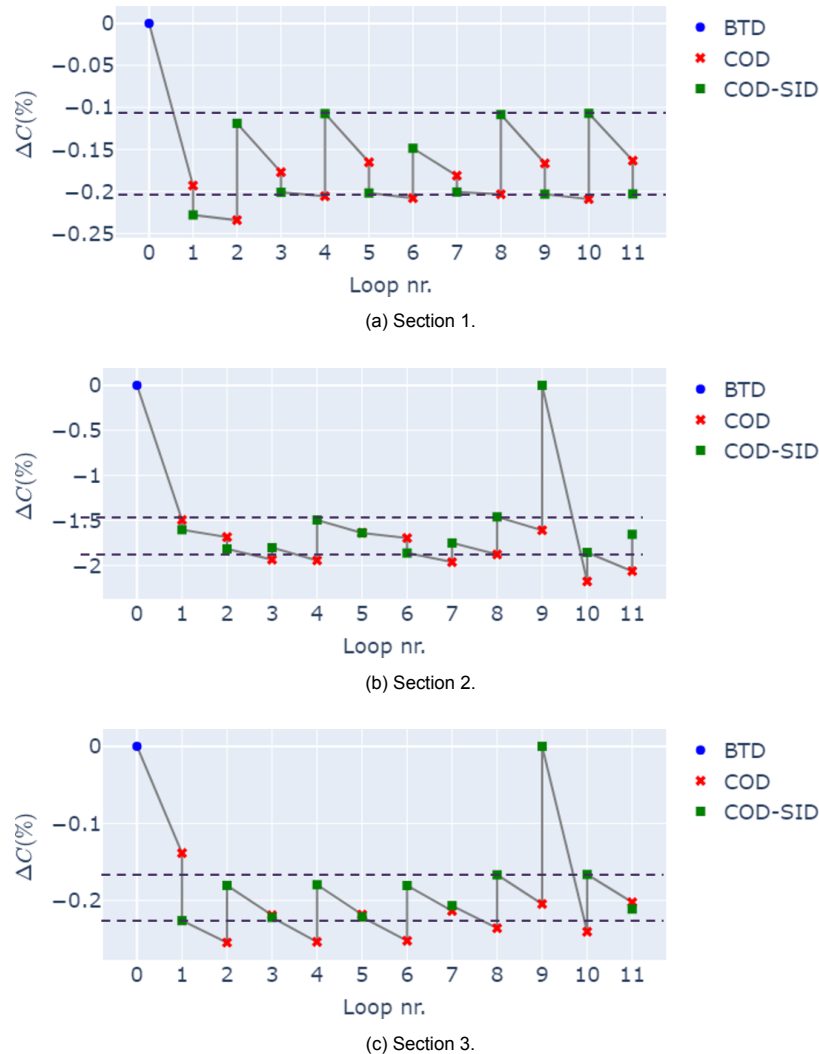


Figure 4.20: Cost results per section for the tower design loop.

No cost convergence

What can be observed is that for none of the sections, the tower design loop converges. In each case, the cost optimization model finds a better design, but the tower design software has to increase the shell thicknesses in some designs.

Patterns in tower design loop

On closer inspection of the figures, a pattern can be observed for each section. In sections 1 and 3, the cylindrical sections, the pattern repeats every two loops. In section 2, the pattern appears to repeat every four loops, but more iterations have to be run to verify the pattern. The phenomenon occurs because the cost optimization model uses the thickness interpolation of the COD-SID of the previous loop. Because of the changes in design, the objective function has different behavior. The

cost reductions also appear to stay within bands. The upper and lower band values are given in table 4.6. This gives some stability to the tower design loop.

Table 4.6: Bandwidths of the tower design loop

	Lower ΔC	Upper ΔC
Section 1	-0.20	-0.11
Section 2	-1.86	-1.46
Section 3	-0.22	-0.18

4.6.4. Mitigation of the vulnerabilities

The vulnerabilities can be mitigated by tweaking the tower design loop. Two changes are made. Firstly, in the number of cost optimization model iterations and secondly in the tower design loop iterations. The final tower design loop is shown in figure 4.21. Each mitigation is explained in its own paragraph.

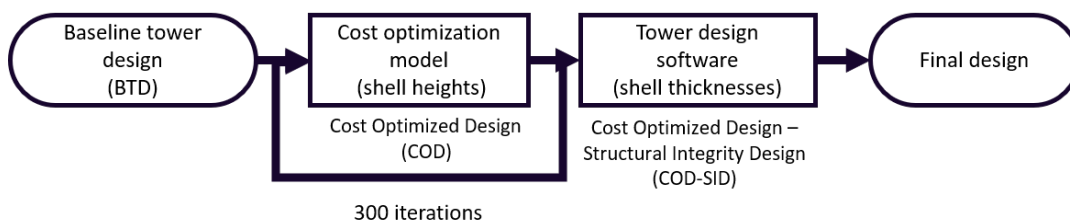


Figure 4.21: Steps in the cost optimization model.

Number of cost optimization model iterations

The local minima study has shown that the cost optimization model has many local minima. Especially for section 2, a range of minima was observed. To mitigate this vulnerability, the cost optimization model was run 300 times in every iteration of the larger tower design loop. The section design with the largest cost reduction was used. This brute force approach increases the chance to find the global minimum, although it is impossible to know for sure if the global minimum was found.

Number of tower design loops

The convergence study has shown that the best design for sections 1 and 3 was found after one iteration, while in section 2, after two iterations, the lower bandwidth was reached. The tower design comparison showed little changes in thickness distributions. Because the cost reduction yields good results after one iteration, the choice was made to simplify the tower design loop to make just one loop. In future research, a method to stabilize the tower design loop has to be found.

Performance of the tower design loop

In the current implementation, the tower design loop takes 27 minutes to run for a new project, as can be seen in table 4.7. The tower design software takes 6 minutes is ran twice; first, to establish the BTD, the second time to ensure the structural integrity of the tower. The cost optimization takes roughly 15 minutes to complete. The cylindrical sections require fewer iterations than the conical ones.

Table 4.7: Tower design loop performance.

	Cost optimization model	Tower design software	Total
Iteration time	+/- 3 s	+/- 6 min	-
Iterations	300	2	-
Cost optimization time	15 min	6 min	27 min

5

Case studies

Three scenarios were developed to test the tower design loop in, a high manufacturing cost, a lower manufacturing cost, and a high material cost scenario. The first two scenarios are explained in a dedicated section. Each section starts with an explanation of the scenario parameters, which is followed by the cost analysis and the tower design comparison. A problem with the optimizer is that the number of shells per section is an input. The effect of varying the number of shells is studied at last in section 5.3.

5.1. High manufacturing cost scenario

The first case study is the high manufacturing cost scenario, such as manufacturing the tower in Europe or the US. In paragraph 5.1.1, the cost functions and cost breakdowns per section are given. Knowing the relative share of each cost function in the total is important for interpreting the results. The cost analysis is given in paragraph 5.1.2, and the section is ended with a tower design comparison.

5.1.1. Scenario parameters

The supply chain consists of supplier 1 and manufacturer 4. The cost functions for material procurement, material transport and manufacturing cost are given in sections 3.3, 3.4, and 3.5 respectively. All time-dependent cost functions and discrete choices have been set to constant values in the optimization. The implemented cost functions are explained in the first paragraph. With these cost functions and the BTM, a breakdown per cost function per section can be made, explained in the last paragraph.

Changes to the cost model

In the material procurement phase, the steel price and CO₂ fluctuate over time. These time-dependent cost functions are set to a constant value in the cost optimization model.

The steel grade and the number of shells per section are discrete choices. Direct-search methods do not handle discrete choice well. This problem is resolved by using inputs for the decisions in the model and leave them out of the optimization variables. For the steel grade, this is not a big issue as most offshore towers are made from the same steel grade. However, the number of shells in a section can change per design and can influence costs to a large extent. The number of shells determines the number of the design variables. Unfortunately, the optimizer cannot handle a varying number of design variables; thus, this input is kept constant. To evaluate the effect the number of shells has on production, the sensitivity study in section 5.3 was done.

Cost breakdowns

The relative share of each cost function in production cost affects the focus of the optimizer. From figure 5.1 can be derived that roughly 35% can be attributed to material and material transport cost, which depend heavily on plate mass. About 50% of production cost is beveling and welding cost, where the cost driver is welding volume.

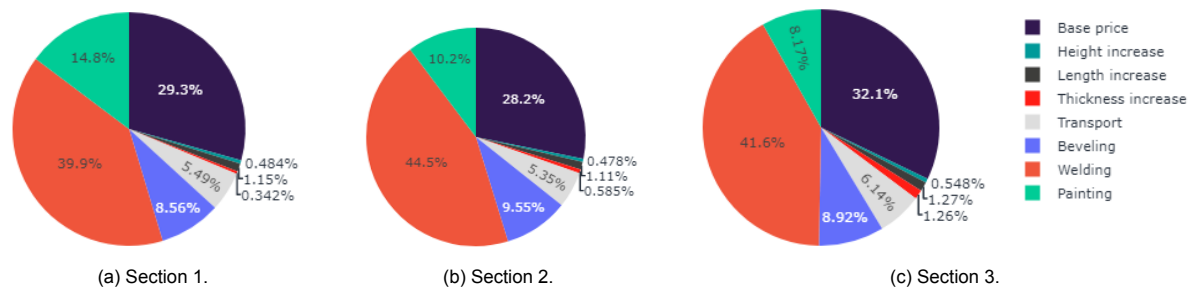


Figure 5.1: Section cost breakdowns of the baseline tower design for supplier 1 and manufacturer 4.

5.1.2. Cost analysis

The cost reductions per section and phase are given in table 5.1 and visually shown in figure 5.2. What can be derived is that the production cost has decreased for all sections in the Cost-Optimized Design (COD). The Tower Design Software (TDS) step actually reduced production cost even further. The production cost reductions were in all sections driven by the decrease in manufacturing costs. With these results, several aspects of the optimizer can be analyzed.

The effect of optimizing shell heights

The use of shell heights as design variables enables a trade-off between material, transport, and manufacturing cost. This is proof that optimizing shell heights are one valid approach to optimizing for production cost.

Manufacturing cost over material cost

The reduced production cost is primarily the result of the decreased manufacturing cost, which has a roughly 50% share of production cost. Manufacturing cost depends on the weld volume, and apparently, the benefit of reducing weld volume outweighs the increase in material and transport costs. This effect is seen in all sections, although most extreme in section 2. This shows the importance of including manufacturing costs in the tower optimization process.

Cost differences between COD and COD-SID

The COD and the COD-SID show deviations in their cost results and shell masses. This indicates that the post-processing SID changes the tower design slightly. The largest difference is seen in section 2, where the SID reduced costs even more. The changes in sections 1 and 3 are relatively small. These deviations show there is an inaccuracy in the structural integrity assumptions in the optimization model. In the tower design analysis, these effects are studied in-depth.

Tower mass \neq material cost

In all cost-optimized sections, the change in mass does not equal the change in material cost. Although the changes are minor, they do indicate that the material cost functions concerning plate height c_h , length c_l , and thickness c_t play a role in the search for the optimal design. Moreover, it is the first to prove that a minimum mass design does not equal a minimum cost design.

Minimum cost \neq minimum mass

The results for all sections show that the lowest cost was achieved by increasing section mass in order to reduce the manufacturing cost. This contradicts the current assumption in the industry that the lowest mass equals the lowest cost.

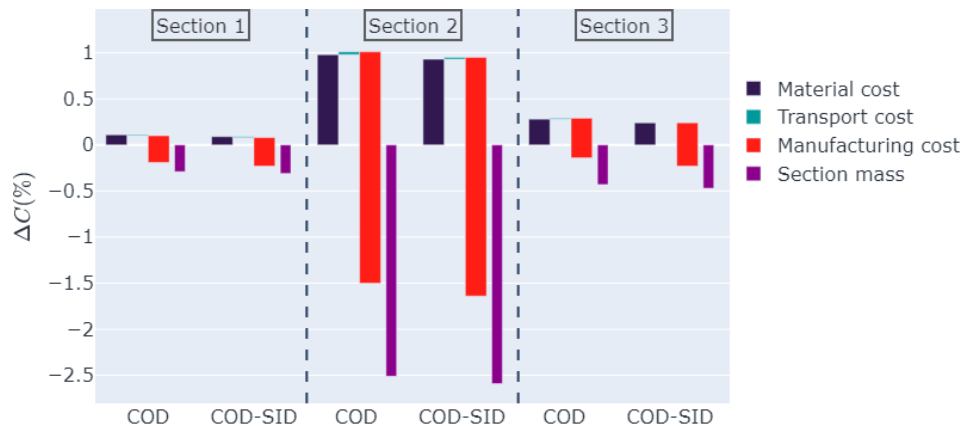


Figure 5.2: Optimization cost deviations per section.

Table 5.1: Results for the COD and COD-SID. Comparison against the baseline tower design.

		COD	COD-SID
Section 1	Production cost	-0.19	-0.23
	Material cost	0.11	0.09
	Transport cost	-0.01	-0.01
	Manufacturing cost	-0.29	-0.31
	Shell mass	-0.09	-0.13
Section 2	Production cost	-1.50	-1.64
	Material cost	0.98	0.93
	Transport cost	0.03	0.02
	Manufacturing cost	-2.51	-2.59
	Shell mass	0.78	0.63
Section 3	Production cost	-0.14	-0.23
	Material cost	0.28	0.24
	Transport cost	0.01	0.0
	Manufacturing cost	-0.43	-0.47
	Shell mass	0.20	0.10

5.1.3. Tower design analyses

The cost results in the previous paragraph can be explained by a comparison of the Baseline Tower Design (BTD), Cost-Optimized Design (COD), and Cost-Optimized Design - Structural Integrity Design (COD-SID). With the designs at hand, the reduction of the manufacturing cost and the increase in material cost can be explained.

Reasons for the manufacturing cost reductions

The manufacturing cost reduction results from the elongation of the bottom shells and the shortening of the top shells in each section. This effect can be seen especially well in figure 5.3c. Shell heights 25, 26, 27, and 28 visibly increased, while shell heights 15, 16, 17, and 18 decreased. The reason is that the top part has a lower thickness, which requires less weld volume to join plates together. In the bottom part, the shell thickness is higher, which increases the weld volume needed to join plates. The shell thickness is constrained to the BTD thickness interpolation line. Therefore, it becomes beneficial to raise the height of the bottom plates to reduce the required weld volume. The benefit overrules the increase in material cost.

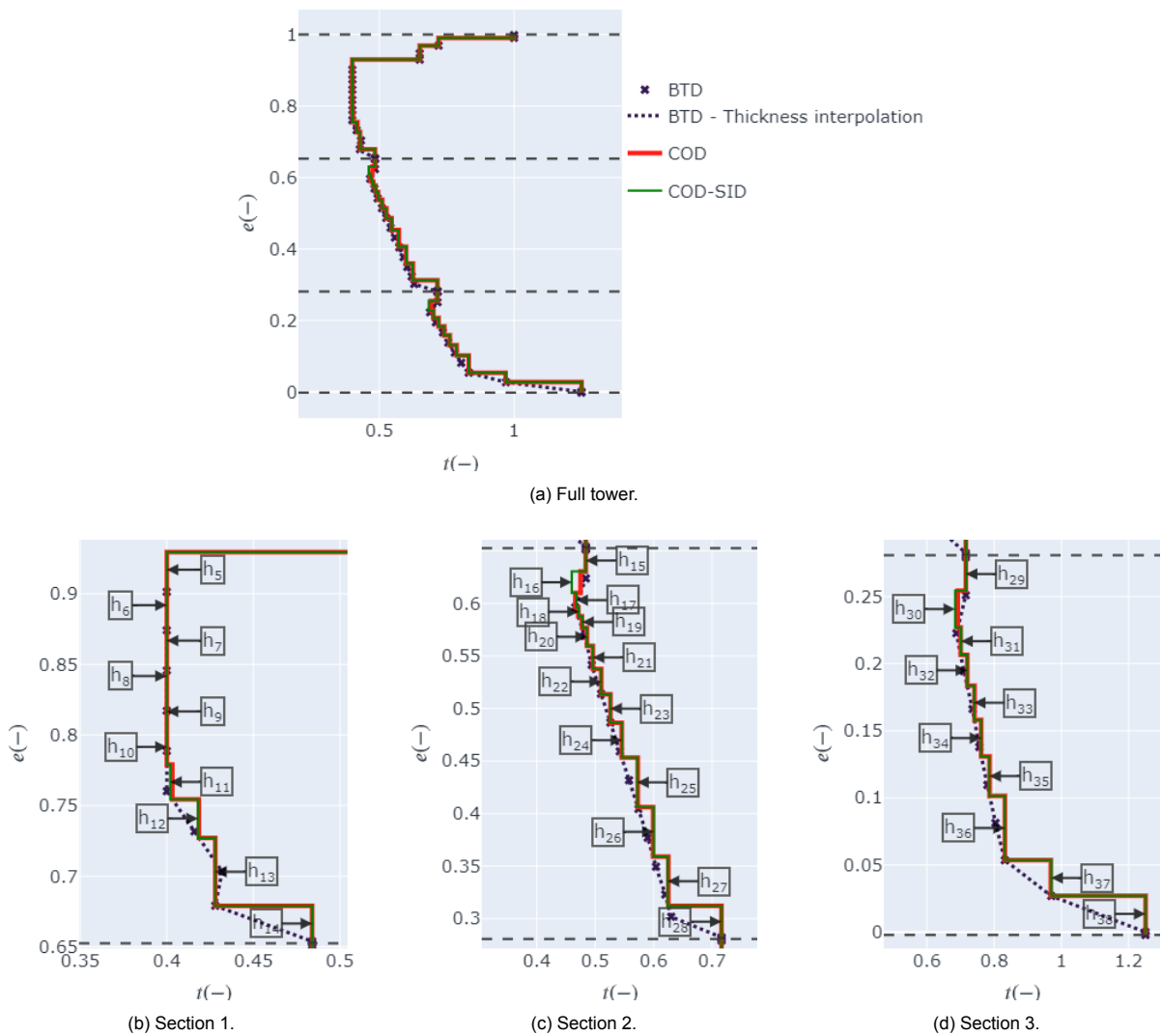


Figure 5.3: Thickness distributions for the BTD and COD.

Effect of plate height cost function

The high shells at the bottom of the plate and low shells at the top increase the plate height cost function. This can be observed in the COD cost breakdown for section 2, shown in figure 5.4. The share of the plate height cost increased from 0.48% in the BTD to 1.32% in the COD. The difference in costs explains the deviation between the section mass and material cost changes.

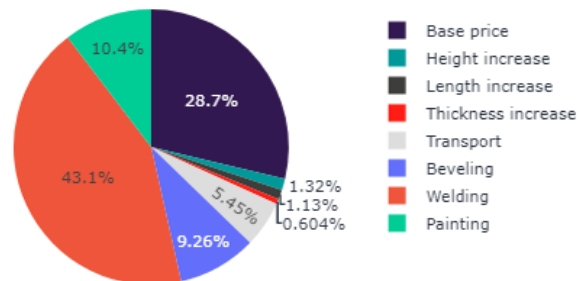


Figure 5.4: COD cost breakdown of section 2.

5.2. Low manufacturing cost scenario

The idea behind the low manufacturing cost scenario (CS2) is that it represents a manufacturer in Asia. Comparing the results from this scenario against the Europe/US scenario (CS1) can show the effect a different supply chain has on tower design. First, the scenario parameters are discussed. This is followed by a cost analysis of the Europe/US COD-SID and the Asia COD-SID with the current scenario parameters. The section ends with a comparison in tower designs.

5.2.1. Scenario parameters

The case study parameters from paragraph 5.1.1 are used and the manufacturing cost functions are scaled by a factor of (1/3), shown in figure 5.5.

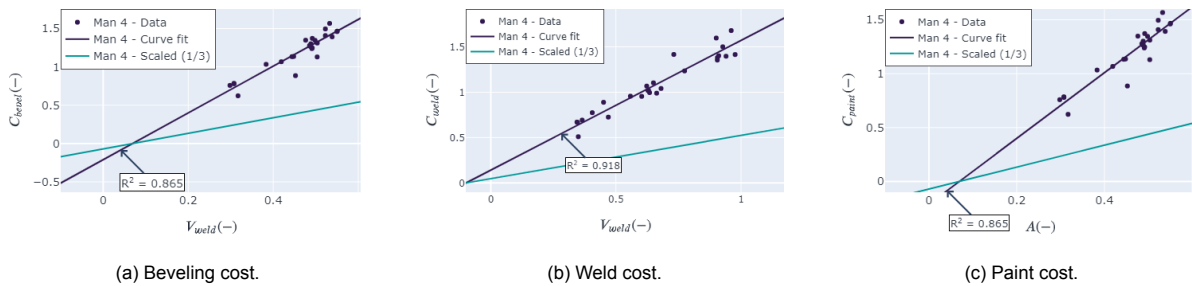


Figure 5.5: Scaled manufacturing cost functions used in case study 2.

The cost breakdowns that follow from the scaled manufacturing cost functions are shown in figures 5.6a, 5.6a, and 5.6a. For all sections, the share of beveling and welding cost reduced from 55% in the Europe/US scenario to roughly 30% of production cost in the Asia scenario. This is due to the fact that the material and material transport costs remained the same while the manufacturing cost decreased.

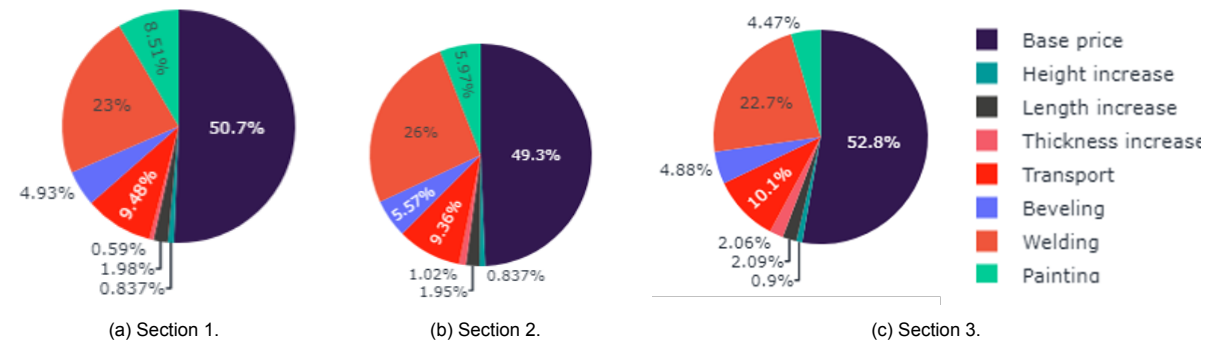


Figure 5.6: Section cost breakdowns of baseline design for supplier 1 and the scaled manufacturing cost functions.

5.2.2. Cost analysis

The cost of the Europe/US and the Asia COD-SID is calculated with the Asia cost functions and compared against the BTD costs. The comparison shows the effect of designing a tower for one manufacturer while it will be built by another manufacturer. The results can help identify the effect of the supply chain on the optimum design of the tower.

Effect of supply chain

The cost reductions for the Europe/US (CS1) and Asia (CS2) design are given in table 5.2 and visually shown in figure 5.7. All sections designed for the Europe scenario show an increase in production cost if it is built in Asia. The reason is that the reduction was driven by lower manufacturing costs. Unfortunately, in the current setting, manufacturing makes up a smaller share of production costs which decreases this effect. The result is most striking for the conical section 2, where the cost reduction was $\Delta C = -1.64\%$ and increased to $\Delta C = 0.04\%$.

If the tower was designed for the Asia supply chain, the sections would show a small cost reduction. The largest cost reduction can be observed in section 2, with a $\Delta C = -0.27\%$.

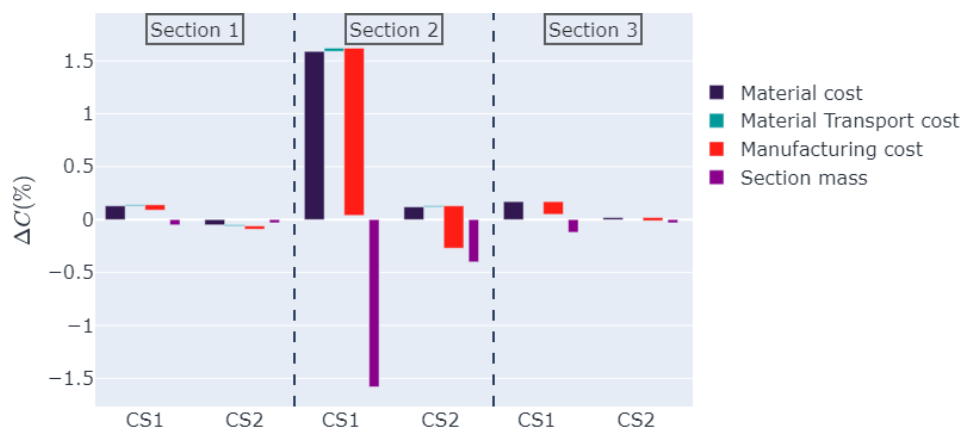


Figure 5.7: Phase costs and section mass results for the COD-SID-CS1 and COD-SID-CS2.

Table 5.2: Results for the COD-SID-CS1 and COD-SID-CS2. Comparisons made against the baseline tower design of each case.

		COD-SID CS1 (CS2 parameters)	COD-SID CS2 (CS2 Parameters)
Section 1	production cost	0.08	-0.09
	Material cost	0.13	-0.05
	Transport cost	0.01	-0.01
	Manufacturing cost	-0.05	-0.03
	Shell mass	0.05	-0.04
Section 2	production cost	0.04	-0.27
	Material cost	1.59	0.12
	Transport cost	0.03	0.01
	Manufacturing cost	-1.58	-0.4
	Shell mass	0.52	0.07
Section 3	production cost	0.05	-0.01
	Material cost	0.17	0.02
	Transport cost	0.0	0.0
	Manufacturing cost	-0.12	-0.03
	Shell mass	0.01	0.0

5.2.3. Tower design comparison

The cost differences between COD-SID-CS1 and COD-SID-CS2 can be explained by their tower designs, shown in figure 5.8. The figure shows the shell thicknesses of the BTD with the purple marker 'x'. In figure 5.8a markers were added for clarity. In figure 5.8b and 5.8c, only the BTD markers are shown for the same reason.

Minor improvements in section 1

The attachment in section 1 at $e \approx 0.71$ increases the shell thickness locally. With a slight change in the height of shell 13, this bulge in thickness is eliminated. This is an unexpected benefit of cost optimization.

Smaller design changes in section 2

In section 2, the thickness distribution of CS2 is closer to the BTD than the design of CS1. The reason for this is the smaller impact a reduction of welding volume has on costs. In the BTD, the shell heights are equally distributed, which yields the least excess material. Because the relative share of material cost is larger in this scenario, the optimizer changes the design less.

The drawback is that the optimization does not push the shells to the top of section 2, while in CS1, that is the place where the largest mass reduction was found. This problem can be resolved by using a thickness distribution with a higher discretization (based on more shells in the section).

Negligible design changes in section 3

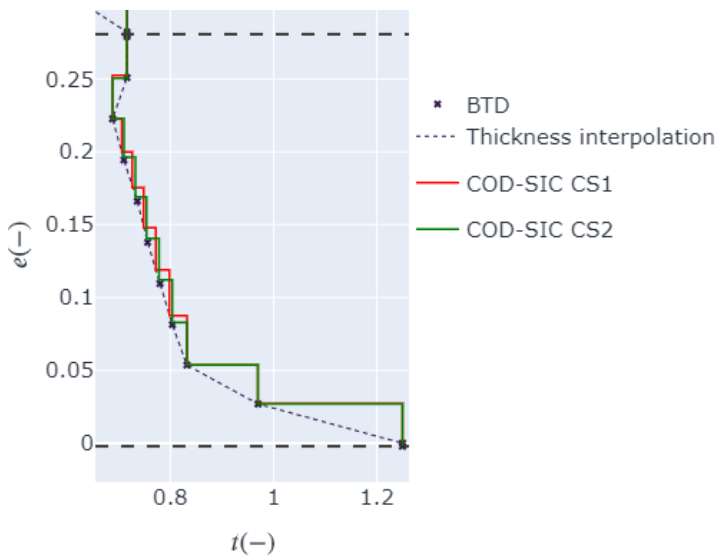
In section 3, the tower design of CS2 shows negligible differences compared to the BTD. The reason is that this section has very few 'effective' design variables. Changing the heights bottom two shells (37 and 38) and the top two shells (29 and 30) adds a large amount of excess mass. Therefore, the optimizer is unlikely to change these variables. This leaves only six shells in the middle part, while in section 2, there are 11 shells. Therefore, the optimizer has less freedom to change the shell heights.



(a) Section 1.



(b) Section 2.



(c) Section 3.

Figure 5.8: Thickness distributions for the BTD and COD.

5.3. Sensitivity study into number of shells

The previous case studies show that the largest cost reductions are due to lower weld volume. Another way to reduce weld volume is to reduce the number of shells in a section. This sensitivity study ran for scenarios CS1 and CS2, and a third extremely high material cost scenario CS3. The last scenario was added to explore an edge case with the cost optimization model.

5.3.1. Scenario parameters

The parameters of the previous scenarios are used. The fourth is a high material cost scenario. This simulates the current market conditions where the price for hot-rolled shells in the US is $c_{base} = 1800\$/tonne$. This scenario is simulated by scaling the material cost functions c_{base} , c_h , c_t , and c_l with a factor of three.

The number of shells per section is given in table 5.3. Only feasible designs, meaning the plate height constraint is not violated in the cost-optimized design, are evaluated. This determines the minimum number of shells per section.

Table 5.3: Parameters for the sensitivity study into the number of shells per section.

	N_{min}	N_{max}	N_{BTD}
Section 1	10	18	14
Section 2	8	18	14
Section 3	9	18	13

5.3.2. Cost analysis

The cost analysis was done based on the Cost-Optimized Design - Structural Integrity Design (COD-SID)s. First, the optimum number of shells is discussed, after which each section is analyzed separately.

Optimum number of plates

The results for sections 1 to 3 are shown in figures 5.9, 5.10, and 5.11 respectively. It shows that for scenarios 1 and 2, the lowest-cost tower designs have the least amount of shells. The largest cost reductions are found in the high manufacturing cost scenario, with a 15-20% decrease in cost per section. These designs also show the highest mass, which is a cost driver in the assembly and installation phase.

The different optimum in number shells is found in the high material cost scenario. The cost reductions are also a factor five smaller. It shows that the market circumstances also influence the optimum number of shells.

Cost reductions in section 1

Figures 5.9a and 5.9b show that the number of shells can be reduced to 11 without additional tower mass. Basically, this is a free lunch. For $N_{plates} = 10$, the mass increases roughly 1% in both scenarios, and the production cost decrease 16% and 7%. This incurs a trade-off with the assembly and installation costs because tower mass is a cost driver in those phases.

The cost reductions are mostly driven by the reduced number of plates, not by the cost optimization model. This conclusion is drawn because the cost reductions are an order larger than in the previous studies. Also, as the number of shell decrease, so does the freedom of the optimizer to change the shell heights. This limits the effect the optimizer has on tower design at a smaller number of shells.

The optimum number of shells changes in the high material cost scenario in figure 5.9c from $N_{plates} = 10$ to $N_{plates} = 12$. The price of excess material increased, which outweighed the decrease in weld costs.

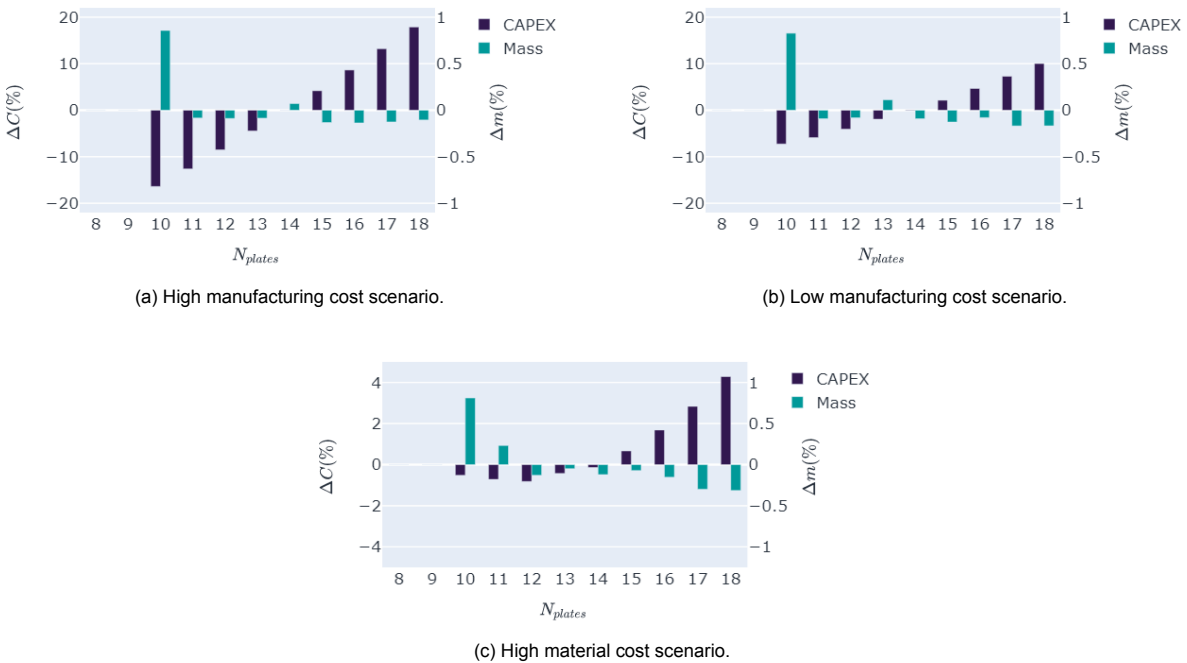


Figure 5.9: Results for varying number of shells in section 1 for several case studies.

Cost reductions in section 2

Section 2 is the section with the most local minima and has the largest benefit from cost optimization. For scenarios 1 and 2, the cost reductions are an order larger than the difference in local minima; thus, the effect is neglected.

In all scenarios, it is beneficial to reduce the number of plates. For the high and low manufacturing cost scenarios, the lowest production cost was achieved by using the minimum number of shells $N_{plates} = 8$. In the high material cost scenario (CS3), the lowest production cost was found at $N_{plates} = 9$. The cost reductions are also an order smaller than in scenarios 1 and 2.

The mass of section 2 appears to have a negative linear relationship with the number of plates in all figures. It is a logical conclusion if explained from the cost optimization perspective. The thickness interpolation is a continuous line, and the shell thicknesses are a discretization of that line. Therefore, a higher number of shells creates smaller bins and a better approximation of the interpolated line. This effect decreases the excess steel and lowers the section mass. The trend line figure 5.10a does show a higher trend line, which is caused by the high manufacturing cost. For $N_{plates} \leq 11$ the section mass increase is still relatively similar. However, for a higher number of shells, the difference in section mass increases. This is the consequence that in scenario 1, reducing weld length over the increase in section mass is more beneficial than in scenarios 2 and 3. Thus, as the number of shells increases and the optimizer gets more freedom to change the shell heights, this trade-off becomes more clear.

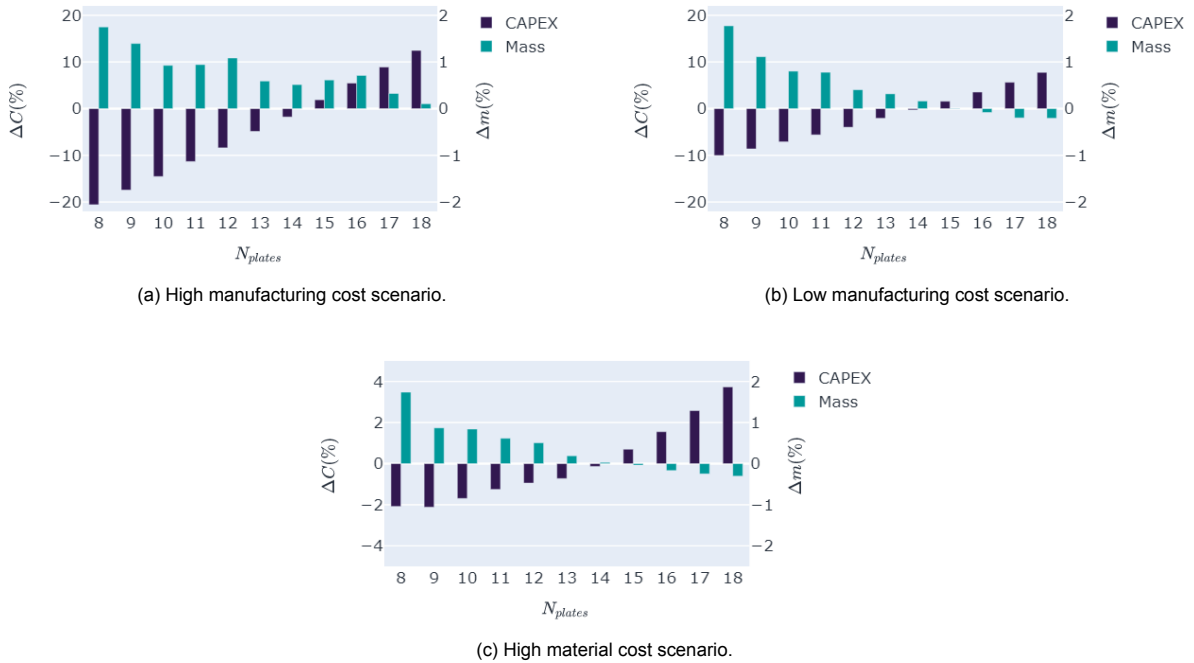


Figure 5.10: Results for varying number of shells in section 2 for several case studies.

Cost reductions in section 3

In section 3, the optimum number of shells varies for each scenario. In scenario 1, the minimum number of plates, $N_{plates} = 9$, gives a production cost reduction of 14.5%. For scenario 2, the optimum is $N_{plates} = 10$ and in scenario 3, the lowest cost is achieved by using $N_{plates} = 13$.

In scenario 1 in figure 5.11a, the optimum number of shells incurs a mass increase of 4.2%. Thus, the trade-off between cost reduction in the material procurement, material transport, and manufacturing phases has to be weighed against possibly higher costs due to additional tower mass in the section transport, assembly, and installation phases.

The results of scenario 2 in figure 5.11b shows production cost reduces with less number of shells in the section until $N_{plates} = 10$. The increase in cost for $N_{plates} = 9$ can be attributed to the large increase in section mass, which incurs additional material costs.

The optimum number of shells in scenario 3 is $N_{plates} = 13$, the same number as in the baseline tower design. The reason is that in this scenario, the material cost functions are scaled a factor 3. The section mass increases with the number of plates, and with the high material cost functions, the decrease in manufacturing expense does not outweigh the increase in material cost anymore. The share of the height cost function in production cost grows from 1.2% for $N_{plates} = 13$ to 5.4% for $N_{plates} = 9$, as can be seen in figure 5.11d.

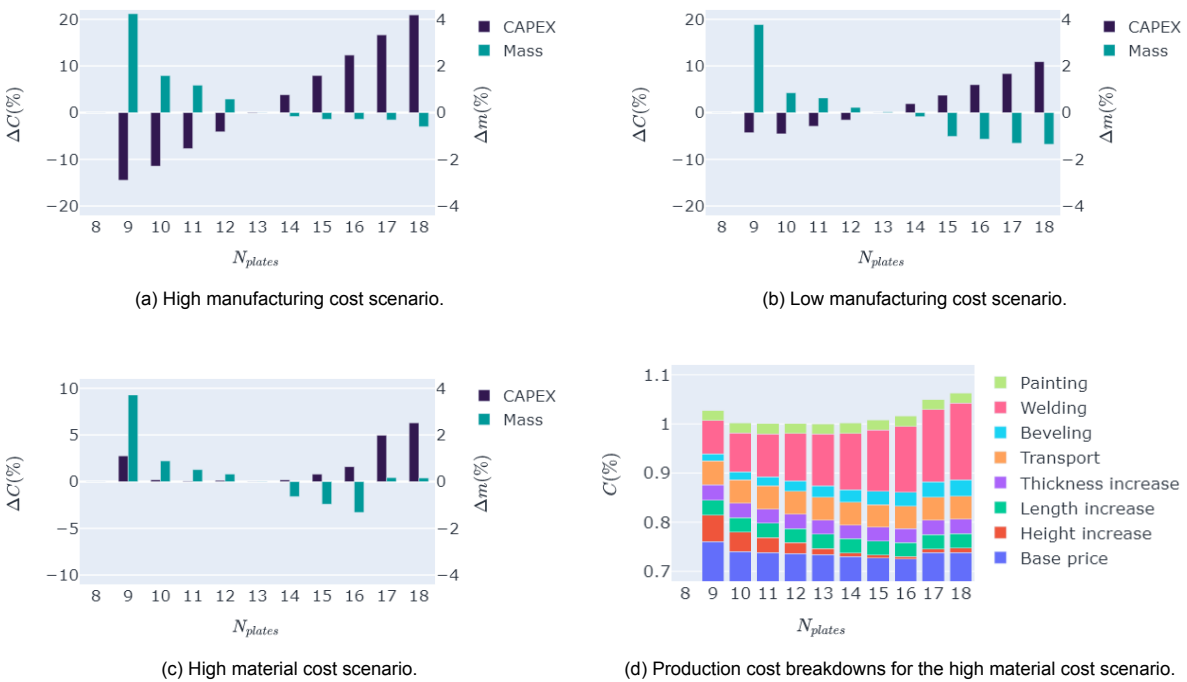
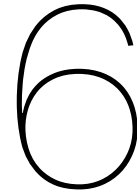


Figure 5.11: Results for varying number of shells in section 3 for several case studies.



Conclusions and recommendations

6.1. Conclusions

The goal of wind turbine manufacturers is to lower the cost of energy. One way to do so is to decrease the tower cost. Currently, the industry focuses on minimizing mass, assuming that mass is the main cost driver. Tower costs are estimated with a fixed steel price. Whole optimization methods are built on this assumption. However, the assumption is not validated, and engineers suspect that improvements can be made. This led the industry partner SGRE to ask the following thesis objective:

”Evaluate the production costs and tower design of a cost-optimized tower against a reference tower.”

In a literature study on tower cost optimization models, the main problem was identified. No detailed cost model was available for offshore towers. Therefore, the first objective was to develop a component-level cost model. The second objective was to propose a tower cost optimization model, and the final objective was to compare a cost-optimized tower against a reference tower on the differences in production costs and tower design. Each objective is discussed separately.

On the cost model

A cost model was built for the material procurement, material transport, and manufacturing phase. From the found cost function, it can be concluded that reliable cost estimates are possible if the cost functions from the three phases are included. The current approach, which uses a fixed steel price to estimate costs and justify the mass minimization, is shortsighted. In the material phase, it was found that the steel price suppliers charge is dependent on the plate dimensions. For extreme dimensions, the increase in steel price can be 22%. The newly added phases are the material transport and manufacturing phases. In the former, costs are a function of plate mass and length. In the latter, the most important parameters are weld volume and tower area. Mass does not play a role. To provide reliable cost estimates, engineers have to account for all cost functions.

Another conclusion is that one of the most important drivers in the cost model is the choice of supplier or manufacturer. Logically, each supplier and manufacturer has its own cost structure and asks for different prices. This results in unique cost functions per supplier and manufacturer. The implication of this finding is large for the cost optimization, which uses the cost functions to minimize costs. If the cost functions are highly dependent on the supply chain, the effect of varying the supply chain must be investigated.

On the cost optimization model

The proposed Cost Optimization Model (COM) optimized the shell heights of a section with fixed outer geometry. The result is a Cost-Optimized Design (COD) which may not be structurally sound. That is what the Tower Design Software (TDS) does. It calculates the minimum required shell thickness for the Structural Integrity Design (SID). The iterating between Cost Optimization Model (COM) and

Tower Design Software (TDS) gives a tower design loop. The idea was that the loop has to convergence to a design where the COD and SID are the same.

It can be concluded that the tower design loop minimizes production costs with structurally sound designs. Unfortunately, no convergence was achieved between the COD and SID, but the cost results for both designs stay within a reasonable bandwidth. The COM has a local minima problem. Cylindrical sections showed few dominant minima, resulting from a local minimum in a material cost function. Developing a different cost function can solve this problem. In the conical section, the minima were spread over a range, which was the result from the additional function that was applied to calculate the shape of rectangular steel plate for a conical section. This last problem is hard to mitigate.

On the production costs and tower designs

Two tests were run to study the influence of different cost functions (the supply chain) and one sensitivity study in the optimum number of shells per section. In the first two tests, the tower design loop ran for a high manufacturing cost and a low manufacturing cost scenario. The production costs were analyzed per section production phase. In the final test, the tower design loop ran for a range of shells in three cost scenarios, high and low manufacturing costs, and high material costs. The results were the changes in cost and mass per section.

It can be concluded from the sensitivity study that the lowest cost design has the minimum amount of shells possible, except in the high material cost scenario. However, this design also showed a large increase in section mass $\Delta m \approx +2 - 4\%$. Therefore, engineers have to assess to what extent the mass increase affects costs in the assembly and installation phase.

Another conclusion is that the COM is most effective in conical sections, with cost reductions of $\Delta C \approx -1.9\%$. However, in the cylindrical sections, the reductions were in the range of $\Delta C \approx -0.2\%$.

The last conclusion is that the engineers have to design towers for the supply chain. It was found that the cost reductions for a section optimized for supply chain A were be eradicated if it is built by supply chain B. This is the consequence of the different cost functions in each supply chain.

Proposed engineering guidelines

The conclusions can be rewritten to general engineering guidelines. These guidelines are steps that can be followed at the start of each project.

1. Perform the sensitivity study at the start of a project.
2. Assess the mass induced costs from the assembly and installation phase.
3. Choose the optimum number of shells.
4. Design the tower for the supply chain.

6.2. Recommendations for future research

Given the conclusions mentioned above and a reflection on the thesis, several recommendations for future research are given.

Research into cost modeling

In future research, a cost model for flanges has to be developed. In the current COM, the outer geometry was fixed, and the flange dimensions do not change. However, if a study into the optimum section dimensions is done, the flange costs can play a vital role.

Another improvement can be made in the accuracy of the welding and painting cost function. For the welding cost, including the weld shape can improve the curve fit. For the painting cost, the cost of paint material fluctuations can be studied.

Another improvement is to extend the quantitative cost model with functions for the section transport, assembly, and installation phase. If the section dimensions are included in the optimization, they will definitely affect costs in these phases. The

Research into cost optimization

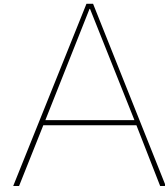
In future research, a genetic algorithm is proposed for cost optimization. The reason is threefold. First, the largest cost reductions were achieved by varying the number of shells in a section. However,

this is a discrete input that is hard to handle for gradient-based and direct search algorithms. A genetic algorithm handles discrete inputs better. Secondly, the optimization showed a lot of local minima, especially in the conical middle section. A genetic algorithm is more likely to find the global optimum efficiently. Finally, the computation time of one cost optimization model iteration is below one second. One of the benefits of using gradient-based and direct-search algorithms over genetic algorithms is the shorter computation time. If the genetic algorithm would take 1000 times longer, it would still only be 15 minutes, which is reasonable in an engineering context. Therefore, the drawback of genetic algorithms is not an issue.

The second topic for future research would be to include the outer geometry in the optimization routine. However, changing the outer geometry has a major influence on the vessel stow, which is the main cost driver in the section transport phase. Also, this would change the flange dimensions, and a cost function for the flange has to be found.

Minimum CO₂ design

It is known that steel production and transport are large producers of greenhouse gasses. The cost model approach can also be used to develop a tower CO₂ emissions model per phase. Several researchers have studied the emissions of CO₂ for steel and transport; thus, a model can be built. With such a model, multi-objective optimization can be done to see the trade-off between tower cost and CO₂. This may be an interesting study with the increasing pressure from society and governments to reduce greenhouse gasses.



Qualitative interview data

Table A.1: Answers to interview questions.

Date	12/10/2020
Topic	General cost modelling
Phase	All
Job title	Quotation engineer
Question	
1	Material: net and gross tower weight, plate and flange dimensions, steel grades, number of sections, flange types, testing, manufacturing location. Material transport: Transport can be done either by road or sea transport. Road is cheaper than sea. There are road limitations on plate length, flange diameter and mass. No knowledge on other phases.
2	No knowledge on specific cost estimation techniques. Must check with other cost engineers. -
3	No knowledge on cost modelling. Please check with other engineers. -
4	Yes. [Cost engineer], [Material procurer], [Project manager], [Production procurer]
Date	10/11/2020
Topic	Optimizing for cost in the offshore tower design process
Phase	-
Job title	Tower engineer
Question	Phrase
1	Tower mass contributes most to tower costs.
2	Other wind energy players use a constant cost factor, which is often the steel price. However, this can be improved.
3	We do not know if the cost model (Farkas) is correct. It is the only model I found in literature for modelling tower costs.
4	No
Date	12/15/2020
Topic	Cost engineering for offshore towers
Phase	All
Job title	Cost engineer
Question	Phrase
1	Main driver is material cost.

	In manufacturing, the cost of manufacturing materials vary per manufacturer. of weld, weld material
	... Cutting, beveling, rolling, welding and painting contribute to about 80% of manufacturing costs. The rest is storage, handling of materials, ...
	For cutting, the cut length is most important.
	... beveling cost are influenced by the type of the weld, bevel length and plate thickness.
	Rolling the plate length and thickness are most influential
	The type of weld, weld volume and testing influences the weld costs
	Painting is dependend on the area and the cost of paint materials.
2	Never seen this before. It can be right but
3	Material: The cost factor (price per tonne) is dependend on tower parameters. Therefore, using a fixed cost factor is not sufficient.
4	No
Date	2/5/2021
Topic	Procurement of materials
Phase	Material
Job title	Material procurer
Question	Phrase
1	The plate costs depend on plate width, height, length
	Steel grade has a large impact
	Non-destructive testing influences the plate costs tremendously
	Cost factor varies per plate manufacturer
	Flange cost are dominated by the diameter and weight
	... little reliable data on flange cost is available.
	Flange and plate are the largest driver of material cost. Other components are the internals and bolts.
2	Step wise increase in cost factor adder.
3	Material costs can be modelled with a base price (cost factor) and adders (cost factor increases). The adders are dependent on the plate height, width, length, steel grade and type of testing. A fixed base price (cost factor) does cover the fluctuating cost factor.
4	[Production procurer]
Date	2/9/2021
Topic	Pre-assembly costs
Phase	Assembly
Job title	Project manager
Question	Phrase
1	Assembly strategy affects the phase cost to most.
	Crane costs are the second largest cost component. The crane day-rate depends on the type of crane which is selected based on the maximum section mass and tower height.
2	Manual calculation of assembly costs.
3	No cost model available.
4	[Commercial site manager]
Date	11/2/2021
Topic	Pre-assembly strategies and costs
Phase	Assembly
Job title	Commercial site manager
Question	Phrase

- 1 Land lease are largest cost component. The required area a matter of decision-making towards the uncertainty of inflow and outflow of turbine components. There are two components to the land-lease, the buffer area and the assembly area. A large buffer area allows for more flexibility on the inflow and outflow of components but increases the assembly phase costs.
The strategy depends on the reliability of the inflow and outflow. The inflow can be affected by problems of all previous steps in the supply chain. The outflow can be affected by the installation downtime due to weather.
- 2 Manual calculation of assembly costs.
- 3 No cost model available.
- 4 -

Date 12/2/2021
Topic Procurement of flanges
Phase Material
Job title Material procurer
Question Phrase

- 1 Flange diameter is the most important cost driver.
Flange costs scale non-linear with diameter. After 7.2m, the cost have a large increase.
No useable data available for modelling costs.
- 2 Manual calculation of flange costs.
- 3 No cost model available.
- 4 -

Date 19-02-2021
Topic Cost of manufacturing towers
Phase Manufacturing
Job title Production procurer
Question Phrase

- 1 The manufacturing cost is mostly dominated by cutting, beveling, rolling, welding and painting.
Current cost estimation techniques fail to properly estimate costs.
- 2 Scaling the cost for each process with the tower mass. This does not yield good results. Deviations of 40%-50% are quite common.
- 3 [Farkas cost model] Might be useful. Never seen it and relationships look weird.
- 4 -

Date 24-02-2021
Topic Case studies on CAPEX costs
Phase All
Job title Project manager
Question Phrase

- 1 Tower mass is most important.
no data available on CAPEX of one project.
- 2 No knowledge of cost models.
- 3 No model presented
- 4 -

Date 2/26/2020
Topic Transport of sections
Phase Section transport

Job title	Transport procurer
Question	Phrase
1	The cost transport of sections highly dependent on the market conditions (amount of available ships, possibility of return freight) The section diameters, mass and length are most important. Costs depend on the vessel day rate and amount of trips necessary. However, determining the amount of sections that a vessel can have is a manual job. No model can grasp that cost dynamic. Therefore, modelling cost is not feasible for this phase.
2	[Irawan] Cost model is weigh to simplistic. Does not represent reality in any way.
3	We model the time for each action and manually determine the amount of ships and number sections per ship.
4	-
Date	8/3/2021
Topic	Cost in the installation phase
Phase	Installation
Job title	Installation procurer
Question	Phrase
1	Vessel rent is largest cost component in installation. Type of vessel is determined by the heaviest part to be lifted (usually a tower section) and the maximum height it can reach. Installation costs can increase a lot due to weather downtime. This is a complicated aspects to model.
2	Similar to Sarker cost model.
3	[Sarker cost model] The cost model is similar but simpler than what they use. The model of SGRE is extended with a weather downtime factor.
4	-

B

Derivation of plate dimensions

This chapter describes the derivation of the rectangular plate dimensions for cylindrical and conical shell. This is necessary for conical shells, because there is a cutting loss in the manufacturing process, shown in figure B.1. In the calculation for the cylindrical shell, described in section B.1, there are no cutting losses, which means the shell mass is equal to plate mass. For the conical shell, the rolled out shape is different from the rectangular plate and a formula is derived to make a more accurate estimate of the plate dimensions and mass, which affects the material costs. This derivation is explained in section B.2.

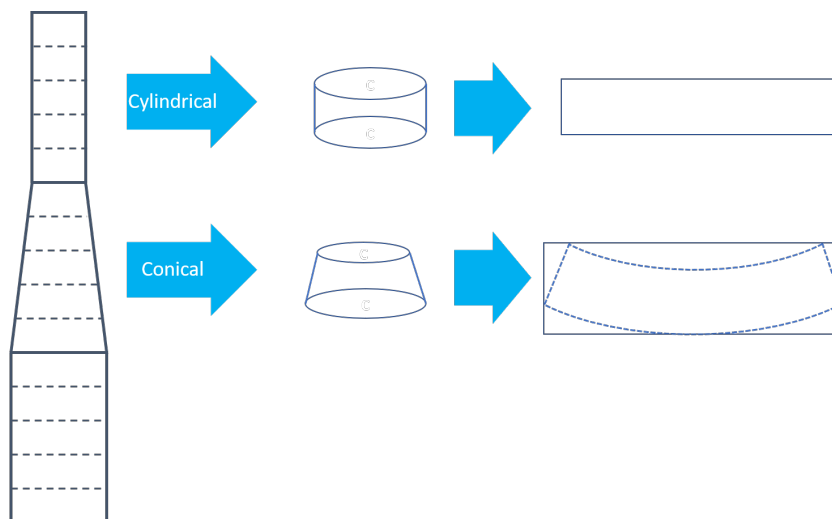


Figure B.1: Necessary plate shape for cylindrical and conical shells.

B.1. Cylindrical shell - plate mass

The plate mass of a cylindrical shell is given in equation B.1.

$$m_{plate_i} = \pi h d t \quad (B.1)$$

The shell height, diameter, and thickness are h , d , and t respectively.

B.2. Conical shell - plate mass

Determining the plate mass of a conical shell is done through trigonometry. The conical shell is rolled open which results in a banana-shaped plate or semi ring $ABCD$, as is shown in figure B.1. The rectangle encapsulating the semi ring is the area of the procured plate. The derivation of the plate height PR and length EF is as follows.

First, the sides AD and BC are extended to intersect in S . The top angle between lines DS and CS is theta θ and the length is l . The top circumference is equal to two times $l - h$ times θ , shown in equation B.2, and the bottom diameter is equal to two times l times θ , shown in figure B.3.

$$2(l - h')\theta = \pi d_1, \text{ where: } h' = \sqrt{h^2 + \left(\frac{d_1 - d_2}{2}\right)^2} \quad (\text{B.2})$$

$$2l\theta = \pi d_2 \quad (\text{B.3})$$

By isolating l in equation B.2 and substituting it in B.3 results in formula B.4 for theta. Isolating theta and substituting it in equation B.3 gives the equation for l in B.5.

$$\theta = \frac{\pi(d_2 - d_1)}{2h'} \quad (\text{B.4})$$

$$l = \frac{h'}{1 - \frac{d_1}{d_2}} \quad (\text{B.5})$$

With the top angle θ known, the plate height and length can be calculated through trigonometry, shown in equations B.6 and B.7 respectively.

$$PR = SR - SP$$

$$SR = l$$

$$SP = (l - h') \cos \theta$$

$$h_{plate} = PR = l(1 - \cos \theta) + h' \cos \theta \quad (\text{B.6})$$

$$EP = EA + AP$$

$$EA = h' \sin \theta$$

$$AP = (l - h') \sin \theta$$

$$l_{plate} = 2EP = 2l \sin \theta \quad (\text{B.7})$$

The mass of the plate is the area of the plate times the shell thickness, shown in equation B.8. Substituting equation B.6 and B.7 result in a formula that is only depend on the top diameter d_1 , bottom diameter d_2 , shell height h , and the thickness t . The formula $g_1(d_1, d_2, h)$ calculates the area.

$$m_{plate} = A_{plate}t = h_{plate}l_{plate}t \quad (\text{B.8})$$

$$= (1 - (l - h') \cos \theta) 2l \sin \theta t$$

$$= (l^2 (2 \sin \theta - \sin 2\theta) + lh' \sin 2\theta) t \quad (\text{B.9})$$

$$= g_1(d_1, d_2, h)t \quad (\text{B.10})$$

Plate mass vs. shell mass

Comparing the plate and shell mass of a conical section shows that the difference in mass is largest for small shell heights h and a large δd , as can be seen in the 3D plot in figure B.3c.

Two conclusions can be drawn from figures B.3a and B.3b. From the the former, it shows that the mass difference scales linearly with delta δ . The second figure shows that relative difference in mass scales inversely linear with the plate height. This shows that for small heights in the range

can be derived from figure B.3a, is that the difference between the plate mass m_{plate} and shell mass m_{shell} scales linearly with the increase in bottom diameter if the top diameter is fixed. This means that for conical shells with large differences in top and bottom diameter, the error in material cost can be large. Including this formula in the cost calculation yields a more accurate result.

$$d_1 = d_2 - 2\frac{h}{\tan \theta} \quad (\text{B.11})$$

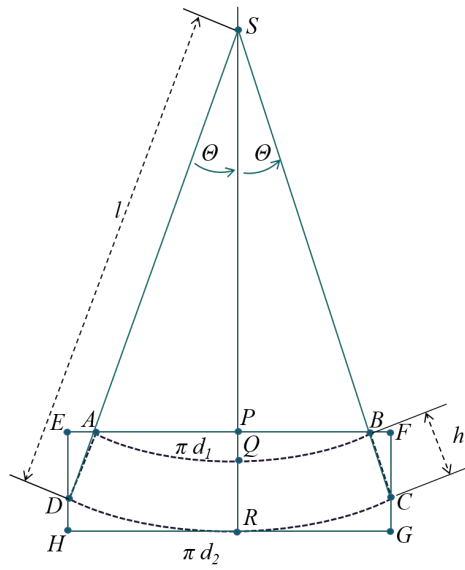
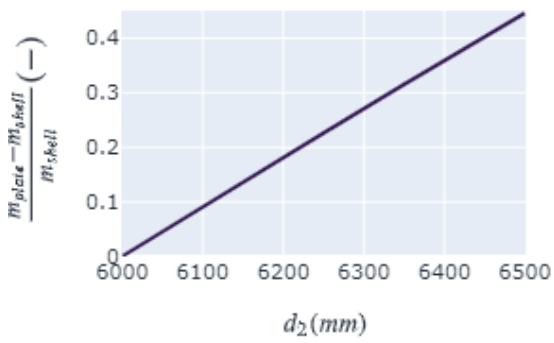
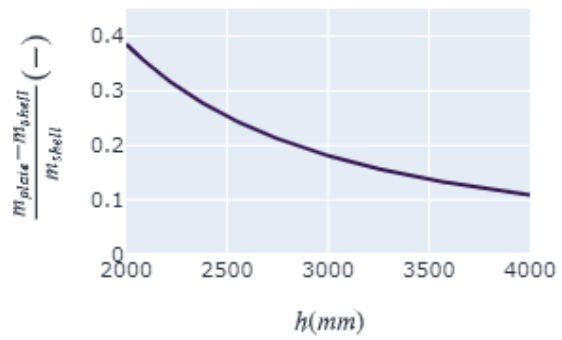


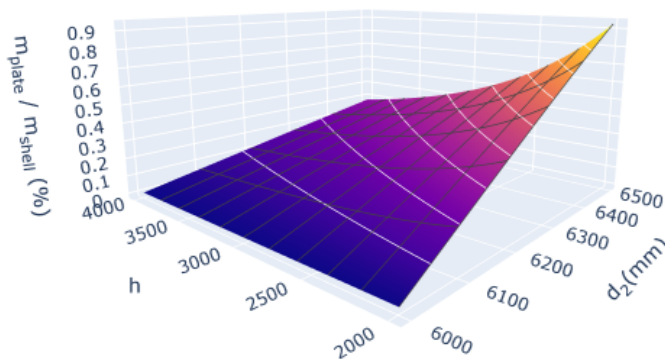
Figure B.2: Plate geometry of a conical shell.



(a) Mass difference w.r.t shell bottom diameter ($d_1 = 6000\text{mm}$, $h = 3000\text{mm}$).



(b) Mass difference w.r.t shell height ($d_1 = 6000\text{mm}$, $d_2 = 6200\text{mm}$)



(c) Mass difference w.r.t bottom diameter and shell height.

Figure B.3: Plate and shell mass difference w.r.t to shell height and bottom diameter.

References

- [1] M. Kauffman, “IPCC report: ‘Code red’ for human driven global heating, warns UN chief,” *UN News*, Aug. 2021. [Online]. Available: <https://news.un.org/en/story/2021/08/1097362#:~:text=%20IPCC%20report%3A%20%E2%80%98Code%20red%E2%80%99%20for%20human%20driven,out.%20The%20IPCC%20scientists%20warn%20global..%20More%20>.
- [2] International Electrotechnical Commission, *Wind energy generation systems. design requirements for fixed offshore wind turbines Part 3-1*, en. 2019, OCLC: 1121278946, ISBN: 978-2-8322-6600-7.
- [3] O. Nekeman and M. Zaayer, “A parametric cost model for offshore wind turbine tower design,” Ph.D. dissertation, Delft University of Technology, Dec. 2020.
- [4] I. sources, *Best practices in industry tower design and optimization*, 2020.
- [5] I. E. Commission, *Wind energy generation systems - Part 1: Design requirements*, 2018.
- [6] N. Maljaars, “Support structure optimization,” Ph.D. dissertation, Delft University of Technology, May 2017.
- [7] H. M. Negm and K. Y. Maalawi, “Structural design optimization of wind turbine towers,” en, *Computers & Structures*, vol. 74, no. 6, pp. 649–666, Feb. 2000, ISSN: 00457949. DOI: 10.1016/S0045-7949(99)00079-6. [Online]. Available: <https://linkinghub.elsevier.com/retrieve/pii/S0045794999000796> (visited on 12/07/2020).
- [8] P. Uys, J. Farkas, K. Jármai, and F. van Tonder, “Optimisation of a steel tower for a wind turbine structure,” en, *Engineering Structures*, vol. 29, no. 7, pp. 1337–1342, Jul. 2007, ISSN: 01410296. DOI: 10.1016/j.engstruct.2006.08.011. [Online]. Available: <https://linkinghub.elsevier.com/retrieve/pii/S0141029606003464> (visited on 12/07/2020).
- [9] J. Farkas and K. Jármai, *Optimum Design of Steel Structures*, en. Berlin, Heidelberg: Springer Berlin Heidelberg, 2013, ISBN: 978-3-642-36867-7 978-3-642-36868-4. DOI: 10.1007/978-3-642-36868-4. [Online]. Available: <http://link.springer.com/10.1007/978-3-642-36868-4> (visited on 10/30/2020).
- [10] M. Muskulus and S. Schaffhirt, “Design Optimization of Wind Turbine Support Structures—A Review,” en, *Journal of Ocean and Wind Energy*, vol. 1, no. 1, p. 12, 2014.
- [11] K. O’Leary, “Optimization of composite material tower for offshore wind turbine structures,” en, *Renewable Energy*, p. 15, 2019.
- [12] S. Yoshida, “Wind Turbine Tower Optimization Method Using a Genetic Algorithm,” en, *Wind Engineering*, vol. 30, no. 6, pp. 453–469, Dec. 2006, ISSN: 0309-524X, 2048-402X. DOI: 10.1260/030952406779994150. [Online]. Available: <http://journals.sagepub.com/doi/10.1260/030952406779994150> (visited on 09/28/2020).
- [13] F. Karpat, “A Virtual Tool for Minimum Cost Design of a Wind Turbine Tower with Ring Stiffeners,” en, *Energies*, vol. 6, no. 8, pp. 3822–3840, Jul. 2013, ISSN: 1996-1073. DOI: 10.3390/en6083822. [Online]. Available: <http://www.mdpi.com/1996-1073/6/8/3822> (visited on 09/28/2020).
- [14] R. Harrison and G. Jenkins, “Cost modelling of horizontal axis wind turbines,” Sunderland, UK, Tech. Rep. ETSU Report W/34/00170/REP, 1993, pp. 315–323.
- [15] L. Fingersh, M. Hand, and A. Laxson, “Wind Turbine Design Cost and Scaling Model,” en, Tech. Rep. NREL/TP-500-40566, Dec. 2006, NREL/TP-500-40566. DOI: 10.2172/897434. [Online]. Available: <http://www.osti.gov/servlets/purl/897434-Feoadi/> (visited on 09/04/2020).

- [16] T. Ashuri, M. Zaaier, J. Martins, G. van Bussel, and G. van Kuik, "Multidisciplinary design optimization of offshore wind turbines for minimum levelized cost of energy," en, *Renewable Energy*, vol. 68, pp. 893–905, Aug. 2014, ISSN: 09601481. DOI: 10.1016/j.renene.2014.02.045. [Online]. Available: <https://linkinghub.elsevier.com/retrieve/pii/S0960148114001360> (visited on 09/28/2020).
- [17] M. Shafiee, F. Brennan, and I. A. Espinosa, "A parametric whole life cost model for offshore wind farms," en, *The International Journal of Life Cycle Assessment*, vol. 21, no. 7, pp. 961–975, Jul. 2016, ISSN: 0948-3349, 1614-7502. DOI: 10.1007/s11367-016-1075-z. [Online]. Available: <http://link.springer.com/10.1007/s11367-016-1075-z> (visited on 09/18/2020).
- [18] C. A. Irawan, N. Akbari, D. F. Jones, and D. Menachof, "A combined supply chain optimisation model for the installation phase of offshore wind projects," en, *International Journal of Production Research*, vol. 56, no. 3, pp. 1189–1207, Feb. 2018, ISSN: 0020-7543, 1366-588X. DOI: 10.1080/00207543.2017.1403661. [Online]. Available: <https://www.tandfonline.com/doi/full/10.1080/00207543.2017.1403661> (visited on 11/12/2020).
- [19] B. R. Sarker and T. I. Faiz, "Minimizing transportation and installation costs for turbines in offshore wind farms," en, *Renewable Energy*, vol. 101, pp. 667–679, Feb. 2017, ISSN: 09601481. DOI: 10.1016/j.renene.2016.09.014. [Online]. Available: <https://linkinghub.elsevier.com/retrieve/pii/S0960148116308035> (visited on 11/01/2020).
- [20] P. Cicconi, V. Castorani, M. Germani, M. Mandolini, and A. Vita, "A multi-objective sequential method for manufacturing cost and structural optimization of modular steel towers," en, *Engineering with Computers*, vol. 36, no. 2, pp. 475–497, Apr. 2020, ISSN: 0177-0667, 1435-5663. DOI: 10.1007/s00366-019-00709-0. [Online]. Available: <http://link.springer.com/10.1007/s00366-019-00709-0> (visited on 12/07/2020).
- [21] M. Borrego, P. Douglas, and C. Amelink, "Quantitative, Qualitative, and Mixed Research Methods in Engineering Education," *Journal of Engineering Education*, Jan. 2019.
- [22] N. Chism, E. Douglas, and W. Hilson, *Qualitative Research Basics: A Guide for Engineering Educators*. 2008.
- [23] E. Jones, T. Oliphant, and P. Peterson, *SciPy: Open Source Scientific Tools for Python*, Apr. 2021. [Online]. Available: <http://www.scipy.org/>.
- [24] H. Gavin, "The Levenberg-Marquardt algorithm for nonlinear least squares curve-fitting problems," Sep. 2020.
- [25] P. Virtanen, R. Gommers, T. E. Oliphant, M. Haberland, T. Reddy, D. Cournapeau, E. Burovski, P. Peterson, W. Weckesser, J. Bright, S. J. van der Walt, M. Brett, J. Wilson, K. J. Millman, N. Mayorov, A. R. J. Nelson, E. Jones, R. Kern, E. Larson, C. J. Carey, Í. Polat, Y. Feng, E. W. Moore, J. VanderPlas, D. Laxalde, J. Perktold, R. Cimrman, I. Henriksen, E. A. Quintero, C. R. Harris, A. M. Archibald, A. H. Ribeiro, F. Pedregosa, and P. van Mulbregt, "SciPy 1.0: Fundamental algorithms for scientific computing in Python," en, *Nature Methods*, vol. 17, no. 3, pp. 261–272, Mar. 2020, ISSN: 1548-7091, 1548-7105. DOI: 10.1038/s41592-019-0686-2. [Online]. Available: <http://www.nature.com/articles/s41592-019-0686-2> (visited on 06/22/2021).
- [26] N. D. Lagaros and M. G. Karlaftis, "Life-cycle cost structural design optimization of steel wind towers," en, *Computers & Structures*, vol. 174, pp. 122–132, Oct. 2016, ISSN: 00457949. DOI: 10.1016/j.compstruc.2015.09.013. [Online]. Available: <https://linkinghub.elsevier.com/retrieve/pii/S0045794915002722> (visited on 10/30/2020).
- [27] DNV-GL, *Tower.Architect*, 2021. [Online]. Available: <https://www.dnv.com/services/tower-architect-185956> (visited on 04/19/2021).
- [28] Bentley, *Multiple software packages*, 2021. [Online]. Available: <https://www.bentley.com/en/solutions/wind-turbine-structure-design-and-analysis> (visited on 04/19/2021).
- [29] I. sources, *Material costs in the wind turbine tower production process*. Nov. 2020.
- [30] L. Lambert, "Steel prices are up 200%. When will the bubble pop?" *Fortune*, Jul. 2021. [Online]. Available: <https://fortune.com/2021/07/08/steel-prices-2021-going-up-bubble/> (visited on 08/11/2021).

- [31] MEPS, *Europe Steel Prices*, 2021. [Online]. Available: <https://www.meps.co.uk/gb/en/products/europe-steel-prices> (visited on 08/11/2021).
- [32] —, *North America Steel Prices*, 2021. [Online]. Available: <https://www.meps.co.uk/gb/en/products/north-america-steel-prices> (visited on 08/11/2021).
- [33] —, *Asia Steel Prices*, 2021. [Online]. Available: <https://www.meps.co.uk/gb/en/products/asia-steel-prices> (visited on 08/11/2021).
- [34] A. Hasanbeigi, M. Arens, J. C. R. Cardenas, L. Price, and R. Triolo, "Comparison of carbon dioxide emissions intensity of steel production in China, Germany, Mexico, and the United States," en, *Resources, Conservation and Recycling*, vol. 113, pp. 127–139, Oct. 2016, ISSN: 09213449. DOI: 10.1016/j.resconrec.2016.06.008. [Online]. Available: <https://linkinghub.elsevier.com/retrieve/pii/S0921344916301458> (visited on 08/11/2021).
- [35] T. W. Bank, *Carbon Pricing Dashboard*, 2021. [Online]. Available: https://carbonpricingdashboard.worldbank.org/map_data (visited on 08/11/2021).
- [36] I. sources, *Transport cost of sections from manufacturer to landing site*. Feb. 2021.
- [37] —, *Manufacturing costs and models for offshore wind turbine towers*. Feb. 2021.
- [38] —, *Assembly cost for offshore wind farms*. Feb. 2021.
- [39] —, *The state of the art of installation techniques for offshore wind farms*. Jul. 2021.
- [40] J. A. Nelder and R. Mead, "A Simplex Method for Function Minimization," en, *The Computer Journal*, vol. 7, no. 4, pp. 308–313, Jan. 1965, ISSN: 0010-4620, 1460-2067. DOI: 10.1093/comjnl/7.4.308. [Online]. Available: <https://academic.oup.com/comjnl/article-lookup/doi/10.1093/comjnl/7.4.308> (visited on 08/04/2021).
- [41] M. Wright, "Direct search methods: Once scorned, now respectable," in *Proceedings of the 1995 Dundee Biennial Conference in Numerical Analysis*, Harlow, United Kingdom: Addison-Wesley, 1996, pp. 191–208.
- [42] F. Gao and L. Han, "Implementing the Nelder-Mead simplex algorithm with adaptive parameters," en, *Computational Optimization and Applications*, vol. 51, no. 1, pp. 259–277, Jan. 2012, ISSN: 0926-6003, 1573-2894. DOI: 10.1007/s10589-010-9329-3. [Online]. Available: <http://link.springer.com/10.1007/s10589-010-9329-3> (visited on 08/04/2021).